BUCKLING STRENGTH OF IMPERFECT RING-STIFFENED CYLINDERS UNDER COMBINED LOADS

T.S. KHAW, B.Sc.

Submitted as a Thesis for the Degree of

Doctor of Philosophy

University of Glasgow 1980

ACKNOWLEDGMENTS

This thesis is based on the work carried out at the University of Glasgow from November 1975 to October 1978 in the Department of Naval Architecture and Ocean Engineering. The final part of the work was carried out from March 1980 to May 1980. The financial support from the Faculty of Engineering Scholarship Fund, University of Glasgow, is fully acknowledged.

The author wishes to express his thanks to his supervisor, Professor D. Faulkner, for his valuable advice and guidance, without which this work would have been impossible. Thanks are also due to the members of staff of the Department for their co-operation, and particularly to Dr. Cameron for his encouragement, and Mr. Miller for his assistance in literature collection.

Finally, I am very grateful to the consultants of the Computer Service, University of Glasgow, for their expert advice and guidance.

CONTENTS

CHAPTER 6/

CONTENTS (Cont'd) Page

SUMMARY

Two computer programs, one for interframe collapse and the other for overall collapse as influenced by initial imperfections, have been developed and the results compared with experiments and with present design codes.

A treatment is presented for the buckling strength analysis of ring stiffened cylinders under external hydrostatic pressure and axial compression. The energy method by Ritz approach is used because of its adaptability to the solution of complicated buckling forms. Equations accounting for non-uniform and uniform lateral pre-buckling displacements are presented in this thesis. The effect of uniform and non-uniform lateral pre-buckling displacements on collapse pressure under uniform external pressure is shown by means of numerical examples. Such effect does not yet appear to have been carried out. Comparison with classical Von Mises equation for elastic buckling under uniform external pressure is good for the case of uniform lateral pre-buckling displacement.

Factors such as initial shape imperfections due to fabrication, welding and cold-bending residual stresses of the shell are considered. The technique used to model such imperfections is solely the author's original contribution. An approximate method using the secant modulus is introduced to account for inelastic behaviour. These factors are considered to be the most important adverse features which distinguish offshore structural response from that of aerospace structures. The effect of strain reversal is assumed to be small and negligible. Ideal elastic perfectly plastic behaviour (with no strain hardening) is assumed for the material.

Quantitative imperfection studies defining the sensitivity of interframe shell buckling to the form and amplitude of initial distortion and residual stresses have been carried out. Such studies do not yet appear to have been carried out. The effects of initial geometrical shape imperfections are shown to be most serious with axial compressive load. This/

This is followed by external pressure and the less sensitive radial (lateral) pressure loading. A study of the effects of welding residual stresses on interframe collapse pressure under uniform external pressure confirms that the compressive welding residual stresses of the shell is detrimental to buckling strength of cylindrical shells. The cold-bending residual stresses in the shell have negligible effect on the collapse pressures of the shell. Comparisons are made with the BS5500 design code and the DnV Rules for interframe collapse. For overall collapse comparison with BS5500 design code is included. Results obtained by the present theory are also compared with results obtained by finite difference dynamic relaxation and finite element methods. Comparisons with experimental data for both interframe and overall collapse behaviour under uniform external pressure demonstrate good agreement with the theory.

CHAPTER 1 INTRODUCTION AND AIM

1.1 INTRODUCTION

The use of fabricated stiffened and unstiffened cylinders is a growing phenomenon in structural engineering. Currently cylinders of relatively large diameters are commonly in use in offshore structures - pressure hulls of submersibles, components of deep-water drilling rigs, storage tanks and sea-bed installations of various kinds - and also increasing applications in various other civil engineering structures.

The last few years' offshore oil and gas exploration boom, especially in the North Sea, together with a progressive move into deeper and more hostile waters, has created a demand for bigger offshore platforms either floating or fixed for exploration and production purposes. This situation has created a lot of problems for the designers. A clear example of rapid development insufficiently backed up by research exists today - the intensive design and construction activity of North Sea oil platforms. These are, in effect, the second generation of such structures; the originals were developed for drilling and production in the Gulf of Mexico. The latest structures are designed for deeper water and a generally more hostile environment than those in America.

For hydrodynamic reasons, elements of the steel structures often take the form of large cylinders made of relatively thin plating. As offshore structures become larger with the move into deeper waters, it seems inevitable that there will be a steady progression to an increasingly thin-walled nature in their components. This is especially true of the supporting legs and jackets which are in effect cylindrical shells with longitudinal and/or circumferential stiffeners. Buckling is the primary form of ductile failure for thin-walled steel components and, for supporting legs, is associated with compressive loading coming from external hydrostatic pressures and the deadweight of the superstructure. This is augmented by bending and torsional effects arising from/

from wave and wind loads. These loading conditions can be multiple, and during the launching and subsequent working life of the platform can occur in various combinations. Each main component of loading is associated with one or more mode of buckling and it is possible that, when combinations of loading components occur, the various buckling modes will interact. It is here that difficulties will arise.

Two primary design problems emerge with the use of these cylinders. On one hand, the designer is faced with an immediate lack of reliable design guidance. The lack of experimental evidence on probable strength levels for these cylinders hinders classification societies in their attempts to provide designers with safe, but relatively economical cylinder design guidance. On the other hand, there is also a major lack of knowledge about the behaviour of such cylinders under various loadings - axial compression, external hydrostatic pressure and longitudinal bending moment.

Many of the design rules to counteract buckling have been derived from the aerospace industry based on tests of aluminium cylinders with stiffening fins machined or riveted in place. Much of this work was carried out during the early 1960s for the design of rocket bodies which were subsequently proof-tested. Now the rules are being applied to very much bigger cylinders constructed by welding from high-strength steel.

The difficulty in formulation of offshore design codes is shown by the fact that, out of the classification societies involved with offshore structures, only Det norske Veritas (DNV)[1]* has so far produced a comprehensive set of rules concerning offshore cylindrical structures. They treat unstiffened cylinders, ring stiffened cylinders, stringer stiffened cylinders, and ring and stringer stiffened cylinders. Loadings covered include axial compression, bending, external pressure, shear, or any combination of these actions. The bases for these rules are adapted from NASA 'Shell Analysis Manual'[2]. They assume similar types of behaviour as in aero-structures and suggest the use of similar types of buckling strength curves. This rather free transfer from aero-space technology leaves many shortcomings which are clearly outlined in references (3), (4), (5) and (6).

---

*References listed at back

Buckling failure of most cylindrical components occurring in offshore installations takes place inelastically (elasto-plastic), in a way which depends more or less strongly on imperfections, including particularly initial deformations of shell plating, stiffeners and residual stresses caused by welding and cold-forming. Generally stiffened cylinders of this type are normally proportioned to fail by elastic/inelastic interframe buckling of the shell plating with hoop stresses close to yield level. As yet there is no satisfactory solution for overall collapse of stiffened cylinders and so existing design codes[7,8,9] require high factors of safety against elastic general instability and against frame tripping, and specify maximum permissible out-of-circularity to avoid frame yield. These procedures make no explicit allowance for residual stresses.

Experimental studies of the buckling of ring-stiffened cylinders under external pressure have shown that collapse of the shell plating between ring frames is frequently preceded by the yield of shell material. This would indicate that inelastic shell buckling may be an important consideration in the strength design of pressure vessels, particularly when it is realised that residual welding and cold-bent stresses often induce inelastic behaviour at pressures well below the design strength. Such cylinders are likely to lie in the range $35 < R/t < 150$ for which buckling occurs inelastically.

In recent years the finite element approach has largely superceded the type of elementary approach and several computer packages are available which are capable of examining instability problems in a wide variety of geometries, such as thin cylindrical shells, conical shells and domes. However, because of their generality and size, these routines are often too costly to use. This much more superior technique of finite element or finite difference method requires extensive computer time for development. At the time when this work began the University of Glasgow had no computer facilities but was sharing the Newcastle Computer (NUMAC), hence resulting in a bad turn-round for a job. Bearing this in mind a reasonable method had to be adopted to suit the facilities available.

1.2 AIM

As a result of the previous considerations, it appears desirable to concentrate attention on the energy method and to develop a technique to allow for the following complications:

a) initial out-of-circularity (initial shape imperfections)

b) residual stresses due to welding and cold-bending

c) inelastic behaviour

d) various boundary conditions

e) under external hydrostatic pressure and axial compression

The purpose of the present work is to develop an economical analytical technique to predict the buckling pressures of ring-stiffened cylinders under external pressure and axial compression. Ring stiffeners and transverse diaphragms (intermediate deep ring frames) provide the most effective means of reinforcing cylindrical shell under external pressure. This form of reinforcement is universally used in the pressure hulls of submarines, submersibles and offshore structures. Failure of a ring stiffened cylinder under external pressure may occur in any of the following modes:

i) Shell instability (interframe buckling)

Interframe shell buckling between rings usually occurs when the shell is stiffened by relatively heavy rings. The shell wall buckles between the rings, while the rings remain essentially circular. The buckling pattern is characterised by the formation of lobes or waves around the circumference. The minimum number of circumferential buckle waves is equal to two, corresponding to buckling into an oval shape. For closely spaced cylinders, the number of circumferential waves is usually much greater than two. Buckling of cylindrical shells induced by external pressure can take place in two basic modes, axisymmetric buckling, during which/

which circumferential corrugations develop along the axis and asymmetric buckling, whereby inward and outward lobes appear alternatively around the circumference. Buckling modes involve a number of n of circumferential waves which increases as the length reduces. In very short cylinders ($\ell/\sqrt{Rt} < 1$) buckling occurs in an axisymmetric (n = 0) mode. Cylinders of such range are not very practicable in engineering usage. Hence much attention will be on asymmetric buckling mode.

ii) General instability (overall instability)

General instability or overall instability refers to the simultaneous buckling of the shell and stiffening rings causing an overall collapse at the critical load. Under external pressure, the general instability buckle-wave form is such that the longitudinal half-wave length is normally equal to the length of the cylinder between bulkheads, and the minimum number of circumferential waves is equal to two or more. General instability is strongly influenced by the frame-spacing and the geometrical properties of the stiffening rings and is likely to be sensitive when the rings are light. The general instability of ring stiffened cylinders can be divided into two types:

a) the general instability under external pressure of circular cylindrical shells with evenly spaced, equal strength ring frames. Non-uniform frame spacing will not be considered here.

b) the general instability under external pressure of circular cylindrical shells of evenly spaced, equal strength ring frames with heavy intermediate ring frames.

In most practical cases, however, collapse by general instability will involve yielding of stiffeners and will be influenced by out-of-circularity and residual stresses caused by welding and possibly cold-bending. Only type (a) will be considered in this thesis. A good theoretical background for general instability of type (b) can be found in references (10),(11),(12),(13).

iii) Local instability of ring stiffeners

In designing the stiffening rings for cylinders, major attention is usually given to the strength of the ring in its own plane. There is also a possibility that a ring may trip, that is, it may buckle or deform laterally. If such deformation became large, the support furnished by the ring to the cylinder may be seriously impaired. The reinforcing efficiency of a ring stiffener increases with each of the following three parameters: Ix_o, A_f and e.

For a given cross-sectional area the most efficient stiffener is obtained when most of the stiffener material is contained in a flange which is connected to the shell by means of a long thin web. The extent to which this can be done effectively is determined by the phenomenon of local instability. A web which is too thin will buckle as thin shell and a section which has too little resistance to bending or twisting out of the plane will develop some form of bending or torsional instability. The analysis of local instability of ring stiffeners needs complex numerical technique and is a major subject by itself. Therefore it will not be pursued here, but some good literature on the subject can be found in references (14), (15), (16) and (17).

2.1 SHELL INSTABILITY

The problem of the shell instability proved of interest as early as 1888 when Bryan[18], employing a strain energy approach, obtained a solution for the buckling of a thin-walled infinitely long circular cylindrical shell under uniform external lateral pressure. Later Southwell[19] obtained a solution for the buckling of a short tube, but his result unfortunately contained an unknown parameter. Then Von Mises[20] made a break-through when he obtained the elastic buckling pressure of a thin shell, simply-supported at its edges and subjected to uniform external lateral pressure. Von Mises derived three separate shell differential equations based on equilibrium of the shell, and by substituting an assumed deflection configuration into these equations, he obtained the required solution. Later in 1929 he extended the solution to include the effect of uniform axial pressure[21]. But as in the previous case, he assumed a deflection configuration which allowed no rotational restraint at the edges. Attempting to verify the second Von Mises formula by experiment, Windenburg and Trilling[22] noticed that for long thin shells, agreement was reasonable, but for shorter shells there was little connection. They concluded that the longer shells buckled elastically, while the shorter ones collapsed by a yield-buckling mode. Unfortunately the models of Windenburg and Trilling were fabricated by rolling and soldering and this introduced much distortion to many of the models. These initial imperfections would affect the cylinders, but was not considered by Von Mises.

In 1941 Sturm[23] carried out a theoretical and experimental investigation on the buckling of thin cylindrical shells under lateral pressure and external pressure. Although he buckled several tubes, many of these were of little use because they were fabricated by welding and rolling and suffered considerable distortion. In the theoretical approach Sturm made many simplifications to his elastic shell equilibrium equations and these have made the predictions of his solutions too inconsistent. The possibility of shorter shells buckling inelastically was/

was pointed out by Sturm and he suggested that an "effective" modulus, related to the tangent and secant moduli, should be employed instead of the elastic modulus. However, this modification does not appear to solve the problem.

Nash[24] recognised the inadequacy of the Von Mises approach, insofar as that only certain buckling forms can be considered, and using a new strain energy expression, he obtained the elastic buckling pressure for a cylindrical shell with its edges fixed. The solution proved to be even further out with the existing experimental observations than the Von Mises solution.

A much more recent investigation of shells which buckle in the inelastic range was presented by Reynolds[25]. The author obtained two inelastic solutions, one based on failure by buckling and the other failure by yield. The first solution involved the use of the secant and tangent moduli, and by relating these two functions to the experimental stress intensity obtained from simple mechanical tests, it was possible to calculate the inelastic buckling pressures at certain stress intensities. The other solution employed the Hencky-Von Mises criterion for yielding and also the Von Sanden-Gunther[26] stress analysis, and from these Reynolds obtained an applied pressure-stress intensity relationship. The plotting of the pressure-stress intensity relationship from these two solutions on the same axis, found the two curves to intersect at a point, and the pressure at this point was taken as the inelastic buckling pressure. Both shape imperfections and residual stresses are ignored. Agreement with observations were shown by the author to be good. However, it was shown later in (27) that the Reynolds solution is too inconsistent.

In 1962 Reynolds[28] developed a small deflection analysis for the elastic interbay buckling of ring-stiffened cylindrical shells in which the influence of the rings on deformations before and during buckling was considered. Tests were carried out with a machined, ring-stiffened cylinder subjected to external hydrostatic pressure. The theory predicted with accuracy the elastic buckling for closely spaced ring stiffeners, at least where stiffeners were external. The solutions predicted much higher buckling pressures when compared with welded models.

One major setback in comparing the relative merits of these solutions is the lack of experimental work in accurately perfect machined models. Another missing consideration is the effect of boundary conditions on the buckling pressure. When small elastic stiffening rings bound a shell, there is a possibility that these may afford only partial constraint to rotation of the edges. Ross[27], employing the energy method, obtained the following solutions for inter-frame shell instability:

i) partially fixed edges
ii) totally fixed edges
iii) simply supported edges

He represented the pre-buckling stresses by the membrane stresses. However, comparison with experimental results is too inconsistent.

None of the above authors has considered the effect of shape imperfections (initial out-of-circularity) in their analyses. This effect and its detrimental influence on cylinders has been pointed out as early as 1945 by Koiter[29]. Effect of shape imperfections on buckling of thin cylinders under various loadings has been studied by many authors[31, 32, 33, 34, 35, 36, 37, 38]. Therefore, any theoretical analysis of shell instability will be incomplete and irrelevant without considering the effect of initial out-of-circularity. Many authors have shown great difficulties in explaining the results of experimental with theoretical solutions. The theory available or being developed was for perfect structures, whereas the models employed for confirmation were imperfect.

2.2 GENERAL INSTABILITY

General instability or overall instability was first pointed out by Tokugawa[39]. He obtained a solution for this mode by a similar approach to that of Von Mises, but careful examination of his result reveals that it is only a combination of a ring buckling formula and a shell buckling expression, each taking place separately. This assumption is incorrect because it does not represent an overall behaviour and no allowance was made for the number of ring stiffeners nor for the length of unsupported span.

For/

For several years after Tokugawa's work the ring stiffeners were designed by many methods based on this approach and it was not until 1950 that Salerno and Levine[40, 41, 42] resolved this inadequacy. They represented a buckling configuration extending over the whole shell-frame assembly and substituting this and its various derivatives into a strain energy expression, they obtained the buckling pressure by minimising the total potential. Salerno and Levine employed in their expressions items such as extensional strain energy, bending strain energy, axial and radial potential, and many other terms, but unfortunately neglected the fact that the radius of the centre of the frames may be different to the radius of the mid-surface of the shell. Also, in comparing the buckling pressure, they neglected the pre-buckling deformations altogether. Because of this shortcoming and because of certain errors in their energy expressions, the analysis is not considered correct.

Kendrick[43, 44, 45] noticed this and made the simplifying assumption of uniform lateral and axial contraction prior to buckling. He assumed simply-supported edges and introduced a '1-cos' term in the buckling displacements to allow for the sagging of the shell plating during buckling. Kendrick found lower buckling pressures than the solutions of Salerno and Levine. Although his method was simpler than that of Salerno and Levine, it neglected only trivial terms - shear, torsion, out-of-the plane bending and twisting of the frames. The range of application of the simplifying assumption concerning pre-buckling deformation is very limited and its effect will be pointed out later in this thesis.

Nash[46] did not accept Kendrick's view that the shear, torsion, out-of-the plane bending and twisting of the frames were negligible, nor did he accept Kendrick's belief that the magnitude of rotational restraint at the edges has no serious effect on the buckling pressure. He took all of these into account and found that the difference in the predicted buckling pressure was indeed significant.

Kaminsky[47] attempted to find out more clearly the difference in buckling strength for clamped end and hinged end cylinders by comparing Kendrick's/

Kendrick's solution with a clamped ends solution obtained through the strain energy expressions used by Kendrick. This too was found to have significant variations.

Reynolds and Blumenberg[48] tested without destroying four accurately machined models, the edges of these being subjected to various boundary conditions. The authors found from their observations that the boundary conditions of the models had an appreciable effect on the buckling pressure. Their experimental results of almost simply-supported edges was in good agreement with the simply-supported edges solution of Kendrick, part III[45].

There are various assumptions and simplifications in Kendrick's Part III theory, so complete agreement with test results cannot be expected.

a) Out-of-plane bending, torsional and warping terms are omitted when strain energy in the ring stiffeners was evaluated

b) Neglected that the radius of the centre of the frames may be different to the radius of the mid-surface of the shell

c) The pre-buckling deformations were considered uniform that the discontinuity effects imposed by the stiffeners were neglected

This feature has not yet been investigated in the case of general instability. However, it shall be considered in this thesis. Finite pre-buckling displacements have a profound effect on the bifurcation load[50]. To ignore these displacements, as is done in most instability analyses, is to invite major errors, usually on the unsafe side. It will be shown later that this effect is serious and detrimental. Most of the authors mentioned above represented the pre-buckling stresses by the membrane stresses.

d) The theories available or developed were for perfect structures, whereas the models employed for confirmation were imperfect due to normal processes of fabrication.

In 1962 Roxburgh[49] employed a uniform radial displacement and a uniform longitudinal contraction for the pre-buckling deformations, and thus neglecting the sagging of the shell plating between the frames. This is particularly serious in widely framed cylinders. Further, a uniform radial displacement does not satisfy the boundary conditions neither at the frames nor at the bulkheads. On close examination Roxburgh used only linear terms for shear expression for the shell plating. Inclusion of higher order terms in the shear expression would lower the buckling pressure significantly.

In 1976 Creswell[13] used Reynolds[28] energy terms for the elastic analysis of overall instability for ring-stiffened cylindrical shells. Fourier functions are used to represent the buckling displacements. In the general case, arbitrary frame sizes and spacings, matrix dimension is 3NfNs, where Ns is the number of frame-spaces and Nf is the limit to the number of basis functions required to represent the buckling displacements. This form of representation of the buckling displacements resulted in (60 x 60) matrices for a solution which could be obtained by the present theory requiring only (5 x 5) matrices within a few per cent of the former. The cost of running such a computer program is obviously too expensive for design purposes. The theory only considered perfect cylinder and only limited comparison was made[51]. A comparison will be shown later between the present theory and that of Creswell's. The work of Creswell is more general in the manner that unequal ring frame spacing is allowed.

There is still no satisfactory inelastic solution for an overall collapse. For a reasonable solution of such kind one would require a huge computer program by finite element or finite difference technique representing each individual frame and shell elements throughout the whole length of the cylinder. Because of this enormous task attention has been focused on problems of the frame-shell combination failure by buckling rather than on overall collapse. Smith and Kirkwood[52] developed a finite-element computer program in which the frame cross-section (and shell) is subdivided into fibres or layers over its depth and which allows for the influence of initial deformations and residual stresses/

stresses to be included. The program considered progressive yielding and strain reversal and it has been used to examine these effects for cold-bent and shell deformations.

A complete analysis of the buckling of ring stiffened cylinders would be extremely lengthy since each frame would undergo different deformations and would go plastic at different pressures. It is necessary to make some sweeping approximations in order to produce a practicable solution. Kendrick[53] used an approach to consider the behaviour of a stiffener near to the centre of the cylinder length and to modify a single stiffener analysis so that the following obvious requirements are satisfied:

a) The elastic stresses in the stiffener for zero out-of-roundness are the same as for the ring stiffened cylinder

b) The elastic buckling pressure should be the same as for the ring stiffened cylinder

c) The plastic limit load assuming perfect circularity should be the same as for the ring-stiffened cylinder

d) The elastic stresses caused by an initial out-of-roundness in a pure buckling mode should be the same as for the ring-stiffened cylinder.

He concluded that the collapse load of a ring stiffener can be greatly reduced by the presence of cold-bending stresses, which is not surprising as it has already been confirmed by previous work[52]. This simple modification to the ring stiffener theory could lead to an under-estimate of the true collapse pressure.

It must be reminded that the previous works by Smith[52] and Kendrick[53] are aimed at the effect of cold-bending stresses in the ring stiffeners on the collapse pressure, as this is the common practice of fabrication of ring frames in navy submarine construction. In the offshore industry most ring frames are fabricated from cut-outs, and/

and welded together and hence the absence of cold-bending stresses.

In the field of finite difference energy method, several authors have made much contribution[54, 55, 56, 57]. Most of the works are applicable to perfect structures and are meant for the aeronautical industry. In the aeronautical field much of the work on cylinders is based on the principle of 'smeared theory'. A good guidance in this field is available from references[58, 59, 60, 61, 62, 63, 64]. The smeared theory technique has its limitations. It assumes that both the shell plating and the ring frames have the same yield strength. Secondly, the increase in critical load due to stiffeners or stringers is the same as that obtained by uniform thickening of the shell with the same amount of material. This second assumption is definitely not true as it depends on the frame spacing and perhaps for very close spacing the differences might be insignificant. Finally, this technique of smeared theory is not applicable to offshore industry as the geometry, material and fabrication processes of the cylinders are different as that of the aerospace industry.

3.1 BASIC CONCEPTS

The principal sources of non-linear structural behaviour are non-linearities in the material properties and the geometric non-linearities caused by rotations of structural elements. Since the latter is the physical reason for static instability, we shall consider its effect and influence.

Buckling of a structure occurs either at a bifurcation point or at a limit point. A bifurcation point indicates a load level at and above which some new deformation mode is possible. The existence of a bifurcation point indicates only that the equilibrium on the primary path loses its stability. The structural behaviour at and beyond this point is governed by the conditions on the secondary path. This secondary equilibrium path can be stable (Fig. 1) or unstable (Fig. 2), symmetric or asymmetric. An unstable bifurcation point indicates an imperfection sensitive structure.

A limit point (Fig. 3) corresponds to the maximum of the load-displacement curve visualising the primary equilibrium path. Under a load exceeding this maximum, there exists no equilibrium configuration in the immediate neighbourhood. For shells of general shapes, buckling or collapse will in most cases occur through the passing of a limit point.

The influence of initial shape imperfections on the stability behaviour of thin shells is most important. The equilibrium path for imperfect cylindrical shells corresponds to substantially lower load levels (Fig. 4). The dramatic reduction of the critical buckling load for cylinders has received both experimental and analytical confirmation[65, 66]. The central significance of the shape of the secondary equilibrium path in determining the influence of initial imperfections is evidenced by the tremendous reduction of the bifurcation buckling load. Lack of knowledge of this secondary path introduces an element of uncertainty.

The/

The energy method by Ritz approach is used because of its adaptability to the solution of complicated buckling forms. Briefly the basis of the energy method is as follows. Strain energies of shell and ring frames, and external load potential, are expressed in terms of the displacements from the unstressed state. Total displacements are then expressed as a sum of displacements along the axisymmetric primary path, and the asymmetric secondary path on buckling. The critical pressures are the pressures at which there exists a non-trivial solution for the buckling displacements, which satisfies the condition that the total potential of the system plus its loads is minimies with respect to the buckling displacements. Both the primary path and secondary path must satisfy the boundary conditions of the structure. To find the critical pressures it is then only necessary to solve an eigen-value problem of the form:

$$([a] - \phi_1 [b])[X] = 0 \qquad (1)$$

where [X] is the buckling deformation vector. Matrix [a] is a stiffness matrix derived from the strain energy of the shell and ring frames and [b] is a load-geometric matrix derived from the (negative) change in potential of the external loads, and the (positive) work done by stresses developed on the primary path immediately before the onset of secondary deformation.

3.2 ASSUMPTIONS

The formulation is based on the usual assumption of the thin shell theory:

1. The shell is assumed to be isotropic and its thickness is small compared to its radius so that the problem is restricted to two dimensions. The co-ordinates are as defined in Fig. 5.

2. Stresses normal to the midplane of the shell and the stiffener axis are ignored and the transverse shear deformation is neglected in both the shell and the stiffener/

2. (Cont'd)

stiffener, so that the hypothesis of preservation of straight normals during deformation is retained.

3. The Kirchoff assumption will be used to relate the deformation of the shell and frame fibres distant from the shell-median surface to the displacements of the shell-median surface. The external load will be taken to act at that same surface.

4. Kendrick's non-linear extensional strain-displacement expressions will be used in the derivation.

5. The ring stiffeners are of solid rectangular or 'T' cross-section.

6. Ring stiffeners are to be fabricated from cut-outs and not by cold-bending. Hence there is no residual stresses due to cold-bending (Fig. 6).

7. Stress-strain curves are irreversible. That is the effect of strain reversal is neglected.

8. Material has ideal elastic perfectly plastic behaviour with no strain-hardening.

9. There is no initial tilt in the ring stiffeners.

3.3 MATHEMATICAL FORMULATION

The total potential energy S_T of a system is defined by:

$$S_T = S_s + S_b + S_f + W_d \qquad (2)$$

where S_S is the extensional strain energy of the shell

S_b is the bending strain energy of the shell

S_f is the strain energy of the ring frames

and W_d is the work done by the external loadings

The effect of welding residual stresses is outlined at the end of this chapter.

For any cylindrical element the strain energy is defined as:

$$\tfrac{1}{2} \iiint \sigma\varepsilon \; R \; d\theta dx dz \tag{3}$$

Applying the thin-shell theory, the constitutive (stress-strain law) relations are:

$$\sigma_x = \frac{E}{1-\mu^2} (\varepsilon_x + \mu\varepsilon_\theta) \tag{4a}$$

$$\sigma_\theta = \frac{E}{1-\mu^2} (\varepsilon_\theta + \mu\varepsilon_x) \tag{4b}$$

$$\sigma_{x\theta} = \frac{E}{2(1+\mu)} \varepsilon_{x\theta} \tag{4c}$$

The extensional kinematic (strain-displacement) equations are from Ref. (67).

$$\varepsilon_x = U_x + \tfrac{1}{2}(W_x^2 + V_x^2 + 2W_{ox} W_x) \tag{5a}$$

$$\varepsilon_\theta = \frac{(V_\theta - W)}{R} + \frac{1}{2R^2}(W_\theta^2 + U_\theta^2 - 2WV_\theta + 2W_{o\theta}W_\theta - 2W_o W) \tag{5b}$$

$$\varepsilon_\theta = \frac{U_\theta}{R} + V_x + \frac{1}{R}(W_\theta W_x + W_{o\theta}W_x + W_{ox}W_\theta) \tag{5c}$$

where: $U_x = \frac{\partial U}{\partial x}$, $W_{ox} = \frac{\partial W_o}{\partial x}$, $V_x = \frac{\partial V}{\partial x}$, etc.

Substituting equations (4), (5) into (3) and retaining only third order terms, we get

$$\begin{aligned}
\bar{S}_s = \frac{ERt}{2(1-\mu^2)} \alpha \iint [& U_x^2 + U_x (W_x^2 + V_x^2 + 2W_{ox} W_x) \\
& + \frac{1}{R^2} (V_\theta - W)^2 + 2\mu U_x (V_\theta - W)/R \\
& + \frac{1}{R^3} (V_\theta - W)(W_\theta^2 + U_\theta^2 - 2WV_\theta + 2W_{o\theta}W_\theta - 2W_o W) + \frac{\mu}{R} (V_\theta - W)(W_x^2 + V_x^2 + 2W_{ox}W_x) \\
& + \mu \frac{U_x}{R^2} (W_\theta^2 + U_\theta^2 - 2WV_\theta + 2W_{o\theta}W_\theta - 2W_o W) + \tfrac{1}{2}(1-\mu)\left(\frac{U_\theta}{R} + V_x\right)^2 \\
& + (1-\mu)\frac{1}{R}\left(\frac{U_\theta}{R} + V_x\right)(W_\theta W_x + W_{o\theta}W_x + W_{ox}W_\theta) \;] \, dx d\theta
\end{aligned} \tag{6}$$

Omission of the fourth and higher order terms

The admissibility of the omission of terms of the fourth and higher order may be examined through calculations and comparison with the remaining contributions in the energy equations. Such comparisons have been carried out by Koiter in Ref. (29), page 293. It has been extensively proved by Koiter that the fourth and higher order terms may indeed be neglected if:

$$1 - \frac{\lambda^*}{\lambda} << 6(1-\mu^2)$$

where the ratio $\frac{\lambda^*}{\lambda}$ is defined in Fig. (45) and is termed the reduction factor.

For welded cylinders, the reduction factor can go as low as 0.30 depending on the R/t and ℓ/R ratio and the degree of imperfections. The reduction factor is always positive. Hence in practice the above inequality is well satisfied and the omission of the fourth order terms may indeed be neglected. The inclusion of higher order terms would lead to more complex mathematical formulation and this is unnecessary unless one is looking at the post-buckling behaviour. One may argue that a more refined shell theory is more necessary than higher order terms.

The bending strain energy expressions are, from Ref. (68) as suggested by Kendrick, such that near agreement with the Vlasov[69] differential equations can be obtained.

$$S_b = \frac{ERtk}{2(1-\mu^2)} \alpha \int\int [R^2 W_{xx} + (W_{\theta\theta}+W)^2/R^2 + \tfrac{1}{2}(1-\mu)(W_{x\theta}-U_{\theta}/R)^2$$

$$+ \frac{3}{2}(1-\mu)(V_x + W_{x\theta})^2 + 2\mu W_{xx}(W_{\theta\theta}+V_{\theta}) + 2RU_x W_{xx}] \, dx d\theta \qquad (7)$$

The term α will be unity for an elastic solution and less than unity for an inelastic solution. This point will be discussed later. The limits of integrations will be from ℓ to 0 and 2π to 0 for interframe instatibility, and from L to 0 and 2π to 0 for an overall instability. Also $S_f = 0$ for interframe buckling.

The/

The strain energy expressions for the ring frames are adopted from Refs. (45) and (28), but modified to suit the co-ordinate system as shown in Fig. 5.

$$S_f = \frac{EA_f\alpha_f}{2(R-e)} \sum_{i=1}^{N} \int_o^{2\pi} [(W_{\theta\theta} + V_\theta)\frac{e}{R^2} - \varepsilon_\theta]^2 d\theta \quad x = i\ell$$

$$+ \frac{EI_{xo}\alpha_f}{2(R-e)} \sum_{i=1}^{N} \int_o^{2\pi} (W_{\theta\theta} + V_\theta)^2 \frac{1}{R^2} \, d\theta \quad x = i\ell$$

$$+ \frac{EI_{zo}\alpha_f}{2(R-e)^3} \sum_{i=1}^{N} \int_o^{2\pi} [eW_{x\theta} - U_{\theta\theta} + (R-e)W_x]^2 d\theta \quad x = i\ell$$

$$+ \frac{GC_r\alpha_f}{2(R-e)^3} \sum_{i=1}^{N} \int_o^{2\pi} [U_\theta + RW_{x\theta}]^2 \, d\theta \quad x = i\ell \qquad (8)$$

where ε_θ is given in eq. (5b).

Work done by the external pressure on an imperfect cylinder can be derived as follows:

Initial volume of cylinder VOL 1 $= \frac{1}{2}\int\int (R-W_o)^2 d\theta dx$

Deformed volume of cylinder VOL 2 =

$$\frac{1}{2}\int\int (R-W-W_o)^2 (1+U_x)(1+V_\theta/R) \, d\theta dx$$

Change in volume (VOL 2 - VOL 1) =

$$\frac{1}{2}\int\int [W^2 - 2RW + 2W_oW - 2R(W_o+W)(U_x + V_\theta/R) + RU_xV_\theta + R^2U_x + RV_\theta] dx d\theta$$

Hence work done by the radial (lateral) pressure component:

$$W_{p1} = -\frac{pl}{2}\int\int [2W_oW - 2RW + W^2 - 2R(W_o+W)(U_x + V_\theta/R) + RU_xV_\theta + RV_\theta] d\theta dx \qquad (9)$$

and work done by the axial pressure component

$$W_{p2} = -p_2 R^2/2 \int\int U_x \, d\theta dx \qquad (10)$$

where $$W_d = W_{p1} + W_{p2} \qquad (11)$$

For axial compression $W_d = W_{p2}$ and for radial pressure only $W_d = W_{p1}$.

During/

During buckling, the system passes from an initial or pre-buckling equilibrium state, in which all deformations are axisymmetric, to the buckled or asymmetric state. The interaction state is defined as the interaction behaviour between the pre-buckled state and buckled state. The total displacements are then expressed as a sum of displacements along axis-symmetric primary path and the asymmetric secondary path on buckling. The overall diagrammatic representation of buckling behaviour could be expressed as below:

PRE-BUCKLED STATE ⟶ INTERACTION STATE ⟶ BUCKLED STATE

The pre-buckling state is a self-equilibrium state. For an initially circular cylindrical structure the primary deformation is axis-symmetric. The effect of initial shape imperfections is small and negligible at the pre-buckled state, unless the initial shape imperfections are purely axis-symmetric, which is not possible in welded cylinders.

A set of appropriate pre-buckled displacements could be assumed as follows:

$$\begin{aligned} u &= f(x) \\ v &= 0 \\ w &= f(x) \end{aligned} \qquad (12)$$

Hence

$$\begin{aligned} U^T &= u + U \\ V^T &= V \\ W^T &= w + W \end{aligned} \qquad (13)$$

Where the subscript T denotes total displacements at buckled state, the small letters u, v, w represent pre-buckling displacements, and capital letters U, V, W represent additional displacements due to buckling. Substituting equations (13) into (6), we get:

$$\begin{aligned} W_s = \frac{ERt}{2(1-\mu^2)} \alpha \iint [& -(M_2+M_1)(W_x^2 + V_x^2 + 2W_{ox}W_x) - 2\frac{1}{R^2}M_1(V_\theta - W)(V_\theta + W_o) \\ & - (M_1+\mu M_2)\frac{1}{R^2}(W_\theta^2 + U_\theta^2 - 2WV_\theta + 2W_{o\theta}W_\theta - 2W_oW) \\ & + 2M_3U_x(W_x + W_{ox}) + 2\mu M_3\frac{1}{3R}(V_\theta - W)(W_x + W_{ox}) - 2\mu M_1U_x\frac{(V_\theta + W_o)}{R} \\ & + (1-\mu)M_3\frac{1}{3R}(U_\theta/R + V_x)(W_\theta + W_{o\theta})] \, d\theta dx \end{aligned} \qquad (14)$$

where:

$$M_1 = \frac{w}{R}\ ,\ M_2 = -\frac{\partial u}{\partial x}\ ,\ M_3 = \frac{\partial w}{\partial x}\quad \text{(derivative of eq. (12))}$$

and the term w_s shall denote this work done due to the interaction behaviour, and must be added to eq. (2) to complete the equilibrium of the system.

In the case of overall instability the same procedure should be applied to eq. (8) resulting in the additional work done due to the ring frames as:

$$W_f = \frac{EA_f\alpha_f}{2(R-e)} \sum_{i=1}^{N} \int_o^{2\pi} [-M_1(W_\theta^2 + U_\theta^2 - 2WV_\theta + 2W_{o\theta}W_\theta - 2W_oW)$$

$$+ M_1(V_\theta+W_o)(W_{\theta\theta}+V_\theta)\frac{e}{R} - M_1(V_\theta+W_o)(V_\theta - W)]d\theta \qquad x = i\ell \qquad (15)$$

where $M_1 = w/R$

Similarly eq. (15) has to be included in eq. (2) to complte the equilibrium system for an overall instability.

3.4 REPRESENTATION OF THE PRE-BUCKLING DISPLACEMENTS

Both Kendrick[68] and Reynolds[28] have in their analyses made the simplifying assumption of uniform lateral and axial contraction prior to buckling. Roxburgh[50] used a better assumption, but still in error because the assumed pre-buckling displacements do not satisfy the boundary conditions. The function f(x) in eq. (12) has to be of the form that satisfies the boundary conditions and physically sound. For simple supported edges:

$$\frac{\partial w}{\partial x} \neq 0 \quad \text{and} \quad \frac{\partial^2 w}{\partial x^2} = 0 \quad \text{at} \quad x = 0 \text{ and } x = \ell \text{ or } L$$

For partial fixed edges:

$$\frac{\partial w}{\partial x} \neq 0 \quad \text{and} \quad \frac{\partial^2 w}{\partial x^2} \neq 0 \quad \text{at } x = 0 \text{ and } x = \ell \text{ or } L$$

For clamped edges:

$$\frac{\partial w}{\partial x} = 0 \quad \text{and} \quad \frac{\partial^2 w}{\partial x^2} \neq 0 \quad \text{at} \quad x = 0 \text{ and } x = \ell \text{ or } L$$

In the case for overall buckling behaviour the "1 - Cos" form has to be introduced to allow for the effect of sagging of shell plating between the ring frames.

i) Simple supported edges:

Recalling eq. (12), the axis-symmetric pre-buckling displacements satisfying the above conditions are assumed as follows:

$$\begin{aligned} \frac{\partial u}{\partial x} &= \text{constant} \\ v &= 0 \\ w &= w_2 \sin\left(\frac{\pi x}{\ell}\right) \end{aligned} \tag{16a}$$

Initially a form of $u = u_2 \cos\frac{\pi x}{\ell}$ was adopted, but it was found to give higher buckling load than that suggested in eq. (16a) - See Fig. 7.

After some numerical observation a uniform axial contraction is adopted for the u function.

In the case of overall instability the following pre-buckling displacements are assumed:

$$\begin{aligned} \frac{\partial u}{\partial x} &= \text{constant} \\ v &= 0 \\ w &= w_1 \sin\frac{\pi x}{L} + w_2\left(1-\cos\frac{2\pi x}{\ell}\right) \end{aligned} \tag{16b}$$

The $\left(1 - \cos\frac{2\pi x}{\ell}\right)$ term is to allow for the effect of sagging of shell plating between the ring frames. w_1 and w_2 are arbitrary constants to be determined from the pre-buckling equilibrium state.

ii) Partially fixed edges

The pre-buckling displacements assumed are as follows:

$$\begin{aligned} \frac{\partial u}{\partial x} &= \text{constant} \\ v &= 0 \\ w &= w_2\left(\sin\frac{\pi x}{\ell} + \sin^2\frac{\pi x}{\ell}\right) \end{aligned} \tag{17a}$$

For overall instability the following displacements are adopted:

$$\begin{aligned} \frac{\partial u}{\partial x} &= \text{constant} \\ v &= 0 \\ w &= w_1\left(\sin\frac{\pi x}{L} + \sin^2\frac{\pi x}{L}\right) + w_2\left(1 - \cos\frac{2\pi x}{\ell}\right) \end{aligned} \tag{17b}$$

iii) Clamped edges

For interframe instability the pre-buckling displacements are:

$$\frac{\partial u}{\partial x} = \text{constant}$$

$$v = 0 \qquad (18a)$$

$$w = w_2\left(1 - \text{Cos}\frac{2\pi x}{\ell}\right)$$

For overall instability the pre-buckling displacements are:

$$\frac{\partial u}{\partial x} = \text{constant}$$

$$v = 0 \qquad (18b)$$

$$w = w_1\left(1 - \text{Cos}\frac{2\pi x}{L}\right) + w_2\left(1 - \text{Cos}\frac{2\pi x}{\ell}\right)$$

3.5 REPRESENTATION OF THE BUCKLING DISPLACEMENTS

The choice of the buckling displacements has to be made such that the amount of computer time required to solve the problem is not too excessive. From the experience of several authors[27,43,44,45,47] the following buckling displacements are adopted for various boundary conditions:

i) Simple supported edges

For interframe instability:

$$U = A_1 \text{Cos}\, n\theta\, \text{Cos}\frac{\pi x}{\ell}$$

$$V = B_1 \text{Sin}\, n\theta\, \text{Sin}\frac{\pi x}{\ell} \qquad (19a)$$

$$W = C_1 \text{Cos}\, n\theta\, \text{Sin}\frac{\pi x}{\ell}$$

$$W_o = C_o \text{Cos}\, n\theta\, \text{Sin}\frac{\pi x}{\ell}$$

For/

For overall instability:

$$U = A_1 \text{Cos } n\theta \text{ Cos}\frac{\pi x}{L}$$

$$V = B_1 \text{Sin } n\theta \text{ Sin}\frac{\pi x}{L} + B_2 \text{Sin } n\theta \left(1 - \text{Cos}\frac{2\pi x}{\ell}\right) \qquad (19b)$$

$$W = C_1 \text{Cos } n\theta \text{ Sin}\frac{\pi x}{L} + C_2 \text{Cos } n\theta \left(1 - \text{Cos}\frac{2\pi x}{\ell}\right)$$

$$W_o = C_{o1} \text{Cos } n\theta \text{ Sin}\frac{\pi x}{L} + C_{o2} \text{Cos } n\theta \left(1 - \text{Cos}\frac{2\pi x}{\ell}\right)$$

ii) Partially fixed edges

For interframe instability:

$$U = A_1 \text{Cos } n\theta \text{ Cos}\frac{\pi x}{\ell}$$

$$V = B_1 \text{Sin } n\theta \left(\text{Sin}\frac{\pi x}{\ell} + \text{Sin}^2 \frac{\pi x}{\ell}\right) \qquad (20a)$$

$$W = C_1 \text{Cos } n\theta \left(\text{Sin}\frac{\pi x}{\ell} + \text{Sin}^2 \frac{\pi x}{\ell}\right)$$

$$W_o = C_o \text{Cos } n\theta \left(\text{Sin}\frac{\pi x}{\ell} + \text{Sin}^2 \frac{\pi x}{\ell}\right)$$

For overall instability:

$$U = A_1 \text{Cos } n\theta \text{ Cos}\frac{\pi x}{L}$$

$$V = B_1 \text{Sin } n\theta \left(\text{Sin}\frac{\pi x}{L} + \text{Sin}^2 \frac{\pi x}{L}\right) + B_2 \text{Sin } n \left(1 - \text{Cos}\frac{2\pi x}{\ell}\right) \qquad (20b)$$

$$W = C_1 \text{Cos } n\theta \left(\text{Sin}\frac{\pi x}{L} + \text{Sin}^2 \frac{\pi x}{L}\right) + C_2 \text{Sin } n\theta \left(1 - \text{Cos}\frac{2\pi x}{\ell}\right)$$

$$W_o = C_{o1} \text{Cos } n\theta \left(\text{Sin}\frac{\pi x}{L} + \text{Sin}^2 \frac{\pi x}{L}\right) + C_{o2} \text{Cos } n\theta \left(1 - \text{Cos}\frac{2\pi x}{\ell}\right)$$

iii)/

iii) Clamped edges

For interframe instability:

$$\begin{aligned} U &= A_1 \text{Cos}\, n\theta\, \text{Cos}\frac{\pi x}{\ell} \\ V &= B_1 \text{Sin}\, n\theta\, (1 - \text{Cos}\frac{2\pi x}{\ell}) \\ W &= C_1 \text{Cos}\, n\theta\, (1 - \text{Cos}\frac{2\pi x}{\ell}) \\ W_o &= C_o \text{Cos}\, n\theta\, (1 - \text{Cos}\frac{2\pi x}{\ell}) \end{aligned} \tag{21a}$$

For overall instability:

$$\begin{aligned} U &= A_1 \text{Cos}\, n\theta\, \text{Cos}\frac{\pi x}{\ell} \\ V &= B_1 \text{Sin}\, n\theta\, (1 - \text{Cos}\frac{2\pi x}{L}) + B_2 \text{Sin}\, n\theta\, (1 - \text{Cos}\frac{2\pi x}{\ell}) \\ W &= C_1 \text{Cos}\, n\theta\, (1 - \text{Cos}\frac{2\pi x}{L}) + C_2 \text{Cos}\, n\theta\, (1 - \text{Cos}\frac{2\pi x}{\ell}) \\ W_o &= C_{o1} \text{Cos}\, n\theta\, (1 - \text{Cos}\frac{2\pi x}{L}) + C_{o2} \text{Cos}\, n\theta\, (1 - \text{Cos}\frac{2\pi x}{\ell}) \end{aligned} \tag{21b}$$

As mentioned in Ref. (44)(80) there are other possible forms of buckling displacements which cater for "infinite" cylinders. The term "infinite" is not clearly defined by Kendrick[80]. A more appropriate non-dimensional parameter is necessary in order to draw a line between "finite" and "infinite" cylinders.

The form of buckling displacements suggested by Kendrick[80] for "infinite" cylinders are:

$$\begin{aligned} U &= 0 \\ V &= B_1 \text{Sin}\, n\theta + B_2 \text{Sin}\, n\theta\, (1 - \text{Cos}\frac{2\pi x}{\ell}) \\ W &= C_1 \text{Cos}\, n\theta + C_2 \text{Cos}\, n\theta\, (1 - \text{Cos}\frac{2\pi x}{\ell}) \\ W_o &= Co_1 \text{Cos}\, n\theta + C_{o2} \text{Cos}\, n\theta\, (1 - \text{Cos}\frac{2\pi x}{\ell}) \end{aligned} \tag{22a}$$

The/

The author disagrees with the form of eq.(22a) for the U-displacement. A rather more correct displacements are:

$$U = A_1 \text{Cos}\, n\theta \, \text{Cos}\frac{\pi x}{L}$$

$$V = B_1 \text{Sin}\, n\theta + B_2 \text{Sin}\, n\theta \, (1-\text{Cos}\frac{2\pi x}{\ell}) \qquad (22b)$$

$$W = C_1 \text{Cos}\, n\theta + C_2 \text{Cos}\, n\theta \, (1-\text{Cos}\frac{2\pi x}{\ell})$$

$$W_o = C_{o1} \text{Cos}\, n\theta + C_{o2} \text{Cos}\, n\theta \, (1-\text{Cos}\frac{2\pi x}{\ell})$$

As we shall see, the latter displacement pattern gives slightly lower buckling pressures and is therefore more correct.

A_1 , B_1 , C_1 , B_2 , C_2 are arbitrary constants to be determined from the minimisation of eq. (2). The terms C_o , C_{o1} , C_{o2} are amplitudes of the shape of imperfections and are known to designers by means of past experience or from collected data.

The (1 - Cos) term is used instead of a $\text{Sin}\frac{\pi x}{\ell}$, to allow for the effect of sagging between ring frames. A $\sin\frac{\pi x}{\ell}$ term would cause a discontinuity at the position of the ring frame, hence not a physical configuration. The (1 - Cos) term is particularly dominant in widely spaced ring stiffened cylinder. It has been shown by Kendrick[45] that to ignore this term is to invite major errors, usually on the unsafe side.

The shape of imperfection has been assumed to resemble the buckling mode. It has been proved numerically that the configuration of the most severe shape of imperfection resembles the buckling mode[52,62,63,67]. The term C_{o1} represents the out-of-circularity of the ring frames and C_{o2} (or C_o) measures the out-of-circularity of the shell between the ring frames. The solutions obtained by this assumed configuration are sufficiently accurate for design purposes.

We/

We shall see later that the solutions obtained are in close agreement with solutions obtained in finite element analysis[52]. The main obstacle is that the true shape of imperfection is not known at design stage, until the cylinder is fabricated. Furthermore, the degree of shape imperfection depends on the fabrication method and this varies from place to place. Most codes are explicity on the degree of out-of-circularity required expressed as the difference between maximum and minimum diameter and BS5500 and ASME use a value equivalent to a departure of 0.5% on radius. This criterion only covers ovality and more complex shapes and localised dents require a different criterion. Various methods of measurement are described in Ref. (34). Since the type of imperfections that the cylindrical structure will exhibit is not yet well known, shells are designed for the 'worst' type of imperfections that are likely to occur. It is now widely accepted that significant advances towards more accurate predictions of the buckling load of thin shells depend on the availability of extensive data of realistic initial imperfections and their correlation with manufacturing techniques[70,71,72,73].

3.6 RESIDUAL STRESSES

3.6.1 Cold bending residual stresses

The residual stresses caused by cold rolling the skin plates to the required curvature must be considered, although it is believed to be less important than those caused by welding and flame cutting.

The simple theoretical model, shown in Fig. A1, comprises an elasto-plastic stress distribution for the bending phase on which is superimposed a reverse elastic distribution due to spring-back. The net final effect is the well known zig-zag stress pattern, the exact form of which depends on the ratio of the radius k to thickness t (see Appendix I). Results at Cambridge by Pascoe[79] on 36 mm plate with σ_y = 470 N/mm² support the validity of this model. Pascoe also showed that the Bauschinger effect made very little difference to the final pattern. If we accept the simple model, the final pattern of circumferential residual stress due to cold bending is as plotted in Fig. A1, depending on the quantity $Et/R\sigma_y$.

The above treatment assumes that the plating is bent once and released. In practice it probably goes through the bending rolls several times before reaching the desired curvature.

In the skin plates the bending operation will give rise also to longitudinal stresses, from the Paisson's ratio effect. These are likely to be less than the circumferential ones and will not be considered in this thesis.

The effect of cold-bending residual stresses on the potential energy of the system can be expressed as follows:

Let S_{cb} be the strain energy due to the cold-bending residual stresses:

$$S_{cb} = \tfrac{1}{2}\iiint \sigma_{cb}\, k_\theta\, R\,dx\,d\theta\,dz \qquad (23)$$

where/

where

k_θ is the circumferential curvature strain given by

$$k_\theta = -\frac{z}{R^2}(W_{\theta\theta} + W) + \frac{z}{R^2} U_{\theta\theta} W_x - \frac{z}{2R} W_x^2$$ up to 2nd order terms.

Substituting for k_θ in eq. (23) we get:

$$S_{cb} = \tfrac{1}{2} R \iiint \sigma_{cb} \left\{ -\frac{z}{R^2}(W_{\theta\theta} + W) + \frac{z}{R^2} U_{\theta\theta} W_x - \frac{z}{2R} W_x^2 \right\} dx\, d\theta\, dz$$

$$S_{cb} = \tfrac{1}{2} R \iint \bar{\sigma}_{cb} \left\{ -\frac{1}{R^2}(W_{\theta\theta} + W) + \frac{1}{R^2} U_{\theta\theta} W_x - \frac{1}{2R} W_x^2 \right\} dx\, d\theta \qquad (24)$$

where

$$\bar{\sigma}_{cb} = \int \sigma_{cb}\, z\, dz \qquad (25)$$

which is derived as follows:

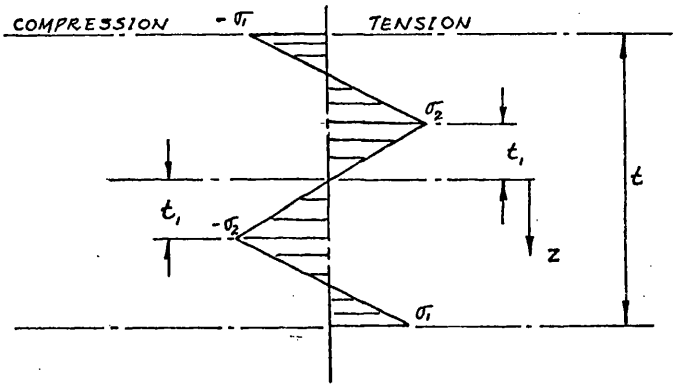

Reference to the figure above, the stress distribution across the shell thickness t can be represented by two simple linear equations.

From A to B and C to D:

$$\sigma_{cb} = \frac{(\sigma_2 + \sigma_1)}{(t/2 - t_1)} z - \frac{(\sigma_2 \frac{t}{2} + \sigma_1 t_1)}{(t/2 - t_1)} \qquad (26)$$

and

From B to C:

$$\sigma_{cb} = \frac{\sigma_2}{t_1} z \qquad (27)$$

$\therefore$ /

$$\therefore \quad \bar{\sigma}_{cb} = \int_{-t_1}^{t_1} \frac{\sigma_2}{t_1} z^2 \, dz + 2\int_{t_1}^{t/2} \left\{\frac{(\sigma_2 + \sigma_1)}{(t/2 - t_1)} z^2 - \frac{(\sigma_2 \frac{t}{2} + \sigma_1 t_2)}{(t/2 - t_1)} z\right\} dz \qquad (28)$$

$$\bar{\sigma}_{cb} = \underline{\sigma_2 \frac{2}{3} t_1^2 + 2\gamma} \qquad (29)$$

where

$$\gamma = \frac{1}{(t/2 - t_1)} \left\{\frac{(\sigma_2 + \sigma_1)}{24} t^3 + \tfrac{1}{2}(t_1^2 - \frac{t^2}{4})(\sigma_2 \frac{t}{4} + \sigma_1 t_1) - (\sigma_2 + \sigma_1)\frac{t_1^3}{3}\right\} \qquad (30)$$

Hence eq. (24) has to be included in eq. (2) to account for the presence of cold bending residual stresses.

Ring Frames

The T-section ring frames are made up of ten or eight sections which are then butt welded together to form a complete ring (Fig. 6b). Each section is built-up from plate in the following manner:

i) Flame cut web segment to correct shape from plate to plate - cutting proceeds continuously around the profile of the segment.

ii) Roll the flame - cut flange strip to the correct curvature

iii) Tack the flange to the web

iv) Complete the web-to-flange welds, with the plates clamped into the jigs to maintain correct curvature and to prevent tilt of web.

The sections are then jigged into the correct circle and joined by full penetration butt welds to form a complete ring.

The above procedure of fabrication is a normal practice carried out in most offshore fabrication yards. There is no cold bending carried out except for the sectional flange strips which are very thin compared with the web depth. Therefore the presence of any cold bending residual stresses in the ring frames can be ignored.

3.6.2 Welding residual stresses

The effect of welding residual stresses on the buckling load of stiffened cylinders is much more serious than that of the cold bending residual stresses. Much work has been done on the measurement of these residual stresses in Cambridge[73,74]. Earlier work on the calculations of deformations of welded metal structures can be found in Reference (75). The effects of residual stresses on the ductile strength of ring stiffened cylinders are outlined by Faulkner in Reference (76).

From the above references a simple mathematical model will be presented here as shown

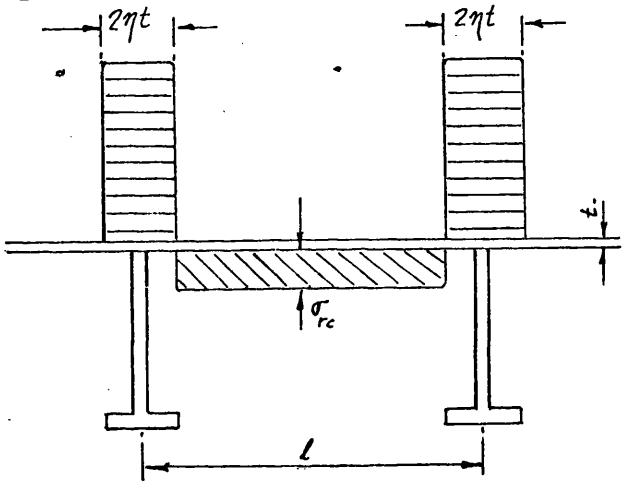

The width ηt of the yield tension block each side of the weld joint is governed by the welding process and, in particular, by the heat input (or rate of weld deposity), yield stress and thickness of the members joined. From experiences gained in weld imperfections of stiffened panel, initial values of η in the range 4.5 - 6 seemed typical. Measurements on larger models suggest much higher values of η[77]. It appears reasonable to assume that the compressive residual stresses σ_{rc} in the plating are balanced by the tension block in the plating.

Then:

$$\frac{\sigma_{rc}}{\sigma_y} = \frac{2\eta}{\ell/t - 2\eta} \qquad (31)$$

There is very scant information on this subject. One value for a specific/

specific submarine[78] gave $\sigma_{rc} = 0.17\ \sigma_y$ as measured. Typical values for σ_{rc} from $0.10\ \sigma_y$ to $0.20\ \sigma_y$ are practical for stiffened welded cylinders.

As outlined by Faulkner[76], for internally stiffened cylinders welding the ring frames to the shell produces interframe compression residual stresses from two sources:

i) from tension block η actions from along-the-weld shrinkage as represented by eq.(31)

ii) from typical interframe shell distortion caused by the welding

The source (ii) cannot be included here as it is already considered for under the effect of shape imperfections, W_o. This supports the logic that welded cylinders can never have perfect circularity.

The effect of welding residual stresses on the potential energy of the system shall now be expressed as follows:

Let S_w be the strain energy due to the welding residual stresses and σ_w the welding residual stresses in the shell plating.

Then:

$$S_w = \tfrac{1}{2}\int\int\int \sigma_w \epsilon_\theta R\, d\theta dx dz \qquad (32)$$

where

$\sigma_w = \sigma_y$ (at the tension block)

and

$\sigma_w = \sigma_{rc}$ (compressive stress at mid-bay, computed by eq.(31)

Substituting/

Substituting for ε_θ from eq. (5b)

$$S_w = \tfrac{1}{2}Rt\int\int\sigma_w\left[(V_\theta - W)/R + \frac{1}{2R^2}(W_\theta^2 + U_\theta^2 - 2WV_\theta + 2W_{o\theta}W - 2W_oW\right] d\theta dx \qquad (32)$$

Hence eq. (32) has to be included in eq. (2) to account for the presence of welding residual stresses in the shell plating. To evaluate eq. (32) step-integration would be performed.

4.1 PREBUCKLING MATRICES

The pre-buckling state is a self-equilibrium state. Substituting the pre-buckling displacements of eq. (12) into eq. (2), where ew. (12) will take the form of eqs. (16) to (18) depending on the boundary conditions and the mode of buckling, interframe or overall buckling, we get in matrix form:

$$u^T = \frac{ERtL}{2(1-\mu^2)} \left| \tfrac{1}{2}[x]^T[r][x] - \phi_1[s]^T[x] \right| \tag{33}$$

where [r] is the stiffness matrix

[s] is the load matrix

This potential energy u^T must be a minimum. Differentiating u^T with respect to vector [x], we get:

$$\frac{\partial u^T}{\partial [x]} = [r][x] - \phi_1[s] = 0 \tag{34}$$

or $$[r][x] = \phi_1[s]$$

The vector [x] can then be solved in terms of ϕ_1, and these are needed to calculate W_s and W_f later on.

4.2 BUCKLING MATRICES

The total potential energy of the buckled state includes the terms W_s and W_f and the terms to account for the presence of residual stresses. The buckling displacements will take the form outlined in eqs. (19) to (22), depending on the boundary conditions and the mode of buckling. After substituting, we get:

$$U^T = \frac{EtTL}{4R(1-\mu^2)} \left(\tfrac{1}{2}[X]^T([a] - \phi_1[b])[X] - \phi_1[c]^T[X]\right) \tag{35}$$

This/

This potential energy U^T must be a minimum. Differentiating U^T with respect to vector [X], we get:

$$\frac{\partial U^T}{\partial [x]} = ([a] - \phi_1[b])[x] - \phi_1[c] = 0$$

$$\text{or} \quad ([a] - \phi_1[b])[X] = \phi_1[c] \tag{36}$$

where

[a] is the stiffness matrix at buckled state

[b] is the load matrix at buckled state

[c] is the column matrix due to initial shape imperfections

For a perfect cylinder, the matrix [c] is a null matrix, and hence reducing equation (36) to simply:

$$([a] - \phi_1[b])[X] = 0 \tag{37}$$

the smallest root of ϕ_1 and hence the buckling pressure is of interest here.

It is easy to solve for the smallest value of ϕ_1 of eq. (37) than eq. (36). Eq. (37) can be written:

$$(I - [d]\phi_1)[x] = 0 \tag{38}$$

where

$$[d] = [a]^{-1}[b]$$

and I is the unit matrix

Let $\beta = 1/\phi_1$ and eq. (38) becomes:

$$(\beta[I] - [d])[x] = 0 \tag{39}$$

The largest root of eq. (39) and the associated vector [x] is easily found by repeated premultiplication of an arbitrary column vector by [d]. The theory is given in Ref. (81) and a numerical example follows:/

follows:

$$[a] = \begin{bmatrix} 274.0 & -145.2 & 5.58 \\ -145.0 & 924.7 & -72.0 \\ 5.58 & -72.0 & 6.69 \end{bmatrix} \qquad [b] = \begin{bmatrix} 135.5 & 191.8 & -432.2 \\ 191.8 & 819.1 & 174.2 \\ -432.2 & 174.2 & 836.2 \end{bmatrix}$$

$$[a]^{-1} = \begin{bmatrix} 0.00453 & 0.00453 & 0.0239 \\ 0.00258 & 0.00816 & 0.0856 \\ 0.0239 & 0.0856 & 1.051 \end{bmatrix} \qquad [d] = \begin{bmatrix} -9.252 & 7.157 & 18.542 \\ -36.09 & 22.09 & 71.92 \\ -434.5 & 257.8 & 883.4 \end{bmatrix}$$

The matrix [d] is now used as a premultiplier on an arbitrary column matrix. A suitable choice of column matrix is as follows, but any will do although a poor choice can slow down the convergence:

$$\begin{bmatrix} 0 \\ 0.10 \\ 1.00 \end{bmatrix}.$$

The last number (β_1 say) in the resulting column matrix is an approximation to the largest eigenvalue β and the matrix is an approximation to the required matrix [X]. Dividing throughout this column matrix by β_1 and repeating the process of premultiplication by [d] leads to a better approxkmation to β_2 and a better approximation to [X] after once again dividing by β_2. This process converges to the exact value of β and [X] after several iterations depending on the size of the matrix [d] and starting value of [X]. The collapse pressure is then given by the dominant root of eq. (39).

Before eq. (36) can be solved a slight modification has to be introduced. Eq. (36) can be rewritten in element form as follows:

$$\left(\begin{bmatrix} a11 & a12 & a13 & 0 \\ a21 & a22 & a23 & 0 \\ a31 & a32 & a33 & 0 \\ 0 & 0 & 0 & 0 \end{bmatrix} - \phi_1 \begin{bmatrix} b11 & b12 & b13 & c1 \\ b21 & b22 & b23 & c2 \\ b31 & b32 & b33 & c3 \\ 0 & 0 & 0 & 0 \end{bmatrix} \right) \begin{bmatrix} X1 \\ X2 \\ X3 \\ 1.00 \end{bmatrix} = 0 \qquad (40)$$

Eq. 40/

Eq. (40) is still mathematically the same as eq. (36) and the zeroes are just dummy elements. From eq. (40) it can be seen how the column matrix [c] affects the collapse pressure through its influence in the load matrix [b]. The inverse of [a] is only performed on non-zero matrix elements, hence the (3 x 3) matrix elements only. If [e] is the inverse of [a], then elements the elements are:

$$[e] = \begin{bmatrix} e11 & e12 & e13 & 0 \\ e21 & e22 & e23 & 0 \\ e31 & e32 & e33 & 0 \\ 0 & 0 & 0 & 0 \end{bmatrix} \qquad (41)$$

The multiplication of matrices [e] and [b] (as in eq. (40)) will give the required matrix [d] which is now (4 x 4) matrix. The problem of eq. (36) is now reduced to the equivalent of eq. (39). Therefore, the iterative process for the smallest value of ϕ_1 is similar to the procedure of eq. (39).

This technique of solving eq. (36) is compared with results obtained by Dynamic-Relaxation Finite difference method for axial compression of unstiffened cylinders with simple supported boundary conditions[82]. The same function is used for shape imperfections in both methods. Numerical examples for cylinder of R = 800 mm, t = 6 mm, = 600 mm are compared and shown in Fig. (8). The results show close agreement with the present technique. A mesh size of (18 x 64) was used in the finite difference program. It is interesting to note that the computer time needed for the finite difference program is enormous - approximately 1000 seconds (cpu time) for each loading point on an ICL 2976 computer, compared with 2 seconds for each buckling load at a specified mode by the present technique. The above comparison is made on elastic solution basis only. The cost of an inelastic solution by the finite difference program is far too frightening to be mentioned here - perhaps not within the scope of the present ICL 2976 computer. A brief description of dynamic relaxation is as follows:

Dynamic/

Dynamic Relaxation is a procedure for moving towards a correct solution from a non-equilibrium starting guess involves the use of dynamic equations. The starting guess with zero velocities is taken as the initial conditions. The static loads are then applied and held constant as the system is allowed to move dynamically until motion dies out. The promise of success soon fades as one tries to apply the method. If the physical characteristics are used to model the mass and damping, one can expect very large transients which persist for long times. This means excessive solution cost and difficulties in controlling spurious oscillations in the solution. An obvious remedy is to assume artificial properties which assure strongly damped responses. The question then shifts to how to estimate those artificial properties. The necessity of obtaining contrived terms for both mass and damping properties detracts further from the method. Other superior methods are reviewed by Crisfield[86] and dynamic relaxation lies low in comparison.

5.1 YIELD FUNCTION

Yield function employed here is that developed by Ivanov and outlined by Robinson[83] and is more accurate than Ilyushin's approximation[84]. Further advantages of Ivanov's yield criterion over Ilyushin's approximation yield function are reviewed by Crisfield[85].

The yield function:

$$f_y^2 = Q_t + \tfrac{1}{2}Q_m + \sqrt{(0.25Q_m^2 + Q^2_{tm})} \qquad (42)$$

where

$$Q_t = \frac{\bar{N}}{N_o^2}$$

$$Q_m = \frac{\bar{M}}{M_o^2}$$

$$Q_{tm} = \frac{\overline{MN}}{M_o N_o}$$

and

$$\bar{N} = N_x^2 + N_\theta^2 - N_x N_\theta + 3N_{x\theta}^2$$

$$\bar{M} = M_x^2 + M_\theta^2 - M_x M_\theta + 3M_{x\theta}^2$$

$$\overline{MN} = M_x N_x + M_\theta N_\theta - \tfrac{1}{2}M_x N_\theta - \tfrac{1}{2}M_\theta N_x + 3M_{x\theta}N_{x\theta}$$

$$N_o = t\sigma_y$$

$$M_o = 0.25\, t\sigma_y^2$$

N_x , N_θ , N_{xy} - forces/unit circumference

M_x , M_θ , $M_{x\theta}$ - bending moments/unit circumference

N_x/

M_x

$$N_x = \frac{\alpha Et}{1-\mu^2} (\varepsilon_x + \mu\varepsilon_\theta) \quad (43a)$$

$$N_\theta^* = \frac{\alpha Et}{1-\mu^2} (\varepsilon_\theta + \mu\varepsilon_x) \quad (43b)$$

$$N_{x\theta} = \tfrac{1}{2}\alpha \frac{Et}{u+w} (\varepsilon_{x\theta}) \quad (43c)$$

$$M_x = \alpha \frac{Et^3}{12(1-\mu^2)} k_x \quad (44a)$$

$$M_\theta = \alpha \frac{Et^3}{12(1-\mu^2)} k_\theta \quad (44b)$$

$$M_{x\theta} = \alpha \frac{Et^3}{12(1-\mu^2)} k_{x\theta} \quad (44c)$$

where $\alpha = E_s/E$

$$k_x = -W_{xx}$$

$$k_\theta = -(W_{\theta\theta} + W)/R^2$$

$$k_{x\theta} = -W_{x\theta}/R - V_x/R + U_\theta/R^2$$

(*includes the residual stresses).

It is clearly obvious that for an elastic solution $\alpha = 1.00$ and for an inelastic solution, α will be less than unity.

The cylinder is divided into mesh size of (9 x 20) for the purpose of computing the yield function, f_y at each nodal point. For an overall instability the arrangement is made such that only 3 or 5 nodes are located between two ring frames in the axial direction, depending on the length of the cylinder.

5.2 ELASTIC SOLUTION

Recall the pre-buckled matrix equation (34) and the buckled matrix equation (36):

$$\text{pre-buckled:} \quad [r]\,[x] = \phi_1[s] \ldots\ldots\ldots (34)$$

$$\text{buckled:} \quad ([a] - \phi_1[b])[X] = \phi_1[c] \ldots (36)$$

The pre-buckled equation is related to the buckled equation through the matrices [b] and [c] - both contain the vector [x]. For an elastic solution and assuming an ideal elastic stress-strain curve, the value of α is one. The case of strain-hardening effect will not be considered here.

The steps taken to arrive at the convergent value of ϕ_1 are as follows:

1. Calculate matrices [r] and [s] and from an initial guess value of ϕ_1 (say zero) and then solve for [x] from eq. (34).

2. Knowing [x], calculate matrices [a], [b] and [c] and solve for the minimum value of ϕ_1 from eq.(36) by iteration - call it ϕ_1^*

3. Compare the value of ϕ_1^* with ϕ_1 used in step 1. If the latter agrees with the former within some small predetermined tolerance, proceed to step 4. If they do not agree use ϕ_1^* as an improved estimate and go to step 1.

4. Use ϕ_1^* and eq. (36) to solve for [X] and then evaluate the total strains (including the residual strains).

The resulting behaviour from equations (34) and (36) under axial compression for various C_o/R values is as shown in Fig. (43).

5.3 INELASTIC SOLUTION

Buckling failure may occur in the inelastic region, particularly in welded and closely framed cylinders - say $\ell/R < \frac{1}{2}$. Elastic buckling is more likely to occur in widely framed cylinders and cylinders with high R/t (say 200) and large C_o/R. In any case, it is necessary to check first whether the failure is due to inelastic or elastic behaviour.

Poison's ratio, μ, is regarded as a variable in the inelastic region[87], and can be accurately expressed as a function of E_s by the equation:

$$\mu = \tfrac{1}{2} - \frac{E_s}{E}(\tfrac{1}{2} - \mu_e)$$

The steps taken to arrive at the convergent value of ϕ_1 for an inelastic solution are as follows:

5. Proceeding from step 4, the yield function at each node of the shell plating is computed. Any yield function greater than one, suggests yielding at the node. The value of α is then reduced - say 0.90, and then proceed to step 1. This cycle goes on until all points have yield function equal to or less than one, with α decreases or increases at each cycle. As α decreases, ϕ_1 decreases, hence lowers the collapse load.

This process of determining the value of α such that the maximum yield function at any nodal point is less than or equal to one, is an iterative procedure and applies only to the shell plating. The yield criterion for the ring frame shall be dealt with separately in a different manner.

5.4/

5.4 YIELDING OF RING STIFFENERS

The problem of stress analysis of ring frame of a stiffened cylinder in an accurate manner is of very great complexity and it is unlikely that a two-dimensional thin shell theory will be able to tackle such a problem. Therefore a very crude approach has to be introduced. In most practical cases, however, collapse by general instability will involve yielding of ring stiffeners and will be influenced by out-of-circularity and residual stresses. Hence it is essential to check whether failure is due to yielding of ring stiffeners or general instability. Failure is assumed to occur when the sum of the circumferential bending stress, σ_b, and the hoop compressive stress σ_{Fc}, reaches yield at the outer fibres of the ring frame. It is implicitly assumed that the total stress is given by the sum of σ_{Fc} and σ_b with sufficient accuracy up to the yield-point of the stress of the material, and that failure is synonymous with the pressure at which yielding in the extreme fibre begins. The latter assumption is, of course, conservative. However, once yielding starts it progresses rapidly and the ultimate pressure is generally not expected to be much greater than the pressure at which yielding begins.

The stresses will be highest in the flange of the frames which are situated at the furthest distance from the rigid ends. For cylinders with an odd number of ring frames, the magnitude of the maximum flange stress is given by:

$$\sigma_F = E\left[(W_{\theta\theta} + V_\theta)\frac{e_{ff}}{R^2} + (W - V_\theta/R\right] \qquad (45)$$

at $\theta = 0$

$x = L/2$

where e_{ff} is the distance of the frame flange from middle surface of the shell. For cylinders with an even number of ring frames the maximum stress will be less than this value but the difference will be negligible unless the number of ring frames is small. The maximum flange/

flange stress may be written:

$$\sigma_F = \sigma_{Fc} + \sigma_b \tag{46}$$

$$\text{and} \quad \sigma_{Fc} = -E(nB_1 - C_1)/R \tag{47}$$

$$\sigma_b = E(nB_1 - n^2 C_1)e_{ff}/R^2 \tag{48}$$

where B_1 and C_1 are calculated from eq.(36).

Hence the yield criteria of the ring frame is:

$$\sigma_{Fc} + \sigma_b = \sigma_{yF} \tag{49}$$

The pressure to cause yielding is then obtained by reducing ϕ_1 of eq.(36) in an iterative procedure such that eq.(49) is satisfied.

Two computer programs, one for interframe collapse, and the other for overall collapse, are developed for the purpose of this analysis.

6.1 COMPARISON WITH VON-MISES CLASSICAL EQUATION FOR INTERFRAMES BUCKLING UNDER UNIFORM EXTERNAL PRESSURE

Von Mises[21] obtained the elastic buckling pressure of a thin shell simply-supported at its edges and subjected to uniform external pressure, by solving three separate shell differential equations based on equilibrium of the shell and substituting an assumed deflection configuration into these equations. Comparisons with Von Mises equation are as shown in Figs. (9),(10),(11) and (12) for various values of ℓ/R and R/t. Good agreement is obtained with Von Mises equation for the case where uniform lateral and axial contraction are assumed in the pre-buckling displacements, $\frac{\partial u}{\partial x}$ = constant and w = constant. For $\ell/R = 0.250$ and $\ell/R = 0.500$ the difference is negligible. For $\ell/R = 0.750$ and $\ell/R = 1.00$, exact agreement with Von Mises equation is obtained. Evidently the energy expressions used here are in agreement with the differential equations obtained by Von Mises.

It is interesting to note that a lower buckling pressure is obtained when the lateral pre-buckling displacement is no longer uniform, as in eq. (16a). It is clearly evident that the generators of the cylinder are no longer straight, but are allowed to vary non-linearly between stiffeners. The former set of pre-buckling displacements assumes that the generators remain straight and hence give a higher buckling pressure. This explanation is comparable with the Foppl[90] formula for the collapse of a circular ring under uniform circumferential load. Another important point no designer can afford to ignore is the type of pressure loading which is often referred to as live loading as opposed to dead loading which does not change direction as the structure deforms. This is one area of application that has received particularly no attention. The assumption that the generators remain straight is an equivalent of a dead load situation, because the pressure is always acting perpendicular to the generators. For rings and some buckling modes of shells the results can be in error by as much as 50%[91]. The error depends very much on the ratio R/t. It is clearly obvious from Figs.(9),(10),(11) and (12) that the gap widens as R/t increases. With the present North Sea offshore structures having R/t as high as 300 restraint/

restraint should be applied as some rules, especially BS 5500, involved the use of Von Mises formula.

6.2 EFFECT OF INITIAL SHAPE IMPERFECTION ON INTERFRAME SHELL BUCKLING

Quantitative imperfection studies defining the sensitivity of interframe shell buckling to the form and amplitude of initial distortions and residual stresses do not yet appear to have been carried out. The most significant initial distortions are those corresponding in form to the interframe shell buckling modes. Figs. (13),(14),(15), (16)and (17) show the initial shape imperfection sensitivity of interframe shell buckling under uniform external pressure for cylinders. It is evident that the sensitivity increases with the ratios R/t and ℓ/R, but is more pronounced with R/t. As no other available study is obtainable, comparison cannot be made here.

Figs. (18),(19),(20),(21) and (22) show the initial shape imperfection sensitivity of interframe shell buckling under radial (lateral) pressure for various R/t and ℓ/R ratios. Again sensitivity is more pronounced for increasing R/t ratio than ℓ/R. On the whole the effect of initial shape of imperfection on buckling load is more sensitive under external pressure than under radial pressure. This is easily explained by the fact that the absence of the axial pressure component reduces the sensitivity under radial pressure loading. It is a well known fact that axial compressive load is the most destructive type of loading. Typical curves of imperfection sensitivity under axial compression are shown in Fig. (23) - the curves are steeper and drop suddenly at small initial imperfection.

It would be incomplete not to mention Koiter's work. He derived the sensitivity of the axial compressive load to initial imperfections as shown in Fig. (45). This is reproduced from Fig. (9) of Ref. (29). A closer examination of the equations in Fig. (45) revealed that they are independent of the ℓ/R ratio. Koiter assumed axi-symmetrical shape imperfections. One must recall that Koiter presented a theory that gives an explanation for the large differences between theoretically and experimentally determined buckling loads. Also the wide scatter in the experimental results is satisfactorily explained by the great sensitivity of the buckling load to small changes in the magnitude of the deviations. Hence, Koiter's work is generally on the adverse factors affecting buckling/

buckling load, rather than on the numerical tool to predict buckling load.

A comparison with the classical solutions of Flugge, Donnel and Timoshenko is shown in Fig. (44).

DnV Rules[1] specify a tolerance on local shell deformation between frames. Tolerances on deviation from circularity specified in the other rules relate primarily to ring frames and do not adequately cover inter-frame shape. The proposal made by Kendrick to the British Standards Institution and accepted by PVE/-/5 Committee allows a maximum tolerance within 0.50% on radius[92][7].

6.3 EFFECT OF COLD-BENDING RESIDUAL STRESSES

Table 1 shows the influence of cold-bending residual stresses in the shell plating on interframe collapse pressure under uniform external pressure. The influence is very small indeed and negligible, but of course it is not the same for ring frame which is an equivalent of a very thick cylindrical shell. The presence of cold-bending residual stresses does not appear to have any significant effect on the interframe collapse pressure. This conclusion is also confirmed by limited experiments employing stress-relief. An attempt to assess the effect of residual stresses on collapse pressures was carried out by Kendrick[80] using two models which were nominally identical except that in one of the models the cold-bending stresses had been removed by heat treatment after cold-bending. The collapse pressure of the models was in fact slightly different, the stress relieved model being the weaker. This was found to be due to the stress relieving having lowered the yield stress by about 7%. Making allowance for the difference in yield stress, it was concluded that the cold-bending did not appear to have any significant effect on the collapse pressure.

6.4 EFFECT OF WELDING RESIDUAL STRESSES

Tables 2, 3 and 4 show the influence of welding residual stresses on interframe collapse pressure under uniform external pressure for simple supported and clamped boundary conditions. It is well established that the compressive residual stresses σ_{rc} are detrimental to ductile strength of both plated structures or cylindrical shells[76]. It is confirmed here that an increase in σ_{rc} follows an increase in the percentage loss of strength - approximately an increase in σ_{rc} results in/

in a same percentage in loss of strength. At a higher ratio of R/t the percentage loss of strength can be enormous, and the same applies to an increase in ℓ/R ratio. For R/t = 200, ℓ/R = 0.675, $\sigma_{rc}/\sigma_y = 0.154$ and $C_o/R = 0.0050$, the percentage loss of strength can be as high as 32% for simple supported edges and 39% for clamped edges. Hence it is obvious that no designer can afford to ignore the effect of welding residual stresses.

6.5 COMPARISON WITH DNV RULES, BS5500 RULES AND EXPERIMENTAL DATA OF FIG. (24) FOR INTERFRAME COLLAPSE PRESSURE UNDER UNIFORM EXTERNAL PRESSURE

The BS5500 design code mentioned here is referred to the proposal made by Kendrick[92] to the British Standards Institution[7], and is based on the experimental data plot of Fig. (24). Fig. (24) is a revised version of Fig. (3) of Ref. (92). It is a plot of well-documented experimental data using the parameters p_c/p_{c5}, p_m/p_{c5} which are defined in Appendix B. This data from about 700 collapsed cylinders covers the range:

$$250 > R/t > 6.0$$

$$50 > \ell/R > 0.04$$

and with cylinders usually less than 2.5 ft. (762 mm) in radius. In most cases the cylinders tested had departures from the mean circle which were much less than 1% of the radius, although in some cases the values were in excess of 1%. Since the majority of cylinders tested have had out-of-roundness values less than 1% it is reasonable to consider that the lower bound curve only applies for cylinders of this accuracy of manufacture. It must be pointed out that Fig. (24) originated from the navy submarine design code[93] for interframe collapse pressure.

The DnV rules of interframe collapse stress is from section C3.4.2.5 and the plasticity reduction factor from section C3.2.1.1 of Ref. (1). The stress level is then converted to pressure by means of pressure = stress x (t/R) for comparison purposes.

Figs. (25),(26),(27,(28) and (29) show the comparison between the present theory, BS5500, DnV Rules and experimental data, for various values/

values of R/t and ℓ/R. The present theory is based on simple supported boundary conditions, $E/\sigma_y = 841$, $\sigma_{rc}/\sigma_y = 0.120$ and $C_o/R = 0.0050$. The experimental data curve refers to the lower bound curve of Fig. (24). As mentioned earlier, BS5500 is based on collected experimental data of cylinders having R/t < 250. This is confirmed here that for values of R/t greater than 250, the present theory predicts lower collapse pressures than permitted by BS5500. The DnV rules on the whole predict higher collapse pressure than BS5500 and in some cases even much higher than the experimental data. This can easily be explained by the fact that the DnV rules are not derived from experimental data like BS5500. The present theory curves on the whole lie lower than the experimental data curve, except for R/t < 150 at ℓ/R = 0.250 and R/t < 125 at ℓ/R = 0.500. This is explained by the fact the simple supported edges are assumed for the present theory but the likely boundary condition for experimental data is between simple supported and clamped condition. This is true in cases of elastic collapse failure. The reverse effect applies when inelastic collapse failure occurs, because the plasticity reduction factor is less for simple supported edges than any other boundary conditions. Secondly, being small scale cylinders (as suggested by the maximum radius being much less than 762 mm) the value of σ_{rc} might even be less than the assumed value of 0.120 σ_y. As we have seen earlier, initial shape imperfections play a more major role than welding residual stresses in the reduction factor of collapse pressure, therefore, it is more likely that the tested cylinders have C_o/R less than 0.0050. Further information on this matter regarding Fig. (24) is not available. Hence, exact comparison is impossible unless one can obtain an experimental curve of tested cylinders having same, or nearly same, C_o/R ratio.

BS5500 curve is derived from the lower bound curve of Fig. (24) by introducing a factor of safety of 1.50. Hence it is only right that BS5500 curve must lie below the present theory curve - and this is true in all cases of ℓ/R ratio and all R/t < 250. It is obvious that the practice of overstretching design rules (in this case R/t > 250) can produce disastrous results. With the present North Sea offshore structures having R/t as high as 300, restraint should be applied when using BS5500 rules, even although it is much more reliable than DnV rules, as far as interframe collapse pressure uniform external pressure is concerned. The pitfalls of extrapolating research information or design rules to areas for which they were never intended cannot be over-emphasised, as such an expedient may often be a recipe for disaster.

6.6 COLLAPSE OF DP1 FRIGG FIELD BUOYANCY TANKS[94]

Engineers in Norway, U.K. and France are wondering whether there was a fundamental design error behind the buckling of all 16 temporary flotation cylinders aboard Elf's Frigg field jacket, DP1. The failure during October 1974 launching operation caused the 6700 ton jacket to hit the bottom buckling two internal legs. Designer McDermott is particularly sensitive about discussing any possibility of error, but informed opinion claims the company may have let its Gulf of Mexico platform design experience, with much lighter structures, guide its choice for inadequate tanks[94]. From the information obtained from Ref. (95) the tanks were designed to withstand a working pressure of 100 psi (694 kN/m^2). From the collapsed sections of tank removed from the Frigg jacket it was observed that on tank after tank the outer shell crumpled between stiffeners to leave a battered steel concertina - indicating interframe collapse failure. With limited information available about the yield stress and degree of initial out-of-circularity, the interframe collapse pressures for varying values of C_o/R and σ_{rc}/σ_y are plotted in Fig. (30). The mean radius of the tank was 800 mm, which exceeded the maximum radius of tested cylinders of BS5500 rules. Hence it can be assumed that the initial out-of-circularity of the Frigg tanks could have a value of 0.005 R or even more. It is obvious from Fig. (3)) that with $C_o/R \geq 0.0040$, failure would occur. BS5500 is reliable at its permitted maximum $C_o/R = 0.0050$, compared with the present theory. The DnV rules (1977 edition) predict a higher value of 686.5 kN/m^2. The DnV rules (1974 edition) give a much higher value of 1035.0 kN/m^2. Since the tanks were designed in 1974 the finger points to DnV rules (1974 edition). Although DnV rules (1977 edition) are a much improved version of the 1974 edition, there are still some doubts. For example, from section C55, Fig. C9.7 of Ref. (1), 1977 edition, DnV maximum permissible C_o/R for Frigg buoyancy tanks is 0.0046. From Fig. (30), for $C_o/R = 0.0046$, the present theory predicts a pressure of about 600 kN/m^2 to 650 kN/m^2, whereas DnV predicts a pressure of 686.5 kN/m^2.

6.7/

6.7 KINRA'S ONE-FIFTH SCALE MODEL TEST[96]

The cylinder is orthogonally stiffened and subjected to uniform external pressure. The model failed due to shell buckling between the rings at a hydrostatic external pressure between 110 psi and 115 psi. The cylinder had 24 stringers of rectangular section of 0.116" by 1.40". The stringers are smeared into an equivalent thickness in order that comparison with the present theory is possible. Hence theoretical predictions should be judged with this in mind. An out-of-roundness of 0.21 inch was mentioned but no further detail measurement was given. With the above information and an assumed value of $\sigma_{rc} = 0.156\ \sigma_y$ the predicted collapse pressures are plotted in Fig. (31). An out-of-roundness of 0.21 inch gives a $C_o/R = 0.0073$ and collapse pressures from Fig. (31) are:

i) p_c = 75 psi for simple supported edges

ii) p_c = 90 psi for partially fixed edges

iii) p_c = 127.5 psi for clamped edges

The predicted collapse pressures are reasonable and sound since the experimental collapse pressures lie between the pressures predicted at simple supported edges and clamped edges. On the whole the results are in good agreement with the collapse pressure.

6.8 COMPARISON WITH MACHINED-MODEL EXPERIMENT FROM REF. (28)

The cylinder was machined and subjected to uniform external pressure. The experimental collapse pressure was 633 psi at a mode of 11 circumferential waves. The experiment was designed to fail by elastic buckling, hence the choice of material of high yield stress of 82500 psi. Comparison with the present theory for different boundary conditions is as shown in Fig. (32). With a buckling mode of n = 11 for the experimental model the simple supported condition is ruled out. An out-of-roundness of $C_o/R = 0.00035$ with clamped edges, the present theory predicts an exact buckling pressure of 633 psi. Such an out-of-roundness is possible to induce through misalignment of lathe shaft when machining. Even for perfect circular cylinder the buckling pressure of 655 psi for clamped edges is in very good agreement with the experimental/

experimental collapse pressure - within 3%. This comparison confirmed that clamped boundary condition is possible in machined cylinder, and secondly, the assumed displacement functions used in the analysis are correct.

6.9 COMPARISON WITH WELDED MODEL EXPERIMENT RESULTS FROM REF. (25)

Five welded cylinders with external ring stiffeners of T-frame were subjected to uniform external pressure. The models are T-2, T-3, T-6, T-2A and T-7A and their properties are listed in Table 5. As in most experiments, no measurement of residual stresses or geometrical imperfections was carried out. Therefore, some assumptions have to be made before comparison with the present theory is possible. A value of $\eta = 4$ is assumed for all models when calculating the compressive residual stresses, σ_{rc}. The predicted pressures are plotted in Figs. (33) (34) (35 (36) and (37). It is interesting to note at this point that material used had very high yield strength, the lowest being 84000 psi, more than twice the strength of the material normally used in offshore structures. As can be seen from the figures, the results on the whole are in good agreement for partially fixed edges and for value of $C_o/R \leq 0.0020$. The value of $C_o/R < 0.0020$ for geometrical imperfections is comparatively lower than those suggested in previous comparison. This can be explained by the fact that externally stiffened cylinders are seen to be significantly stronger than internally stiffened cylinders probably due mainly to the favourable direction of welding distortion associated with external stiffeners. This is also confirmed in Fig. (24) where externally stiffened cylinders are stronger than internally stiffened cylinders.

6.10 AXIAL COMPRESSION

Comparison with experiment under axial compression for interframe shell instability is not possible due to difficulty in obtaining results from ring-stiffened cylinders under axial compression. Most experiments used cylinders with longitudinal stringers. The smearing technique is not possible as in most cases the yield strength of the stringers and the yield strength of the shell plating are different[6, 60, 96]. Secondly, the increase in critical load due to stringers is considerably less than that obtained by uniform thickening of/

of the shell with the same amount of material[60]. Although some experiments for ring-stiffened cylinders under axial compression have been carried out at University College, London, the results are still not available[97]. Therefore, the comparison under axial compression will only be made with unstiffened cylinders and DnV Rules[1].

The stability of cylindrical shells under axial compression has been studied in the past both theoretically and experimentally by very many investigators. The experimental values were much lower than the classical theoretical values and the data had a large scatter band. Initial geometrical imperfections have come to be accepted as the main degrading factor[31]. This is absolutely true and is confirmed in Fig. (23). As can be seen at even a small value of $C_o/R = 0.0005$ a reduction factor of 0.53 is observed for $R/t = 200$. Needless to say the degree of initial geometrical imperfections sensitivity depends on the R/t and ℓ/R ratios of the cylinders. Data collected from 700 experimental results are plotted in Figs. (38), (39) and (40). The data are from 18 publications[98] where all experiments which had buckling stresses exceeding two thirds of the yield stress of the material were disregarded. The reduction factor α_o is a ratio of buckling stress/σ_{cr} where $\sigma_{cr} = 0.605\ Et/R$. All the tested cylinders satisfied the requirements:

i) The largest inward amplitude of initial geometrical imperfections does not exceed $0.04\sqrt{Rt}$.

ii) The effects of non-uniform distribution of the load at the boundaries are alleviated.

iii) The displacements in the plane of cross section are prevented along both edges of the shell.

iv) The length of the cylinder does not exceed $0.95\sqrt{R/t}$.

As shown in Figs. (38), (39) and (40) the present theory curve is based on a simple supported boundary condition, a ℓ/R ratio of one and $C_o = 0.010\sqrt{Rt}$ (a quarter of the maximum allowed). The present theory curves are/

are in close agreement with the experimental data, particularly Fig. (40). There are some scattered data between R/t of 100 and 300 in Fig. (38) lying below the present theory curve. This is because the tested cylinders for these data points were likely to have initial geometrical imperfections greater than the value assumed for the present theory. By assuming a value of $C_o = 0.02\sqrt{Rt}$ these data points can easily be accounted for. The comparison should be judged in mind that the experimental boundary conditions were unlikely to be simple supported, but perhaps near to it. Finally, this comparison proves that initial geometrical imperfections is the main degrading factor. Figs. (38) to (40) are for the length range $0.7 \leq \ell/R \leq 5.5$.

Fig. (41) shows, for various levels of yield stresses, the comparison with DnV Rules (1977 edition) for cylinders under axial compression. The present theory is based on a yield stress of 246 N/mm^2, simple supported boundary conditions and initial geometrical imperfection is based on DnV maximum permissible value taken from C55, Fig. C9.7 of Ref. (1) and reproduced here in Fig. (42). As shown in Fig. (41) the present theory (for $\sigma_y = 246$ N/mm^2) predicts lower values than that permitted by DnV Rules, particularly for R/t > 150. The difference cannot be due to boundary conditions as DnV Rules are based on simple supported boundary conditions. The main reason for the differences lie in the DnV maximum permissible value of initial geometrical imperfection. From Fig. (42), for a same R/t ratio, DnV Rules permit increasing values of C_o/R for increasing ℓ/R ratios. This is surely incorrect, as long cylinders are more sensitive to initial geometric imperfections than short cylinders. Secondly, DnV Rules for axial compression (C3.4.2.1, Ref. (1)) contain no ℓ/R term in reduction factor for $Z \geq 20$. As confirmed earlier, the degree of initial geometrical imperfection sensitivity depends on both R/t and ℓ/R ratios. The comparison shows that DnV Rules are generally less conservative and unreliable for certain range of R/t. The independence of the DnV Rules to ℓ/R is clearly shown by numerical values in Table 13. The elastic buckling stress of the cylindrical shell is calculated by means of classical formula for axial compression, then with modification factors for imperfections and reduction factor for plasticity. The modification factors are independent of the ℓ/R ratio.

Overall Instability/

Overall Instability

Table 6 shows the comparison between the results of Eq. (22a) and Eq. (22b) for various lengths of a cylinder. The comparison is just to demonstrate that the displacement pattern of Eq. (22b) gives slightly lower buckling pressures than Eq. (22a). At critical buckling pressures a difference of 5% is observed throughout.

6.11 COMPARISON WITH KENDRICK PART III

Table 7 shows the comparison between the results obtained from present theory and results from Kendrick Part III. The comparison is based on a numerical example of Ref. (80). Eq. (19b) represents simple supported boundary conditions at the rigid ends of the cylinder. Eq. (20b) and eq. (21b) represent partially fixed edges and clamped edges respectively. Eq. (19c) consists of the same buckling displacements as eq. (19b) but different pre-buckling displacements, that is $\frac{\partial u}{\partial x}$ = constant &, w = constant - uniform lateral and axial contraction prior to buckling. The out-of-plane bending, torsional and warping terms are omitted for the strain energy in the ring stiffeners for eq. (19c). This is done so as to simulate the condition as near as possible to Kendrick's assumptions. It can be seen from Table 7 that the results of eq. (19c) are in good agreement with Kendrick's solution within a few per cent. The slight difference is due to certain different terms used in bending strain energy of the shell. Comparison between eq. (19b), eq. (20b) and eq. (21b) at critical buckling pressures suggests the effect of boundary conditions at rigid end is insignificant for value of L/R < 4.50. For design purposes simple supported condition is sufficient.

The assumption that the generators remain straight (or uniform) is an equivalent of a dead load situation, because the pressure is always acting perpendicular to the generators. Eq. (19c) has pre-buckling displacements that assume such condition. Hence eq. (19b) is more correct than eq. (19c). Hence eq. (19b) and eq. (22b) are of interest here as to which one would predict a lower critical buckling pressure for the cylinder of Table 7. Eq. (22b) gives lower critical buckling pressures than eq. (19b) for $L/R \leq 6$. At $L/R \geq 7.5$ the cylinder buckles in the pattern of eq. (19b). It is interesting at this stage to compare the critical buckling pressures (p_n) predicted by the present theory and that of BS5500 design rules. BS5500 rules for an overall critical buckling/

buckling pressure use the Byrant's formula[99], but introduced an effective length, instead of full length of interframe spacing. The pressure to cause yielding in the ring frame (p_{fy}) calculated by BS5500 is as outlined in Appendix B. For $L/R \leq 6.0$, BS5500 predicts much higher values of p_n than present theory and vice-versa for $L/R \geq 7.5$. This is because Byrant's formula is an approximation of eq. (19b) and the cylinder buckles in the pattern of eq. (22b) for $L/R \leq 6.0$. The p_{fy} of the present theory and BS5500 are based on $C_o/R = 0.0050$ for the ring frame. As p_{fy} depends on p_n therefore it is obvious to see the difference in p_{fy} of BS5500 and present theory for $L/R \leq 6.0$. The small difference between p_n of BS5500 and p_n of present theory for $L/R \geq 7.50$ is due to the fact that Byrant's formula is based on an overall instability of one ring frame, whereas eq. (19b) represents an overall instability of the whole cylinder.

Another numerical example, with the same dimensions as the cylinder in Table 7, except that the interframe spacing is increased to 50 inches, is in Table 8. The aim of this example is to prove that for higher ℓ/R ratio (wider framing spacing) the overall instability of the cylinder follows the pattern of eq. (22b) for greater L/R range. For all values of p_n determined by eq. (22b) the resulted p_{fy} values are lower than that allowed by BS5500. This again proves the close agreement between eq. (19b) and BS5500.

6.12 COMPARISON BETWEEN PRESENT THEORY AND EXPERIMENTAL RESULTS OF REF. (100)

Table 9 shows the comparison between present theory and Creswell's experiment on a machined aluminium cylinder under external pressure. The use of aluminium alloy model is to ensure elastic buckling. The experimental collapse pressure was recorded at 450 psi at a circumferential wave of two. Unfortunately no measurement of initial geometrical imperfections was carried out, and the most likely out-of-circularity mode is n = 2 resulting from ovality of lathe shafts. Therefore, comparison has to be based on assumed values of initial geometrical imperfections. The shell plating is very thin - only 0.030 inch (0.762 mm). Hence any initial out-of-circularity would be more likely to be in the shell plating than in the ring frame. The buckling pressures from eq. (22b) and eq. (19b) for various values of C_{o2} are as shown in Table 9. For a cylinder of such thinness a value of $C_{oz} = 0.20$ mm is possible and eq. (19b) gives a corresponding value/

value of 447.8 psi which is in close agreement with experimental collapse pressure of 450 psi. The comparison should be judged that no exact theoretical comparison is possible without some knowledge about the degree of initial out-of-circularity. Secondly, the very small frame width made strain-gauging of frames impossible and this has inevitably excluded direct observation of the maximum stresses occurring in the frames.

6.13 COMPARISON BETWEEN PRESENT THEORY AND EXPERIMENTAL RESULTS OF REF. (96)

The overall instability of orthogonally stiffened welded steel cylinders under uniform external pressure was carried out by Kinra[96]. An experimental collapse pressure of 270 psi was recorded and an initial out-of-circularity for the ring frame was mentioned as 0.234 inch. Comparison is only possible by smearing all the stringers, as the present theory only considers ring-stiffened cylinders. The results calculated from eq. (19b) and eq. (22b) are as shown in Table 10. A value of $\sigma_{rc} = 0.197\ \sigma_y$ for shell welding residual stresses was assumed. The results from both equations at the same C_{01}/R of Ref. (96) are in close agreement with the experimental collapse pressure. Not surprisingly, BS5500 predicts the same mode of failure as eq. (19b). Unfortunately no strain measurement in the ring frame was recorded and this makes it impossible to confirm whether failure was due to premature yielding in the ring frame or overall instability, as predicted by eq. (22b).

This comparison shows that buckling failure of an orthogonally stiffened cylinder under external hydrostatic pressure can be treated conservatively as that of a ring stiffened cylinder by smearing the stringers.

6.14 INFLUENCE OF OUT-OF-CIRCULARITY ON COLLAPSE STRENGTH

Table 11A shows the comparison between present theory and Smith[52] results obtained by finite element method for externally pressurised ring-stiffened cylinders. The results of Ref. (52) are in close agreement with that of eq. (19b) within a few per cent. Eq. (22b) predicts much lower values. One must not be too hasty to accept results obtained by finite element method as more reliable and accurate than other simple mathematical techniques. Whatever the analytical tool, there are always assumptions made in the analysis. Smith's work assumed that an overall collapse analysis of a stiffened cylinder/

cylinder can be represented by simply the overall collapse analysis of one ring frame with attached strip of shell plating. Although it is claimed that this assumption is accurate enough for long cylinders, the difficulty is how and where would one draw a line between short and long cylinders. As to whether a cylinder would behave as a short or long cylinder depends not only on length but radius, interframe spacing, shell thickness and frame area of the cylinder. A numerical example in Table 11B proves the point. This is a difficult situation as there is no attempt made so far to define the term "long cylinder" in a proper engineering term.

The main aim of this comparison is to show how simple mathematical modes can predict results as close to that of finite element method, not mentioning the higher computer time required for the latter.

6.15 COMPARISON BETWEEN PRESENT THEORY AND FINITE ELEMENT METHOD OF REF. (91)

The comparison is based on numerical example of Ref. (91) for an overall instability of a ring stiffened cylinder under external pressure. The cylinder was modelled by seven sub-structures with a total of 16 triangle elements and 8 stiffener elements in each sub-structure. The stiffener elements use cubic interpolation functions for the displacements. Each sub-structure consisted of one stiffener and its contributing portion of the shell. The end of the cylinder was simply supported with no longitudinal motion allowed. The analysis predicted a buckling pressure of 1525 psi. The analysis allows the loading to change direction as the shell deforms and buckles - a live loading condition. Table 12 shows the results predicted by the present theory. The critical buckling pressures by eq. (19c) and eq. (19b) are 1550.7 psi and 1466.1 psi respectively. Eq. (19b) assumes a non-uniform lateral pre-buckling displacement, whereas eq. (19c) assumes a uniform lateral pre-buckling displacement. Eq. (19b) is close to a live loading condition and its result is within 3.8% of that predicted by finite element method. It is very close indeed, as finite element method depends very much on the mesh size for its accuracy.

CHAPTER 7 CONCLUSIONS AND FUTURE RESEARCH

CONCLUSIONS

Two computer programs, one for interframe collapse and the other for overall collapse as influenced by initial imperfections, have been developed and the results compared with experiments and with present design codes.

Equations accounting for non-uniform and uniform lateral pre-buckling displacements are presented in this thesis. Factors which have a significant effect on the behaviour of ring stiffened cylinders, such as initial geometrical shape imperfections and residual stresses of the shell due to welding and cold-bending, are included in the present theory. The energy expressions used here are in close agreement with the differential equations obtained by Von Mises for interframe buckling under uniform external pressure. This is particularly true when uniform lateral pre-buckling displacements are assumed. However, for non-uniform lateral pre-buckling displacements, the present theory predicts lower buckling pressure than the Von Mises' equations. This is due to the fact that the non-uniform lateral pre-buckling displacements vary non-linearly to accommodate the type of pressure loading which is often referred to as live loading, and changes direction as the structure deforms. Such effect is not accounted for in Von Mises differential equations. The effect of live loading as opposed to dead loading depends on the R/t and ℓ/R ratios and in some cases a difference of more than 10% is obtained.

An examination of the effects of initial geometrical shape imperfections confirms that they are most serious for axial compressive load. This is followed by external pressure and the less sensitive radial (lateral) pressure loading. This is due to the absence of the axial pressure component reducing the sensitivity of the radial pressure loading.

The/

The influence of welding residual stresses of the shell on interframe collapse pressure under uniform external pressure was examined. This confirms that the compressive welding residual stresses of the shell is detrimental to the ductile strength of cylindrical shells. It is shown that as an approximation an increase in the compressive welding residual stresses results in a similar percentage loss in strength. At high ratios of R/t the percentage loss of strength can be very high. Although the effect of cold-bending residual stresses in the shell does not appear to have any significant effect on the collapse pressure of the shell, further experimental verification is necessary.

Comparison with experimental results for interframe collapse and overall collapse under uniform external pressure is good. Interframe collapse by design code BS5500 is adequate for $R/t < 250$. For greater values of R/t further experimental verification is necessary. BS5500 is preferred to the DnV Rules for interframe collapse under external pressure. For overall instability, BS5500 is in good agreement with eq. (19b) of the present theory. Results obtained by the present theory for overall instability are in close agreement with results obtained by finite element methods. In some examples overall collapse pressures from BS5500 are thought to be inadequate when compared with those determined by eq. (22b). Therefore it is advisable to use both equations for an overall collapse prediction. The limited numerical comparisons show that DnV Rules for axial compression for unstiffened cylinders appear to be incompatible with their specified tolerances.

Finally, the buckling failure of an orthogonally stiffened cylinder under external hydrostatic pressure can be treated as conservatively as that of a ring stiffened cylinder by smearing the stringers. This view is supported by the comparison made with experimental results reported by Kinra[96].

FUTURE RESEARCH

There is no theory available which can accurately predict the elasto-plastic behaviour of stiffened cylinders for overall collapse with shape imperfections and residual stresses accounted for. The influence of stiffener tilting on overall collapse strength has received practically no attention at all. The problem including these effects is of very great complexity and it is unlikely that theory will be able to tackle such problems, except in a very crude manner for a long time yet.

Future research should be directed towards cheaper and faster solution techniques for non-linear equations for special problems, such as stiffened cylinders under combined loading. Non-linear finite element or finite difference equations should be solved more cheaply than at present[101]. We are concerned with the behaviour of inelastic materials, where there is a non-linear system to solve at each loading step. This applies both to the quasi-static or dynamic equations of plasticity, and to the problems of large displacement. A general approach to the solution of non-linear systems or the minimisation of non-quadratic functionals, which applies to both finite difference and finite element models, has been successfully used in the field of numerical methods[102, 103, 104]. Other numerical tools that are well adapted to finite difference method are clearly presented in references (105, 106 and 107).

REFERENCES

Abbreviations used:

NCRE Naval Construction Research Establishment, now Admiralty Marine Technology Establishment, UK.

DTMB David Taylor Model Basin, now Naval Ship Research and Development Centre, U.S.A.

ASME American Society of Mechanical Engineers.

NASA National Aeronautics and Space Administration.

NACA National Advisory Committee for Aeronautics.

AIAA American Institute of Aeronautics & Astronauts.

1. DET NORSKE VERITAS: Rules for the Design, Construction and Inspection of Fixed Offshore Structures, 1977 edition and 1974 edition.

2. BAKER, CAPPELI, KOVALEVSKY, RISH, VENETTE: Shell Analysis Manual, NASA CR-912, 1966.

3. RAPTIS, C.: Buckling design for offshore steel structures, M.Sc. thesis, Dept. of Naval Architecture & Ocean Engineering, University of Glasgow, 1978.

4. FAULKNER, D.: Buckling research needs for efficient and safe design of offshore steel structures, Report No. NAOE S76-03, Dept. of Naval Architecture & Ocean Engineering, University of Glasgow, 1976.

5. FAULKNER, D.: Some thoughts on the nature of hazards affecting offshore structures in deeper water, Report No. NAOE S76-04, Dept. of Naval Architecture & Ocean Engineering, University of Glasgow, 1976.

6. WALKER, A.C. and DAVIES, P.: The collapse of stiffened cylinders, Intl. Conf. of Steel Plated Structures, Imperial College, London, paper 33, 1976.

7. British Standards Institute: BS5500, Section 3, 1976.

8./

8. API (American Petroleum Institute): Recommended practice for planning, designing and constructing fixed offshore platforms, API 1975.

9. ISO/TC11: Code for the boiler and pressure vessels, April 1971.

10. KENDRICK, S.: The buckling under external pressure of circular cylindrical shells with equally spaced circular ring frames - Part IV, NCRE Report No. 372, 1957.

11. BLUMENBERG, W.F. and REYNOLDS, T.E.: Elastic general instability of ring-stiffened cylinders with intermediate heavy frames under external hydrostatic pressure, DMTB Report No. 1588, Dec. 1961.

12. BLUMENBERG, W.F.: The effect of intermediate heavy frames on the elastic general instability strength of ring stiffened cylinders under external hydrostatic pressure, DTMB Report No. 1844, Feb. 1965.

13. CRESWELL, D.: Elastic overall instability of ring-stiffened cylindrical shells, NCRE Report No. R643A, Nov. 1976.

14. KENDRICK, S.: The local instability of ring frames, NCRE Report No. R255.

15. WINDENBURG, D.F.: Elastic stability of tee stiffeners, DRMB Report No. 457.

16. KENNARD, E.H.: Tripping of T-shaped stiffening rings on cylinders under external pressure, DTMB Report No. 1079, Nov. 1959.

17. VAUGHAN, H.: The stress distribution in ring frames with initial tilt, NCRE Report No. R476, July 1963.

18. BRYAN, GH: Application of the energy test to the collapse of a long thin pipe under external pressure, Cambridge Philosophical Society Proceedings, Vol. 6, 1888, pp. 287-292.

19. SOUTHWELL, R.V.: On the general theory of elastic stability, Philosophical Transactions of the Royal Society, Vol. 213, Series A, 1913, pp. 187-244.

20. VON MISES, R.: Der Kritische Aussendruck Zylindrischer Rohre, Zeit V.D.1 Vol. 58, 1914, pp. 750-5.

21. VON MISES, R.: Der Kritische Aussendruck Fur allseits belastete Zylindrische Rohre, Fest zum 70, Geburstag Von Prof. Dr. A. Stodola, Zurich, 1929, pp. 418-30. (Also DTMB Translation Report No. 366, 1936).

22./

22. WINDENBURG, D.F. and TRILLING, C.: Collapse by instability of thin cylindrical shells under external pressure, ASME Transactions, Vol. 56, No. 11, pp 819-825, November 1934.

23. STURM, R.G.: A study of the collapsing pressure of thin-walled cylinders, University of Illinois, Bulletin Series no. 329, pp. 1-77, 1941.

24. NASH, W.A.: Buckling of multi-bay ring-reinforced cylindrical shells subject to hydrostatic pressure, Jnl. of Applied Mechanics, Vol. 20, No. 4, pp 469-474, 1953.

25. REYNOLDS, T.E.: Inelastic Lobar buckling of cylindrical shells under external hydrostatic pressure, DTMB Report No. 1392, August 1960.

26. VON SANDEN, K. and GUNTHER, K.: The strength of cylindrical shells, stiffened by frames and bulkheads, under uniform external pressure on all sides, DTMB Translation Report No. 38, March 1952.

27. ROSS, C.T.F.: The instability of ring-stiffened circular cylindrical shells under uniform external pressure, Trans Royal Institute of Naval Architects, pp 375, 1965.

28. REYNOLDS, T.E.: Elastic Lobar buckling of ring-supported cylindrical shells under hydrostatic pressure, DTMB Report No. 1614, September 1962.

29. KOITER, W.T.: On the stability of elastic equilibrium, Ph.D. thesis (1945), University of Delft.

30. KOITER, W.T.: The effect of axi-symmetric imperfections on the buckling of cylindrical shells under axial compression.

31. ARBOCZ and BABCOCK: The effect of general imperfection on the buckling of cylindrical shells, TRANS. ASME, March 1967.

32. DONNELL, L.H. and WAN, C.C.: Effect of imperfections on buckling of thin cylinders and columns under axial compression, Jnl. of Applied Mech., ASME, March 1950.

33. DONNELL, C.H. and WAN, C.C.: Effect of imperfections on buckling of thin cylinders under external pressure, Jnl. of Applied Mech., ASME, December 1956.

34. KENDRICK, S.: Shape imperfections in cylinders and spheres - their importance in design and methods of measurement, Jnl. of Strain Analysis, Vol. 12, No. 2, pp 117-122, 1977.

35. DONNELL, L.H.: Effect of imperfections on buckling of thin cylinders with fixed edges under external pressure, Proc. 3rd US Nat. Congress of .pplied Mech., ASME, 1958.

36./

36. BUDIANSKY, B. and AMAZIGO, J.C.: Initial post-buckling behaviour of cylindrical shells under external pressure, Jnl. Math. Phys., vol. 47, pp 223-235, 1968.

37. GALLETLY, G.D. and BART, R.: The effect of boundary conditions and initial out-of-roundness on the strength of thin-walled cylinders subject to external hydrostatic pressure, Jnl. of Applied Mech., vol. 78, pp 351-358, 1956.

38. AMAZIGO, J.C.: Asymptotic analysis of the buckling of externally pressurised cylinders with random imperfections, Quarterly Applied Math., vol. 31, pp 429-442, 1974.

39. TOKUGAWA, T.: Model experiments on the elastic stability of closed and cross-stiffened circular cylinders under uniform external pressure, Proceedings of the World Engineering Congress, Tokyo, bol. 29, paper No. 651, pp 249-279, 1929.

40. SALERNO, V.L. and LEVINE, B.: Buckling of circular cylindrical shells with evenly spaced, equal strength circular ring frames, Part I, Polytechnic Institute of Brooklyn, Report No. 167, April 1950.

41. SALERNO, V.L. and LEVINE, B.: Buckling of circular cylindrical shells with evenly spaced, equal strength circular ring frames, Part II, Polytechnic Institute of Brooklyn, Report No. 169, June 1950.

42. SALERNO, V.L. and LEVINE, B.: General instability of reinforced shells under hydrostatic pressure, Polytechnic Institute of Brooklyn, Report No. 189, September 1951.

43. KENDRICK, S.: The buckling under external pressure of circular cylindrical shells with evenly spaced, equal strength circular ring frames, Part I, NCRE Report No. R211, February 1953.

44. KENDRICK, S.: The buckling under external pressure of circular cylindrical shells with evenly spaced, equal strength circular ring frames, Part II, NCRE Report No. R263, September 1953.

45. KENDRICK, S.: The buckling under external pressure of circular cylindrical shells with evenly spaced, equal strength circular ring frames, Part III, NCRE Report No. R244, September 1953.

46. NASH, W.A.: General instability of ring-reinforced shells subject to hydrostatic pressure, Proceedings of the Second US National Congress of Applied Mechanics, pp 359-368, June 1954.

47. KAMINSKY, E.L.: General instability of ring-stiffened cylinders with clamped edges under external pressure by Kendrick's method, DTMB Report No. 855, July 1954.

48. REYNOLDS, T.D. and BLUMENBERG, W.F.: General instability of ring-stiffened cylindrical shells subject to external hydrostatic pressure, DTMB Report No. 1324, June 1959.

49./

49. ROXBURGH, P.M.: The deformation of nearly circular stiffened cylinders, NCRE Report No. R472, September 1962.

50. GLAUM, L.W. and BELYTSCHKO, T.L. and MASHUR, E.F.: Buckling of structures with finite pre-buckling deformations - A perturbation, finite lement analysis, Jnl. of Solids Structures, Vol. 11, pp. 1023-1033, 1975.

51. CRESWELL, D.: Elastic overall instability of ring-stiffened cylindrical shells, experimental determination of the elastic collapse pressures of some miniature aluminium stiffened cylinders, NCRE Report R78643B, June 1978.

52. SMITH, C.S. and KIRKWOOD, W.: Influence of initial deformations and residual stresses on inelastic flexural buckling of stiffened plates and shells, Paper 35, Steel Plated Structures Conference, London, July 1976.

53. KENDRICK, S.: The elasto-plastic collapse of ring stiffened cylinders, NCRE Report No. R653, May 1977.

54. BUSHNELL, D., ALMROTH, B. and BROGAN, F.: Finite difference energy method for nonlinear shell analysis, Computers and Structures, bol. 1, pp 361-387, 1974.

55. BUSHNELL, D.: Buckling of elastic-plastic shells of revolution with discrete elastic-plastic ring stiffeners, Jnl. of Solids Structures, vol. 12, pp 51-66, 1976.

56. BUSHNELL, D.: Stress, stability and vibration of complex branched shells of revolution, Computers and Structures, vol. 4, pp 399-435, 1974.

57. BUSHNELL, D.: Analysis of buckling and vibration of ring-stiffened, segmented shells of revolution, Jnl. of Solids Structures, vol. 6, pp 157-181, 1970.

58. BARUCH, M. and SINGER, J.: Effect of eccentricity of stiffeners on the general instability of stiffened cylinderical shells under hydrostatic pressure, Jnl. of Mechanical Engineering Science, vol. 5, no. 1, pp 23-27, 1963.

59. SINGER, J., BARUCH, M. and HARARI, O.: Inversion of the eccentricity effect in stiffened cylindrical shells buckling under external pressure, Jnl. of Mechanical Engineering Science, Vol. 8, pp 363-373, 1966.

60. SINGER, J., ARBOCZ, J. and BABCOCK, C.: Buckling of imperfect stiffened cylindrical shells under axial compression, AIAA Jnl., vol. 9, no. 1 pp 68-75, October 1971.

61. SINGER, J.: Buckling of integrally stiffened cylindrical shells, A review of experiment and theory, Delft University Press, Rotterdam, 1972.

62./

62. SHEINMAN, I. and SIMITSES, G.: Buckling analysis of geometrically imperfect stiffened cylinders under axial compression, AIAA Jnl., vol. 15, no. 3, 1977.

63. SHEINMAN, I. and SIMITSES, G.: The effect of initial imperfections on optimal stiffened cylinders under axial compression, AFOSR-TR-77-0639, School of Engineering Science & Mechanics, Georgia Institute of Technology, Atlanta, Georgia, February 1977.

64. SIMITSES, G., SHEINMAN, I. and GIRI, J.: Nonlinear stability analysis of pressure-loaded imperfect stiffened cylinders, Jnl. of Ship Research, vol. 23, No. 2, pp 123-126, June 1979.

65. BABCOCK, G.: Experiments in shell buckling, Thin-Shell Structures, Chp. 14, edited by Y.C. Fung and E.E. Sachler.

66. ARBOCZ, J.: The effect of initial imperfections on shell stability, Thin-Shell Structures, Chp. 9, edited by Y.C. Fung, and E.E. Sachler.

67. KENDRICK, S.: The deformation under external pressure of nearly circular cylindrical shells with evenly spaced equal strength nearly circular ring frames, NCRE Report No. R259, October 1953.

68. KENDRICK, S.: The buckling under external presure of ring-stiffened circular cylinders, TRANS RINA, pp 139, 1965.

69. VLASOV, V.S.: Basic differential equations in general theory of elastic shells, NACA Technical Memo 1241, February 1951.

70. ARBOCZ, J. and WILLIAMS, J.G.: Imperfection survey on a 10 ft. diameter shell structure, AIAA Jnl., vol. 15, no. 7, pp 949-956, July 1977.

71. COPPA, A.P.: Measurement of initial imperfections on cylindrical shells, AIAA Jnl., vol. 4, No. 1, pp 172-175, January 1966.

72. SINGER, J., ABRAMOVICH, H. and YAFFE, R.: Initial imperfection measurements of integrally stringer-stiffened cylindrical shells, Report TAE No. 330, Dept. of Aeronautical Engineering, Technion Israel Institute of TEchnology, 1979.

73. WHITE, J.D. and DWIGHT, J.B.: Residual stresses and geometrical imperfections in stiffened tubulars, University of Cambridge, Department of Engineering, Report TR.64, 1977.

74. WHITE, J.D. and DWIGHT, J.B.: Residual stresses in large stiffened tubulars, Technical Report No. CUED/C-STRUCT/TR.67, Dept. of Engineering, University of Cambridge, 1978.

75. OKERBLOM, N.O.: The calculations of deformations of welded metal structures, Mashgiz, Moscow, Leningrad, 1955.

76. FAULKNER, D.: Effects of residual stresses on the ductile strength of plane welded grillages and of ring stiffened cylinders, Jnl. of Strain Analysis, Vol. 12, No. 2, 1977.

77./

77. SMITH, C.S.: Compressive strength of welded steel ship grillages, Trans Royal Institute of Naval Architects, 117, 325-359, 1975.

78. FAULKNER, D.: Residual strains measured during the welding frame 59 in Valiant, NCRE Technical Memo TGO/M2, 1962.

79. PASCOE, K.J.: Strength of cold-formed cylindrical steel plates, Jnl. of Strain Analysis, Vol. 6, No. 3, 1971.

80. KENDRICK, S.B.: Externally pressurised vessels in S.S. Gill (ed.), The stress analysis of pressure vessels and pressure vessel components, Pergamon Press, 1970.

81. FRAZER, R.A., DUNCAN, W.J. and COLLAR, A.R.: Elementary matrices, Cambridge University Press, 1947.

82. PAPDIMITRIOU, A.: M.Sc. Thesis (in preparation), Department of Naval Architecture & Ocean Engineering, University of Glasgow.

83. ROBINSON, M.: A comparison of yield surfaces for thin shells, Intl. J.Mech.Sc., Vol. 13, pp 345-354, 1971.

84. ILYUSHIN, A.A.: Plasticite, Editions Eyrolles, Paris, 1965.

85. CRISFIELD, M.A.: Ianov's yield criterion for thin plates and shells using finite elements, TRRL Lab. Report 919, Bridge Design Division, Structures Dept., Transport & Road Research Laboratory.

86. CRISFIELD, M.A.: Iterative solution procedures for linear and non-linear structural analysis, TRRL Lab. Report 900, Transport & Road Research Laboratory, Dept. of Transport.

87. GERARD, G. and WILDHORN, S.: A study of Poisson's ratio in the yield region, NACA Technical Note 2561, June 1952.

88. WILSON, L.B.: The deformation under external pressure of a circular cylindrical shell supported by equally spaced circular ring frames, NCRE Reports Nos. R337A, R337B, R337C, December, 1956.

89. KENDRICK, S.: The deformation under external pressure of nearly circular cylindrical shells with evenly spaced equal strength nearly circular ring frames, NCRE Report No. R259, October 1953.

90. TIMOSHENKO, S.P. and GERE, J.M.: Theory of elastic stability, 2nd Edition, p. 496, McGraw-Hill.

91. JONES, R.F., GOSTELLO, M.G. and REYNOLDS, T.E.: Buckling of pressure loaded rings and shells by the finite element method, Computers & Structures, Vol. 7, pp 267-274, 1977.

92./

92. KENDRICK, S.B.: Collapse of stiffened cylinders under external pressure, Conference on Vessels under Buckling Conditions, I.Mech.E., Dec. 1972.

93. KENDRICK, S.B.: Structural design of submarine pressure vessels, NCRE Report No. R483, March 1964.

94. Offshore Engineer, January 1975.

95. Offshore Engineer, May 1975.

96. KINRA, R.K.: Hydrostatic and axial collapse tests of stiffened cylinders, Offshore Technology Conference, Houston, Texas, Paper 2685, May 1976.

97. DOWLING, P.J. and HARDING, J.E.: Strength of steel jacket leg components, Offshore Technology Conference, Houston, Texas, Paper 3428, May 1979.

98. SAAL, H.: Buckling of circular cylindrical shells under combined axial compression and internal pressure, Conference on Stability of Steel Structures, Liege, April 1977.

99. BRYANT, A.R.: Hydrostatic pressure buckling of a ring-stiffened tube, Report No. NCRE/R306, October 1954.

100. CRESSWELL, D.J.: Elastic overall instability of ring-stiffened cylindrical shells - Experimental determination of the elastic collapse pressures of some miniature aluminium stiffened cylinders, Admiralty Marine Technology Establishment, Report AMTE(S)R78643B.

101. BATHE, K.J.: An assessment of current finite element analysis of non-linear problems in numerical solution of partial differential equations III (Ed. B. Hubbard), Academic Press, New York, 1976.

102. IRONS, B. and ELSAWAF, A.: The conjugate Newton algorithm for solving finite element equations, in Formulations and Computational Algorithms in Finite Element Analysis (Ed. Bathe, Oden and Wunderlich), MIT Press, Cambridge, 1977.

103. RHEINBOLDT, W.C.: Methods for solving systems of non-linear equations, SIAM Conference 14, Philadelphia, 1974.

104. POWELL, M.J.D.: A fast algorithm for non-linearly constrained optimsation calculations, Lecture Notes in Mathematics Vol. 630, Springer-Verlag, Berlin, 1978.

105. KIZNER, W.: A numerical method for finding solutions of non-linear equations, Jnl Soc. of Industrial Applied Mathematics, Vol. 12, No. 2, June 1964.

106. STONE, H.L.: Iterative solution of implicit approximation of multi-dimensional partial differential equations, SIAM Jnl Numerical Analysis, Vol. 5, No. 3, September 1968.

107. ORTEGA, J.M. and ROCKOFF, M.L.: Non-linear difference equations and Gauss-Seidel type iterative methods, Jnl. SIAM Analysis, Vol. 3, No. 3, 1966.

NOMENCLATURE

A_1	axial buckling displacement amplitude
A_f	area of ring frame section
[a]	stiffness matrix of the cylinder
B_1 , B_2	circumferential buckling displacement amplitudes
[b]	load matrix of the cylinder
C_1 , C_2	radial buckling displacement amplitudes
C_o,C_{o1},C_{o2}	initial out-of-circularity amplitude
F_r	torsional constant of the ring frame section
[c]	column matrix due to initial shape imperfections
d	depth of the web of the ring frame
e	distance of the centroid of the frame section from the shell mid-surface; positive for internal frame and negative for external frame
E	Young's modulus of elasticity
E_s	secant modulus
f	width of the flange of the frame
G	shear modulus of elasticity
I_{xo}	moment of inertia of frame section about the axis parallel to the axis of the cylinder which passes through the C.G. of the section (only)
I_{zo}	moment of inertia of frame section about the vertical axis of the frame which passes through the C.G. of the frame section (only)
k	$= t^2/(12R^2)$, shell curvature term
L	distance between rigid and bulkheads
ℓ	distance between ring frames or length of unstiffened cylinder
m	number of buckled longitudinal half-waves
n	number of buckled circumferential waves

NOMENCLATURE (Cont'd)

N	number of ring frames between bulkheads
p_1	radial pressure component of the external pressure
p_2	axial pressure component of the external pressure
p	$= p_1 + p_2$ = external pressure
p_c	interframe collapse pressure
p_{c5}	pressure to cause yielding in the shell midway between stiffeners
p_m	elastic interframe buckling pressure by Von Mises equation
p_n	elastic overall buckling pressure of a perfect cylinder
p_{Fy}	pressure to cause yielding in the ring frame
$[r]$	stiffness matrix of cylinder at pre-buckled state
R	mean radius of the cylinder
$[s]$	load matrix of cylinder at pre-buckled state
S_T	total potential energy of a system
S_s	extensional strain energy of the shell
S_b	bending strain energy of the shell
S_f	strain energy of the ring frames
t	shell thickness
t_f	thickness of the flange of the frame
t_w	thickness of the web of the ring frame
u, u_1, u_2	axial displacements at pre-buckled state
μ	Poison's ratio
μ_e	Poison's ratio in the elastic limit
U	axial displacement at buckled state
v	circumferential displacement at pre-buckled state
V	circumferential displacement at buckled state
w, w_1, w_2	radial displacements at pre-buckled state
W	radial displacement at buckled state

NOMENCLATURE (Cont'd)

W_d	work done by the external loadings
W_o	radial displacement initial shape imperfections
[x]	displacement matrix at pre-buckled state
[X]	displacement matrix at buckled state
Z	$= \ell^2\sqrt{1-\mu^2}/Rt$
ϕ_1	$= p_1R(1-\mu^2)/Et$
ϕ_2	$= p_2R(1-\mu^2)/Et$
α	$= E_s/E$ for shell
α_f	$= E_s/E$ for ring stiffener
K_x	axial curvature strain
K_θ	circumferential curvature strain
$K_{x\theta}$	twisting strain
ε_θ	extensional strain in circumferential direction (hoop)
ε_x	extensional strain in axial direction
$\varepsilon_{x\theta}$	shear strain
$\sigma_\theta, \sigma_x, \sigma_{x\theta}$	their respective stresses
σ_y	yield stress of shell plating
σ_{YF}	yield stress of ring frame
σ_b	circumferential bending stress in the flange of a ring frame
σ_{FC}	circumferential compressive stress in the flange of a ring frame
σ_F	total circumferential stress in the flange of a ring frame
σ_{rc}	compressive welding residual stresses of the shell plating
τ	warping constant of the ring frame section

NOMENCLATURE (Cont'd)

λ_1 = $\pi R/L$

λ_2 = $\pi R/\ell$

λ_3 = $m\lambda_2$

ηt half width of the tension block of welding residual stresses distribution

APPENDIX A

RESIDUAL STRESSES OF SHELL PLATING DUE TO COLD BENDING

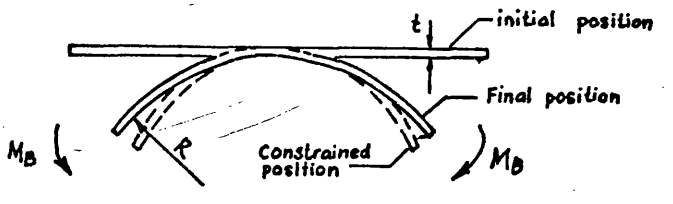

FIG.I —Ring Forming Procedure

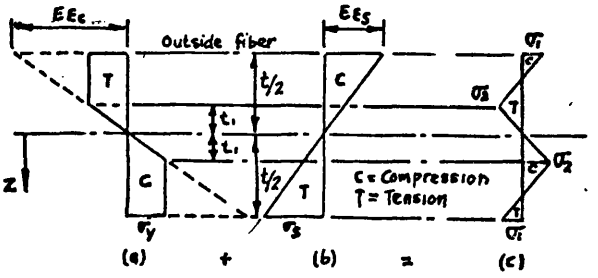

FIG. II —Ring Residual Stresses: (a) Constrained; (b) Springback; (c) Final

Let R be the radius of curvature into which the ring frame is to be formed, R_1 the radius of curvature to produce the elastic-plastic moments required, and R_2 the radius of curvature under the action of elastic springback forces.

M_s = springback moment per unit length

σ_b = bending stresses (hoop)

M_B = applied moment per unit length

By equating the curvatures it follows that $\frac{1}{R} = \frac{1}{R_1} + \frac{1}{R_2}$ ..... (i)

and

static equilibrium equations are:

$$\int_A \sigma_b \, dA = o \qquad \text{..... (ii)}$$

$$\int_A \sigma_b \, z \, dA = M_B \qquad \text{..... (iii)}$$

$$\therefore \quad M_B = 2\sigma_y (t/2 - t_1)(t_1/2 + t/4) + 2\sigma_y t_1^2/3 = \sigma_y (t^2/4 - t_1^2/3)$$

also:

$$t_1 = \sigma_y R_1 / E$$

and $M_s = -M_B = EI/R_2$ where $I = t^3/12$

$$\therefore \quad R_2 = -EI/M_B$$

Substituting for R_2 in (i), we get

$$\frac{1}{R} = \frac{1}{R_1} = \frac{12\sigma_y}{Et^3} \left(t^2/4 - \left(\frac{\sigma_y R_1}{E\sqrt{3}}\right)^2\right) \quad \ldots\ldots\ldots\ldots \text{(iv)}$$

In eq. (iv), R_1, σ_y, E and t are known and therefore R_1 can be easily solved by numerical iteration. Knowing R_1, M_s and M_B can then be calculated.

If σ_s is the springback stress, then $\sigma_s = \frac{M_s z}{I}$

$$\therefore \quad \sigma_S = -\frac{12\sigma_y}{t^3} \left(t^2/4 - \left(\frac{\sigma_y R_1}{E\sqrt{3}}\right)^2\right) \frac{t}{2} \quad \ldots\ldots\ldots\ldots \text{(v)}$$

$$\therefore \quad \sigma_1 = \sigma_y + \sigma_s \quad \ldots\ldots\ldots\ldots \text{(vi)}$$

$$\text{and} \quad \sigma_2 = \sigma_y + t_1 \frac{M_s}{I} \quad \ldots\ldots\ldots\ldots \text{(vii)}$$

Numerical Example:

Given: $R = 800$ mm, $t = 6$ mm, $\sigma_y = 258$ N/mm², $E/\sigma_y = 800$

substituting in eq. (iv)

$$\frac{1}{R} = \frac{1}{R_1} - 6.944 \times 10^{-5} \left(9 - \left(\frac{R_1}{1385.6}\right)^2\right) \quad \ldots\ldots\ldots\ldots \text{(viii)}$$

Solve R_1 by trial-and-error procedure (this can be easily programmed by a simple iterative procedure).

Try/

Try $R_1 = 530$ mm,

Right hand side of eq. (viii) $= \frac{1}{530} - 0.0006148 = 0.00127$

$\therefore \quad R_{cal.} = 786.2$ mm

Next try $R_1 = 536.2$ mm

Right hand side of eq. (viii) $= \frac{1}{536.2} - 0.0006146$

$\therefore \quad R_{cal.} = 799.81$ (near to sufficient accuracy)

Hence $R_1 = 536.2$ mm is the accepted value for eq. (viii) to give a value of R = 800 mm.

Then,

$$t_1 = 0.670 \text{ mm}$$

$$\therefore \quad M_B = 2283.4 \times 10^3$$

and from eqs. (vi) and (vii),

$$\sigma_1 = -0.475\, \sigma_y$$

$$\sigma_2 = 0.670\, \sigma_y$$

This technique of calculating σ_1 and σ_2 are valid for rectangular cross-section only.

Calculated values for $Et/(R\sigma_y) = 20, 150$ are as follows:

$Et/(R\sigma_y)$	σ_1/σ_y	σ_2/σ_y	t_1/t
20	0.496	0.869	0.0435
150	0.499	0.980	0.0065

It/

It is obvious that for $Et/(R\sigma_y) \rightarrow \infty$ $\sigma_1/\sigma_y = 0.500$ and $\sigma_2/\sigma_y = 1.00$

Values of (σ_1/σ_y), (σ_2/σ_y) and (t_1/t) against $Et/(R\sigma_y)$ are plotted in Fig. A1.

REFERENCES:

1. McVEE, J.D.: Residual stresses in cold bent circular ring frame segments of T cross section, NCRE Report No. N194, March 1971.

2. ANNAND, S.C. and GRIFFITH, A.R.: Inelastic buckling of rings with residual stresses, Jnl of Eng. Mechanics Division, October 1973.

APPENDIX B

i) The procedure to calculate the pressure to cause yielding in the extreme fibre of a ring frame under expternal pressure.

The circumferential compressive stress σ_{Fc} in the flange of an internal ring frame derived by Wilson[88] as:

$$\sigma_{Fc} = \frac{p_{Fy} R^2 (1 - \frac{\mu}{2})}{tR_F (1 + \frac{A_1}{(\frac{1}{2} t_w t + \frac{2N_1 t}{\alpha_1})})}$$

where:

p_{Fy} = pressure at which yielding begins in the extreme of a ring frame

R_F = radius to the centroid of the ring section

A_1 = $R^2 A_f / R_f^2$

α_1^4 = $3(1 - \mu^2)/(R^2 t^2)$

N_1 = $[\text{Cosh}(\alpha_1 \ell_1) - \text{Cos}(\alpha_1 \ell_1)]/[\text{Sinh}(\alpha_1 \ell_1) + \text{Sin}(\alpha_1 \ell_1)]$

ℓ_1 = $\ell - \frac{1}{2} t_w$

An approximate circumferential bending stress in the flange of a ring frame derived by Kendrick[89] as:

$$\sigma_b = \frac{E e_{ff} C_{ol} (n^2 - 1)}{nR^2} \frac{p_{Fy}}{(p_n - p_{Fy})}$$

where:

p_n = critical pressure for overall instability of perfect cylinder

C_{01} = initial out-of-circularity amplitude of ring frame

e_{ff} = distance from mid-surface of shell to extreme fibre of the ring frame

The rest of the notations are defined in the nomenclature section.

Equating the sum of circumferential compressive stress and the circumferential bending stress to the yield stress σ_{yF} of the ring frame results in a quadratic equation in p_{Fy}.

$$\sigma_b + \sigma_{Fc} = \sigma_{yF}$$

After substitution we get a quadratic equation of the form:

$$p_{Fy}^2 - p_{Fy} H_1 + H_2 = 0$$

where:

$$H_1 = (D_2/D_1 + p_n + \sigma_{yF}/D_1)$$

$$H_2 = \sigma_{yF} \times p_n/D_1$$

and:

$$D_1 = \sigma_{Fc}/p_{Fy}$$

$$D_2 = E e_{ff} C_{ol} (n^2 - 1)/(n-R^2)$$

Hence minimum p_{Fy} is given by:

$$p_{Fy} = 0.50 \, (H1 - \sqrt{H1^2 - 4H2})$$

This procedure has been adopted in the BS5500[7].

ii) Von Mises equation for elastic buckling pressure under uniform external pressure.

$$p_m = \frac{Et}{R} \frac{1}{(n^2 - 1 + \frac{1}{2}\lambda_2^2)} \left\{ \frac{1}{(n^2 \frac{1}{\lambda_2^2} + 1)^2} + \frac{k^2}{1-\mu^2} [n^2 - 1 + \lambda_2^2] \right\}$$

It is necessary to minimise the buckling pressure with respect to n. This is easily done by a simple computer program. A chart for deforming the number of lobes n for which p_m is a minimum is given in Ref. (7).

Pressure/

Pressure to cause yielding in shell plating midway between stiffeners:

$$p_{c5} = \frac{t\sigma_y}{R(1 \pm \gamma_1 G_1)}$$

$$G_1 = \frac{-2\left[\text{Sinh } \frac{\alpha 1 \ell 1}{2} \text{ Cos } \frac{\alpha 1 \ell 1}{2} + \text{Cosh } \frac{\alpha 1 \ell 1}{2} \text{ Sin } \frac{\alpha 1 \ell 1}{2}\right]}{(\text{Sinh } \alpha_1 \ell_1 + \text{Sin } \alpha_1 \ell_1)}$$

$$\gamma_1 = \frac{A_1 (1 - \frac{\mu}{2})}{(A_1 + twt)(1 + \beta_1)}$$

$$\beta_1 = \frac{2tN_1}{\sigma_1 (A_1 + twt)}$$

where A_1 , α_1 , ℓ_1 are as defined previously.

APPENDIX C

Interframe Buckling

$$a_{11} = 2\alpha\lambda_3^2 + \alpha(1-\mu)n^2(1+k) + 2\alpha RW2(1-\mu^2)n^2$$

$$a_{12} = -4\mu\alpha\lambda_3 nT13 - 2\alpha(1-\mu)n\lambda_3 T14$$

$$a_{13} = 4\mu\alpha\lambda_3 T13 - 2k\alpha(1-\mu)n^2\lambda_3 T14$$

$$a_{22} = 4\alpha n^2 T11 + 2\alpha(1-\mu)\lambda_3^2(1+3k)T15$$

$$a_{23} = -4\alpha nT11 - 6k\alpha(1-\mu)\lambda_3^2 nT15 + 4k\alpha\mu\lambda_3^2 nT16 - 2\alpha RW1n(1-\mu^2)$$

$$a_{33} = 4\alpha T11(1+k(n^2-1)^2) + 4k\alpha\lambda_3^4 T17 + 8k\alpha(1-\mu)\lambda_3^2 n^2 T15$$
$$-8k\mu\alpha\lambda_3^2 n^2 T16 - 2\alpha RRC(1-\mu^2)\lambda_3^2 T1/R + 2\alpha RW1(1-\mu^2)n^2$$

$$b_{11} = 4\alpha x_1 n^2 T4 - 4\alpha\mu x_2 n^2 T6$$

$$b_{12} = -4\alpha\mu x_1\lambda_3 nT9 - 2\lambda_3 nT12I$$

$$b_{13} = -8\alpha\lambda_2 x_1\lambda_3^2 T7 - 4\alpha(1-\mu)x_1\lambda_2 n^2 T10$$

$$b_{22} = 4\alpha x_2\lambda_3^2 T1 + 4\alpha\mu x_1\lambda_3^2 T2 + 8\alpha x_1 n^2 T3$$

$$b_{23} = -8\alpha x_1 nT3 + 4\alpha\mu n(x_2 T5 - 2\lambda_2 x_1\lambda_3 T8) + 4\alpha(1-\mu)x_1\lambda_2 n\lambda_3 T8$$
$$+ 4nT11I$$

$$b_{33} = -4\alpha x_2\lambda_3^2 T1 + 4\mu\alpha x_1\lambda_3^2 T2 + 4\alpha x_1 T3n^2 - 4\alpha\mu x_2 n^2 T5$$
$$+16\alpha\mu x_1\lambda_2\lambda_3 T8 - 4T11I$$

$$c_1 = -8\alpha\lambda_2 x_1\lambda_3^2 T7C_o + 4\alpha\mu x_1\lambda_3 T9C_o - 4\alpha(1-\mu)x_1\lambda_2 n^2 T10C_o$$
$$+4\lambda_3 T12C_o I$$

$$c_2 = 4\alpha x_1 nT3C_o - 8\alpha\mu x_1\lambda_2\lambda_3 nT8C_o + 4\alpha(1-\mu)x_1\lambda_2\lambda_3 nT8C_o$$
$$+ 4nT11C_o I$$

$$c_3 = 4\alpha x_1 T3C_o(n^2-2) - 4\alpha x_2\lambda_3^2 T1C_o + 4\alpha\mu x_1\lambda_3 C_o(\lambda_3 T2 + 2\lambda_2 T8)$$
$$-4\alpha x_2 T5(n^2-1)C_o - 4T11C_o I - 2\alpha RW1(1-\mu^2)C_o(n^2-1)/\phi_1$$

$$r_{11} = 2\alpha T18(1+k) + 2k\alpha\lambda_2^4 T19 + 2\phi_1 T18I - \alpha RRC(1-\mu^2)\lambda_2^2 T21/R$$

$$r_{12} = -2T20(\alpha\mu + \phi_1 I)$$

$$r_{22} = 2\alpha$$

$$s_1 = 2T20I + \alpha RRC(1-\mu^2)T20/(\phi_1 R)$$

$$s_2 = -1.0$$

Simply Supported Edges

$$T1 = \int \cos^2 g \, dx$$

$$T2 = \int \sin g \cos^2 g \, dx$$

$$T3 = \int \sin g \sin^2 g \, dx$$

$$T4 = \int \sin g \cos^2 g \, dx$$

$$T5 = \int \sin^2 g \, dx$$

$$T6 = \int \cos^2 g \, dx$$

$$T7 = \int -0.50 \cos g \sin g \cos g \, dx$$

$$T8 = \int 0.50 \cos g \sin g \cos g \, dx$$

$$T9 = \int \sin g \sin^3 g \, dx$$

$$T10 = \int 0.50 \cos g \cos g \sin g \, dx$$

$$T11 = \int \sin^2 g \, dx$$

$$T12 = \int -\sin^2 g \, dx$$

$$T13 = \int \sin^2 g \, dx$$

$$T14 = \int \cos^2 g \, dx$$

$$T15 = \int \cos^2 g \, dx$$

$$T16 = \int -\sin^2 g \, dx$$

$$T17 = \int \sin^2 g \, dx$$

$$T18 = \int \sin^2 g \, dx$$

$$T19 = \int \sin^{-2} g \, dx$$

$$T20 = \int \sin g \, dx$$

$$T21 = \int \cos^2 g \, dx$$

Partially Fixed Edges

$T1 = \int (\cos g + \sin 2g)^2 \, dx$

$T2 = \int (\sin q + \sin^2 q)(\cos g + \sin 2g)^2 \, dx$

$T3 = \int (\sin q + \sin^2 q)(\sin g + \sin^2 g)^2 \, dx$

$T4 = \int (\sin q + \sin^2 q) \cos^2 g \, dx$

$T5 = \int (\sin g + \sin^2 g)^2 \, dx$

$T6 = \int \cos^2 g \, dx$

$T7 = \int 0.50 (\cos q + \sin 2q) \sin g \, (\cos g + \sin 2g) \, dx$

$T8 = \int 0.50 (\cos q + \sin 2q)(\sin g + \sin^2 g)(\cos g + \sin 2g) \, dx$

$T9 = \int -(\sin q + \sin^2 q) \sin g \, (\sin g + \sin^2 g) \, dx$

$T10 = \int 0.50 (\cos q + \sin^2 q) \cos g \, (\sin g + \sin^2 g) \, dx$

$T11 = \int (\sin g + \sin^2 g)^2 \, dx$

$T12 = \int -0.50 \sin g \, (\sin g + \sin^2 g) \, dx$

$T13 = \int \sin g \, (\sin g + \sin^2 g) \, dx$

$T14 = \int \cos g \, (\cos g + \sin 2g) \, dx$

$T15 = \int (\cos g + \sin 2g)^2 \, dx$

$T16 = \int (\sin g + \sin^2 g)(2\cos 2g - \sin g) \, dx$

$T17 = \int (2\cos 2g - \sin g)^2 \, dx$

$T18 = \int (\sin q + \sin^2 q)^2 \, dx$

$T19 = \int (2\cos 2q - \sin q)^2 \, dx$

$T20 = \int (\sin q + \sin^2 q) \, dx$

$T21 = \int (\cos q + \sin 2q)^2 \, dx$

Clamped Edges

$T1 = \int 4 \sin^2 2g \, dx$

$T2 = \int 4 (1 - \cos 2g) \sin^2 2g \, dx$

$T3 = \int (1 - \cos 2q)(1 - \cos^2 g)^2 \, dx$

$T4 = \int (1 - \cos 2q) \cos^2 g \, dx$

$T5 = \int (1 - \cos 2g)^2 \, dx$

Clamped Edges (Cont'd)

$T6 = \int \cos^2 g \, dx$

$T7 = \int -2\sin 2q \sin g \sin 2g \, dx$

$T8 = \int 2\sin 2q \sin 2g (1-\cos 2g) \, dx$

$T9 = \int \sin g (1-\cos 2q)(1-\cos 2g) \, dx$

$T10 = \int \sin 2q \cos g (1-\cos 2g) \, dx$

$T11 = \int (1-\cos 2g)^2 \, dx$

$T12 = \int -\sin g (1-\cos 2g) \, dx$

$T13 = \int \sin g (1-\cos 2g) \, dx$

$T14 = \int 2\cos g \sin 2g \, dx$

$T15 = \int 4\sin^2 2g \, dx$

$T16 = \int 4(1-\cos 2g)\cos 2g \, dx$

$T17 = \int 16 \cos^2 2g \, dx$

$T18 = \int (1-\cos 2q)^2 \, dx$

$T19 = \int 16 \cos^2 2q \, dx$

$T20 = \int (1-\cos 2q) \, dx$

$T21 = \int 4\sin^2 2q \, dx$

where:

$$g = \frac{m\pi x}{\ell} \quad , \quad q = \frac{\pi x}{\ell}$$

x_1 and x_2 are solutions of eq. (34)

$RW1 = \int \sigma_w \sin^2 g \, dx$

$RW2 = \int \sigma_w \cos^2 g \, dx$

$RRC = \bar{\sigma}_{cb}$ from eq. (29)

$I = 1$ for uniform external pressure

$I = 0$ for axial compression

Overall Buckling

$$a_{11} = 2\alpha\lambda_1^2 + \alpha(1-\mu)(1+k)n^2 + 4(1-\mu^2)\alpha_F n^4 QQ6(H3 + H5)$$
$$+ 2\alpha(1-\mu^2)n^2 RW2 + 2H4(1-\mu)\alpha_F n^2 QQ6$$

$$a_{12} = -4\alpha\mu\lambda_1 nS43 - 2\alpha(1-\mu)\lambda_1 nS48$$

$$a_{13} = -4\alpha\mu\lambda_1 nS45 - 4\alpha(1-\mu)\lambda_2 nS47$$

$$a_{14} = 4\alpha\mu\lambda_1 S43 - 4k\alpha(1-\mu)n^2\lambda_1 S48 - 4H3(1-\mu^2)\lambda_1 QQ5_F n^2(\frac{\ell}{R}n^2 +$$
$$1 - \ell/R) - 2H4(1-\mu)\alpha_F n^2\lambda_1 QQ5 - 4H5(1-\mu^2)\alpha_F n^4(1-\ell/R)\lambda_1 QQ5$$
$$+ 4k\alpha\lambda_1^2 S55 - 2\alpha(1-\mu^2)RRCn^2\lambda_1 S48/R$$

$$a_{15} = 4\alpha\mu\lambda_1 S45 - 8k\alpha(1-\mu)n^2\lambda_2 S47 - 8k\alpha\lambda_1\lambda_2^2 S44$$
$$-4\alpha(1-\mu^2)RRCn^2\lambda_2 S47/R$$

$$a_{22} = 4\alpha n^2 S6 + 2\alpha(1-\mu)\lambda_1^2 S52(1+3k) + 4H2(1-\mu^2)\alpha_F n^2 QQ3(1- /R)^2$$
$$+4H1(1-\mu^2)\alpha_F QQ3n^2$$

$$a_{23} = 4\alpha n^2 S16 + 4\alpha(1-\mu)\lambda_1\lambda_2 S49(1+3k)$$

$$a_{24} = -4\alpha nS6 - 6k\alpha(1-\mu)\lambda_1\lambda_2 S52 + 4k\alpha\mu\lambda_1^2 nS53 - 2\alpha(1-\mu^2)nRW1$$
$$-4H2\alpha_F(1-\mu^2)nQQ3(1-\ell/R-n^2\ell/R + n^2(\frac{\ell}{R})^2) - 4H1(1-\mu^2)\alpha_F QQ3n^3$$

$$a_{25} = -4\alpha nS16 - 12k\alpha(1-\mu)\lambda_1\lambda_2 nS49 + 16k\alpha\mu\lambda_2^2 nS44$$
$$-2\alpha(1-\mu^2)nRW4$$

$$a_{33} = 6\alpha n^2 + 4\alpha(1-\mu)\lambda_2^2(1 + 3k)$$

$$a_{34} = -4\alpha nS16 - 12k\alpha(1-\mu)\lambda_1\lambda_2 nS49 + 4k\alpha\mu\lambda_1^2 nS54$$
$$-2\alpha(1-\mu^2)nRW4$$

$$a_{35} = 6\alpha n - 12k\alpha(1-\mu)\lambda_2^2 n - 8k\alpha\mu\lambda_2^2 n - 2\alpha(1-\mu^2)nRW3$$

$$a_{44} = 4\alpha S6(1+k(n^2-1)^2 + 4k\alpha\lambda_1^4 S50 + 8k\lambda_1^2 n^2(\alpha(1-\mu)S52 -$$
$$\mu\alpha S53) + 4H1(1-\mu^2)\alpha_F QQ3n^4 + 4H2\alpha_F(1-\mu^2)QQ3(n^2\frac{\ell}{R} - 1)$$
$$(n^2\frac{\ell}{R} - 1) + 4H3(1-\mu^2)\alpha_F QQ4\lambda_1^2(n^4(\frac{\ell}{R})^2 + (1-\ell/R)^2 + 2n^2\frac{\ell}{R}(1-\frac{\ell}{R})$$
$$+2H4(1-\mu)n^2\lambda_1^2\alpha_F QQ4 + 2\alpha(1-\mu^2)n^2 RW1 + 4H5(1-\mu^2)\alpha_F n^4\lambda_1^2 QQ4$$
$$(1-\frac{\ell}{R})(1-\frac{\ell}{R}) - 2\alpha(1-\mu^2)\lambda_1^2 RRC\ S52/R$$

Overall Buckling (Cont'd)

$$a_{45} = 16k\alpha\lambda_2^2\lambda_1^2 S51 + 4\alpha S16(1+k(n^2-1)^2) + 16\alpha(1-\mu)\lambda_1\lambda_2 n^2 S49 - 4k\alpha\mu n^2(\lambda_1^2 S54 + 4\lambda_2^2 S44) + 2\alpha(1-\mu^2)n^2 RW4 - 4\alpha(1-\mu^2)RRC\lambda_1\lambda_2 S49/R$$

$$a_{55} = 6\alpha(1+k(n^2-1)^2) + 32k\alpha\lambda_2^4 + 16k\alpha(1-\mu)\lambda_2^2 n^2 + 16k\alpha\mu\lambda_2^2 n^2 + 2\alpha(1-\mu^2)n^2 RW3 - 4\alpha(1-\mu^2)RRC\lambda_2^2/R$$

$$b_{11} = 4\alpha n^2(x_1 S4 + x_2 S7) + 2\alpha\mu x_3 n^2 + 4H_2(1-\mu^2)\alpha_F x_1 n^2 QQ2$$

$$b_{12} = 4\alpha\mu n(x_1\lambda_1 S14 + x_2\lambda_1 S15) + 2\lambda_1 n S43I$$

$$b_{13} = 4\alpha\mu n\lambda_1(x_1 S15 + x_2 S17) + 2\lambda_1 n S45I$$

$$b_{14} = 4\lambda_1 S43I + 4\alpha\lambda_1^2(\lambda_1 x_1 S18 + 2\lambda_2 x_2 S19) - 2\alpha(1-\mu)n^2 (\lambda_1 x_1 S24 + 2\lambda_2 x_2 S26)$$

$$b_{15} = 4\lambda_1 S45I + 8\alpha\lambda_1\lambda_2(\lambda_1 x_1 S19 + 2\lambda_2 x_2 S22) - 2\alpha(1-\mu)n^2 (\lambda_1 x_1 S25 + 2\lambda_2 x_2 S27)$$

$$b_{22} = 4\alpha\lambda_1^2(x_3 S20) + 4\alpha\mu\lambda_1^2(x_1 S8 + x_2 S11) + 8\alpha n^2(x_1 S1 + x_2 S3) + 8H2(1-\mu^2)n^2\alpha_F QQ1\, x_1(1-\ell/R)$$

$$b_{23} = 8\alpha\lambda_1\lambda_2 x_3 S21 + 8\alpha\mu\lambda_1\lambda_2(x_1 S10 + x_2 S13) + 8xn^2(x_1 S3 + x_2 S2)$$

$$b_{24} = -8\alpha n(x_1 S1 + x_2 S3) - 4\alpha\mu n x_3 S40 + 4n S6I - 4\alpha\mu n\lambda_1(\lambda_1 x_1 S8 + 2\lambda_2 x_2 S10) - 4H2(1-\mu^2)\alpha_F x_1 QQ1 n(2-n^2\ell/R) + 2\alpha(1-\mu^2)n\lambda_1 (x_1\lambda_1 S8 + 2\lambda_2 x_2 S10)$$

$$b_{25} = -8\alpha n(x_1 S3 + x_2 S2) - 4\alpha\mu n x_3 S41 + 4n S16I - 8\alpha\mu n\lambda_2(\lambda_1 x_1 S10 + 2\lambda_2 x_2 S9) + 2\alpha(1-\mu)n\lambda_1(\lambda_1 x_1 S11 + 2\lambda_2 x_2 S13)$$

$$b_{33} = 8\alpha\lambda_2^2 x_3 + 16\alpha\mu\lambda_2^2(x_1 S9 + x_2 S12) + 8\alpha n^2(x_1 S2 + x_2 S5)$$

Overall Buckling (Cont'd)

$$b_{34} = -8\alpha n(x_1 S3 + x_2 S2) - 4\alpha\mu n x_3 S41 + 4nS16I - 4\alpha\mu n\lambda_1(\lambda_1 x_1 S11 + 2\lambda_2 x_2 S13) + 4\alpha(1-\mu)n_2(\alpha_1\lambda_2 S10 + 2\lambda_2 x_2 S9)$$

$$b_{35} = -8\alpha n(x_1 S2 + x_2 S5) - 4\alpha\mu n x_3 S42 + 6nI - 8\mu\alpha n\lambda_2(\lambda_1 x_1 S13 + 2\lambda_2 x_2 S12) + 4\alpha(1-\mu)n\lambda_2(\lambda_1 x_1 S13 + 2\lambda_2 x_2 S12)$$

$$b_{44} = 4\alpha x_1^2 x_3 S20 + 4\alpha\mu\lambda_1^2(x_1 S8 + x_2 S11) + 4\alpha n^2(x_1 S1 + x_2 S3) + 4\alpha\mu n^2 x_3 S40 - 4S6I + 8\alpha\mu\lambda_1(\lambda_1 x_1 S8 + 2\lambda_2 x_2 S10) + 4H2(1-\mu^2)\alpha_F x_1 n^2 QQ1$$

$$b_{45} = 8\alpha\lambda_1\lambda_2 x_3 S21 + 8\alpha\mu\lambda_1\lambda_2(x_1 S10 + x_2 S13) + 4\alpha n^2(x_1 S3 + x_2 S2) + 4\alpha\mu n^2(x_3 S41) - 4S16I + 4\alpha\mu\lambda_1(\lambda_1 x_1 S11 + 2\lambda_2 x_2 S13) + 8\alpha\mu\lambda_2(\lambda_1 x_1 S10 + 2\lambda_2 x_2 S9)$$

$$b_{55} = 8\alpha x_3\lambda_2^2 + 16\alpha\mu\lambda_2^2(x_1 S9 + x_2 S12) + 4\alpha n^2(x_1 S21 + x_2 S5) + 4\alpha\mu n^2 x_3 S42 - 6I$$

$$c_1 = -4\alpha\mu C_{o1}\lambda_1(x_1 S14 + x_2 S15) - 4\alpha\mu C_{o2}\lambda_1(x_1 S15 + x_2 S17) - 4\lambda_1 C_{o1} S43I - 4\lambda_1 C_{o2} S45I + 4\alpha C_{o1}\lambda_1^2(\lambda_1 x_1 S18 + 2\lambda_2 x_2 S19) + 8\alpha C_{o2}\lambda_2\lambda_1(\lambda_1 x_1 S19 + 2\lambda_2 x_2 S22) - 2\alpha(1-\mu)n^2 C_{o1}(\lambda_1 x_1 S24 + 2\lambda_2 x_2 S26) - 2\alpha(1-\mu)n^2 C_{o2}(\lambda_1 x_1 S25 + 2\lambda_2 x_2 S27)$$

$$c_2 = 4\alpha n(z_1 S1 + z_2 S3)C_{o1} + 4nI(C_{o1} S6 + C_{o2} S16) - 4\alpha\mu\lambda_1 n C_{o1}(\lambda_1 x_1 S8 + 1\lambda_2 x_2 S10) - 8\alpha\mu n\lambda_2 C_{o2}(\lambda_1 x_1 S10 + 2\lambda_2 x_2 S9) + 2\alpha(1-\mu)n\lambda_1 C_{o1}(\lambda_1 x_1 S8 + 2\lambda_2 x_2 S10) + 2\alpha(1-\mu)n\lambda_1 C_{o2}(\lambda_1 x_1 S11 + 2\lambda_2 x_2 S13) + 4\alpha n C_{o2}(x_1 S3 + x_2 S2) + 4H2(1-\mu)\alpha_F x_1 C_{o1} n(1-\ell/R)$$

c_3 /

Overhall Buckling (Cont'd)

$$c_3 = 4\alpha n C_{o2}(x_1 S2 + x_2 S5) + 4\alpha n C_{o1}(x_1 S3 + x_2 S2) + (6C_{o2} + 4C_{o1} S16)$$
$$-4\alpha\mu n C_{o1}\lambda_1(\lambda_1 x_1 S11 + 2\lambda_2 x_2 S13) - 8\alpha\mu n\lambda_2 C_{o2}(\lambda_1 x_1 S13 + 2\lambda_2 x_2 S12)$$
$$+4\alpha(1-\mu)n\lambda_2 C_{o1}(\lambda_1 x_1 S10 + 2\lambda_2 x_2 S9) + 4\alpha(1-\mu)n\lambda_2 C_{o2}$$
$$(\lambda_1 x_1 S13 + 2\lambda_2 x_2 S12)$$

$$c_4 = 4\alpha C_{o1}\lambda_1^2 x_3 S20 + 8\sigma\lambda_1\lambda_2 C_{o2} x_3 S21 + 4\alpha\mu C_{o1}\lambda_1^2 (x_1 S8 + x_2 S11)$$
$$+8\alpha\mu C_{o2}\lambda_1\lambda_2(x_1 S10 + x_2 S13) + 4\alpha C_{o1}(n^2 - 2)(x_1 S1 + x_2 S3)$$
$$+4\alpha C_{o2}(n^2 - 2)(x_1 S3 + x_2 S2) + 4\alpha\mu C_{o1}(n^2 - 1)x_3 S40 +$$
$$4\alpha\mu C_{o2}(n^2 - 1)x_3 S41 - 4C_{o1} S6I - 4C_{o2} S16I + 4\alpha\mu\lambda_1 C_{o1}(\lambda_1 x_1 S8)$$
$$+2\lambda_2 x_2 S10) + 8\alpha\mu C_{o2}\lambda_2(\lambda_1 x_1 S10 + 2\lambda_2 S9) - 2\alpha(1-\mu^2)(n^2 - 1)$$
$$(RW1\ C_{o1} + RW4\ C_{o2})/\phi_1 + 4H2(1-\mu^2)\alpha_F x_1 QQ1\ C_{o1}(n^2 - 2 + n^2\ell/R)$$

$$c_5 = 8\alpha x_3\lambda_2^2\ C_{o2} + 8\alpha C_{o1}\lambda_1\lambda_2 x_3 S21 + 16\alpha\mu C_{o2}\lambda_2^2(x_1 S9 + x_2 S12)$$
$$+8\alpha\mu C_{o1}\lambda_1\lambda_2(x_1 S10 + x_2 S13) + 4\alpha C_{o2}(x_1 S2 + x_2 S5)(n^2 - 2)$$
$$+4\alpha C_{o1}(n^2 - 2)(x_1 S3 + x_2 S2) + 4\alpha\mu C_{o2}(n^2 - 1)x_3 S42$$
$$+4\alpha\mu C_{o1}(n^2 - 1)x_3 S41 - 4C_{o1} S16I - 6C_{o2} I + 4\alpha\mu\lambda_1 C_{o1}(\lambda_1 x_1 S11 +$$
$$2\lambda_2 x_2 S13) + 8\alpha\mu C_{o2}\lambda_2(\lambda_1 x_1 S13 + 2\lambda_2 x_2 S12)$$
$$-2\alpha(1-\mu)(n^2 - 1)(RW3\ C_{o2} + RW4\ C_{o1})/\phi_1$$

$$r_{11} = 2\alpha S6(1+k) + 2k\alpha\lambda_1^4 S50 + 2\phi_1 S6I + 2H2(1-\mu^2)\alpha_F Q83$$
$$+2H3(1-\mu^2)(1-\ell/R)^2\alpha_F\lambda_1^2 QQ4$$

$$r_{12} = 2S16(\alpha + \phi_1 I) + 8k\alpha\lambda_1^2\lambda_2^2 S51$$

$$r_{13} = 2\mu\alpha S56 - 2\phi_1 S56\ I$$

$$r_{22} = 3(\alpha + k\alpha + \phi_1 I) + 16k\alpha\lambda_2^4$$

$$r_{23} = -2(\mu\alpha + \phi_1 I)$$

$$r_{33} = 2\alpha$$

Overall Buckling (Cont'd)

$s_1 = 2S56\,I + \alpha(1-\mu^2)RRC\ S56/(R\emptyset_1)$

$s_2 = 2I + \alpha(1-\mu^2)RRC^*(R\emptyset_1)$

$s_3 = 1.0$

$H1 = \dfrac{I_{xc}}{tLR(R-e)}$

$H2 = \dfrac{A_f R}{tL(R-e)}$

$H3 = \dfrac{I_{zo} R}{tL(R-e)^3}$

$H4 = \dfrac{C_r R}{tL(R-e)^3}$

$H5 = \dfrac{\Gamma R}{tL(R-e)^5}$

Simply Supported Edges:

$S1 = \int \sin^3 g\, dx$

$S2 = \int \sin g\,(1-\cos h)^2\, dx$

$S3 = \int \sin^2 g\,(1-\cos h)\, dx$

$S4 = \int \sin g \cos^2 g\, dx$

$S5 = \int (1-\cos h)^3\, dx$

$S6 = \int \sin^3 g\, dx$

$S7 = \int \cos^2 g\,(1-\cos h)\, dx$

s8/

Simply Supported Edges (Cont'd)

$S8 = \int \sin g \cos^2 g \, dx$

$S9 = \int \sin g \sin^2 h \, dx$

$S10 = \int \sin g \cos g \sin j \, dx$

$S11 = \int \cos^2 g \, (1 - \cos h) \, dx$

$S12 = \int \sin^2 h \, (1 - \cos h) \, dx$

$S13 = \int (1 - \cos h) \sin h \cos g \, dx$

$S14 = \int \sin^3 g \, dx$

$S15 = \int \sin^2 g \, (1 - \cos h) \, dx$

$S16 = \int \sin g \, (1 - \cos h) \, dx$

$S17 = \int \sin g \, (1 - \cos h)^2 \, dx$

$S18 = \int \sin g \cos^2 g \, dx$

$S19 = \int \cos^2 g \sin g \sin h \, dx$

$S20 = \int \cos^2 g \, dx$

$S21 = \int \cos g \sin h \, dx$

$S22 = \int \sin^2 h \sin g \, dx$

$S24 = \int \sin g \cos^2 g \, dx$

$S25 = \int \cos^2 g \, (1 - \cos h) \, dx$

$S26 = \int \sin h \cos g \sin g \, dx$

$S27 = \int \sin h \cos g \, (1 - \cos h) \, dx$

Simply Supported Edges (Cont'd)

$S40 = \int \sin^2 g \, dx$

$S41 = \int \sin g \, (1 - \cos h) \, dx$

$S42 = \int (1 - \cos h)^2 \, dx$

$S43 = \int \sin^2 g \, dx$

$S44 = \int \sin g \cos h \, dx$

$S45 = \int \sin g \, (1 - \cos h) \, dx$

$S47 = \int \cos g \sin h \, dx$

$S48 = \int \cos^2 g \, dx$

$S49 = \int \sin h \cos g \, dx$

$S50 = \int \sin^2 g \, dx$

$S51 = \int \sin g \cos h \, dx$

$S52 = \int \cos^2 g \, dx$

$S53 = -\int \sin^2 g \, dx$

$S54 = -\int \sin g \, (1 - \cos h) \, DX$

$S55 = \int \sin^2 g \, dx$

$S56 = \int \sin g \, dx$

QQ1/

Simply Supported Edges (Cont'd)

$QQ1 = \Sigma \sin^3 g$

$QQ2 = \Sigma \cos^2 g \sin g$

$QQ3 = \Sigma \sin^2 g$

$QQ4 = \Sigma \cos^2 g$

$QQ5 = \Sigma \cos^2 g$

$QQ6 = \Sigma \cos^2 g$

$RW1 = \int \sigma_w \sin^2 g \, dx$

$RW2 = \int \sigma_w \cos^2 g \, dx$

$RW3 = \int \sigma_w (1 - \cos h)^2 \, dx$

$RW4 = \int \sigma_w \sin g \, (1 - \cos h) \, dx$

Partially Fixed Edges:

$S1 = \int (\sin g + \sin^2 g)^3 \, dx$

$S2 = \int (\sin g + \sin^2 g)(1 - \cos h)^2 \, dx$

$S3 = \int (\sin g + \sin^2 g)^2 (1 - \cos h) \, dx$

$S4 = \int (\sin g + \sin^2 g) \cos g \, dx$

$S5 = \int (1 - \cos h)^3 \, dx$

$S6 = \int (\sin g + \sin^2 g)^2 \, dx$

$S7 = \int (1 - \cos h) \cos^2 g \, dx$

S8/

Partially Fixed Edges (Cont'd)

S8 = $\int (\sin g + \sin^2 g)(\cos g + \sin 2g)^2 \, dx$

S9 = $\int (\sin g + \sin^2 g) \sin^2 h \, dx$

S10 = $\int (\sin g + \sin^2 g)(\cos g + \sin 2g) \sin h \, dx$

S11 = $\int (\cos g + \sin 2g)^2 (1 - \cos h) \, dx$

S12 = $\int \sin^2 h \, (1 - \cos h) \, dx$

S13 = $\int (1 - \cos h) \sin h (\cos g + \sin 2g) \, dx$

S14 = $\int \sin g \, (\sin g + \sin^2 g)^2 \, dx$

S15 = $\int \sin g \, (\sin g + \sin^2 g)(1 - \cos h) \, dx$

S16 = $\int (\sin g + \sin^2 g)(1 - \cos h) \, dx$

S17 = $\int (1 - \cos h)^2 \sin g \, dx$

S18 = $\int \sin g \, (\cos g + \sin 2g)^2 \, dx$

S19 = $\int (\cos g + \sin 2g)^2 \sin h \, dx$

S20 = $\int (\cos g + \sin 2g)^2 \, dx$

S21 = $\int (\cos g + \sin 2g) \sin h \, dx$

S22 = $\int \sin 0h \sin g \, dx$

S24 $\int (\cos g + \sin 2g)(\sin g + \sin^2 g) \cos g \, dx$

S25 = $\int (\cos g + \sin 1g)(1 - \cos h) \cos g \, dx$

S26 = $\int \sin h \cos g \, (\sin g + \sin^2 g) \, dx$

S27/

Partially Fixed Edges (Cont'd)

$S27 = \int \text{Sin } h \text{ Cos } g \ (1 - \text{Cos } h) \ dx$

$S40 = \int (\text{Sin } g + \text{Sin}^2 g)^2 \ dx$

$S41 = \int (\text{Sin } g + \text{Sin}^2 g)(1 - \text{Cos } h) \ dx$

$S42 = \int (1 - \text{Cos } h)^2 \ dx$

$S43 = \int \text{Sin } g \ (\text{Sin } g + \text{Sin}^2 g) \ dx$

$S44 = \int \text{Cos } h \ (\text{Sin } g + \text{Sin}^2 g) \ dx$

$S45 = \int \text{Sin } g \ (1 - \text{Cos } h) \ dx$

$S47 = \int \text{Cos } g \text{ Sin } h \ dx$

$S48 = \int \text{Cos } g \ (\text{Cos } g + \text{Sin } 2g) \ dx$

$S49 = \int \text{Sin } h \ (\text{Cos } g + \text{Sin } 2g) \ dx$

$S50 = \int (2 \text{ Cos } 2g - \text{Sin } g)^2 \ dx$

$S51 = \int \text{Cos } h \ (2 \text{ Cos } 2g - \text{Sin } g) \ dx$

$S52 = \int (\text{Cos } 2g - \text{Sin } g)(1 - \text{Cos } h) \ dx$

$S55 = -\int \text{Sin } g \ (2 \text{ Cos } 2g - \text{Sin } g) \ dx$

$S56 = \int (\text{Sin } g + \text{Sin}^2 g) \ dx$

$QQ1 = \Sigma (\text{Sin } g + \text{Sin}^2 g)^3$

$QQ2 = \Sigma \text{Cos}^2 g \ (\text{Sin } g + \text{Sin}^2 g)$

$QQ3 = \Sigma (\text{Sin } g + \text{Sin}^2 g)^2$

$QQ4 = \Sigma (\text{Cos } g + \text{Sin } 2g)^2$

Partially Fixed Edges (Cont'd)

$QQ5 = \Sigma \text{Cos}\, g\ (\text{Cos}\, g + \text{Sin}\, 2g)$

$QQ6 = \Sigma \text{Cos}^2 g$

$RW1 = \int \sigma_w (\text{Sin}\, g + \text{Sin}^2 g)^2\ dx$

$RW2 = \int \sigma_w (1 - \text{Cos}\, h)^2\ dx$

$RW3 = \int \sigma_w (1 - \text{Cos}\, h)^2\ dx$

$RW4 = \int \sigma_w (\text{Sin}\, g + \text{Sin}^2 g)(1 - \text{Cos}\, h)\ dx$

Clamped Edges:

$S1 = \int (1 - \text{Cos}\ 2g)^3\ dx$

$S2 = \int (1 - \text{Cos}\ 2g)(1 - \text{Cos}\, h)^2\ dx$

$S3 = \int (1 - \text{Cos}\ 2g)^2 (1 - \text{Cos}\, h)\ dx$

$S4 = \int (1 - \text{Cos}\ 2g)\ \text{Cos}\ g\ dx$

$S5 = \int (1 - \text{Cos}\, h)^3\ dx$

$S6 = \int (1 - \text{Cos}\ 2g)^2\ dx$

$S7 = \int (1 - \text{Cos}\, h)\ \text{Cos}^2 g\ dx$

$S8 = \int 4 (1 - \text{Cos}\ 2g)\ \text{Sin}^2 2g\ dx$

$S9 = \int (1 - \text{Cos}\ 2g)\ \text{Sin}^2 h\ dx$

$S10 = \int 2 (1 - \text{Cos}\ 2g)\ \text{Sin}\ 2g\ \text{Sin}\, h\ dx$

$S11 = \int 4\ \text{Sin}^2 2g\ (1 - \text{Cos}\, h)\ dx$

Clamped Edges (Cont'd)

$S12 = \int \sin^2 h\,(1 - \cos h)\,dx$

$S13 = \int 2(1 - \cos h)\sin h \sin g\,dx$

$S14 = \int \sin g\,(1 - \cos 2g)^2\,dx$

$S15 = \int 1 \sin g\,(1 - \cos 2g)(1 - \cos h)\,dx$

$S16 = \int (1 - \cos 2g)(1 - \cos h)^2\,dx$

$S17 = \int \sin g\,(1 - \cos h)^2\,dx$

$S18 = \int 4 \sin g \sin^2 2g\,dx$

$S19 = \int 2 \sin 2g \sin g \sin h\,dx$

$S20 = \int 4 \sin^2 2g\,dx$

$S21 = \int 2 \sin 2g \sin h\,dx$

$S22 = \int \sin g \sin^2 h\,dx$

$S23 = \int \sin g \cos^2 g\,dx$

$S24 = \int 2 \sin 2g\,(1 - \cos h) \cos g\,dx$

$S25 = \int 2 \sin 2g\,(1 - \cos h) \cos g\,dx$

$S26 = \int \sin h \cos g\,(1 - \cos 2g)\,dx$

$S27 = \int \sin h \cos g\,(1 - \cos h)\,dx$

$S40 = \int (1 - \cos 2g)^2\,dx$

$S41 = \int (1 - \cos h)(1 - \cos 2g)\,dx$

$S42 = \int (1 - \cos h)^2\,dx$

Clamped Edges (Cont'd)

$S43 = \int \text{Sin } g\ (1 - \text{Cos } 2g)\ dx$

$S44 = \int \text{Cos } h\ (1 - \text{Cos } 2g)\ dx$

$S45 = \int \text{Sin } g\ (1 - \text{Cos } h)\ dx$

$S46 = \int \text{Sin } g\ \text{Cos } h\ dx$

$S47 = \int \text{Cos } g\ \text{Sin } h\ dx$

$S48 = \int 2\ \text{Cos } g\ \text{Sin } 2g\ dx$

$S49 = \int 2\ \text{Sin } h\ \text{Sin } 2g\ dx$

$S50 = \int 16\ \text{Cos}^2 2g\ dx$

$S51 = \int 4\ \text{Cos } h\ \text{Cos } 2g\ dx$

$S52 = \int 4\ \text{Sin}^2 2g\ dx$

$S53 = \int 4(1 - \text{Cos } 2g)\ \text{Cos } 2g\ dx$

$S54 = \int 4\ \text{Cos } g\ (1 - \text{Cos } h)\ dx$

$S55 = \int -4\ \text{Sin } g\ \text{Cos } 2g\ dx$

$S56 = \int (1 - \text{Cos } 2g)\ dx$

$QQ1 = \Sigma (1 - \text{Cos } 2g)^3$

$QQ2 = \Sigma \text{Cos}^2 g\ (1 - \text{Cos } 2g)$

$QQ3 = \Sigma (1 - \text{Cos } 2g)^2$

$QQ4 = \Sigma 4\ \text{Sin}^2 2g$

Clamped Edges (Cont'd)

$QQ5 = 2 \sin 2g \cos g$

$QQ6 = \cos^2 g$

$RW1 = \int \sigma_w (1 - \cos 2g)^2 \, dx$

$RW2 = \int \sigma_w \cos^2 g \, dx$

$RW3 = \int \sigma_w (1 - \cos h)^2 \, dx$

$RW4 = \int \sigma_w (1 - \cos 2g)(1 - \cos h) \, dx$

where:

$$g = \frac{\pi x}{L} \quad , \quad h = \frac{2\pi x}{\ell}$$

x_1 , x_2 , x_3 are solutions of eq (34)

I = 1 for uniform external pressure

I = 0 for axial compression

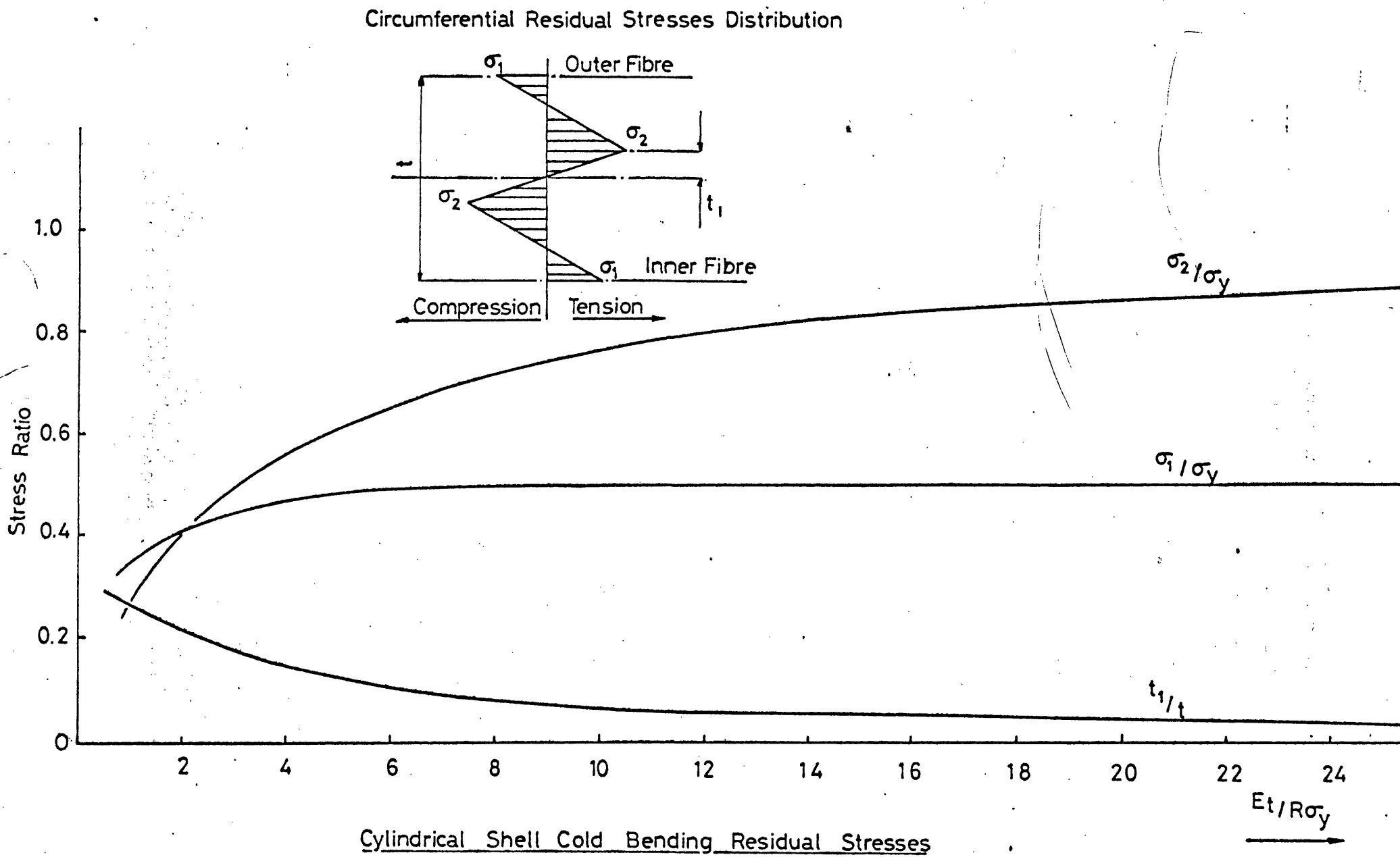

Cylindrical Shell Cold Bending Residual Stresses

Figure A1

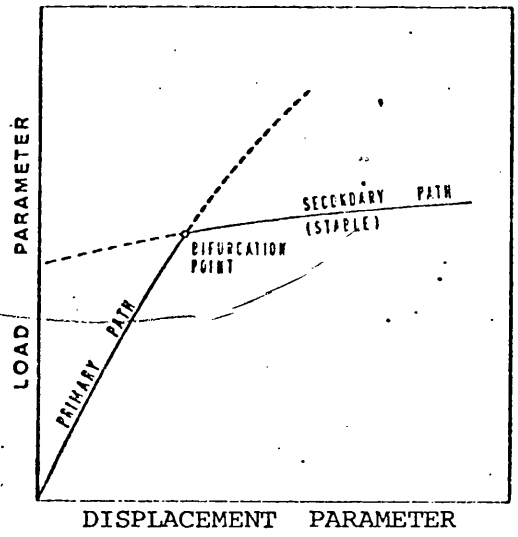

Fig. 1: Stable Bifurcation Point

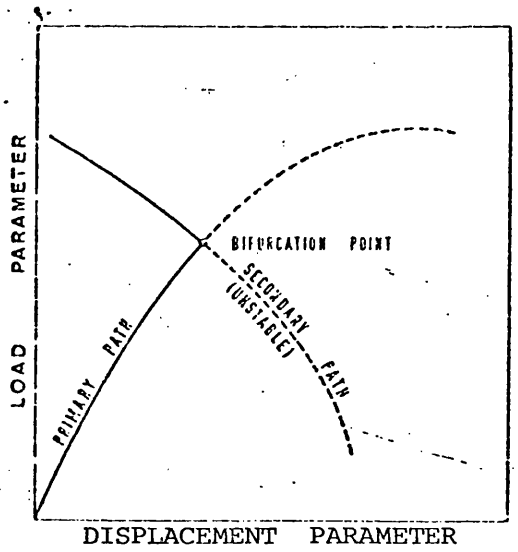

Fig. 2: Unstable Bifurcation Point

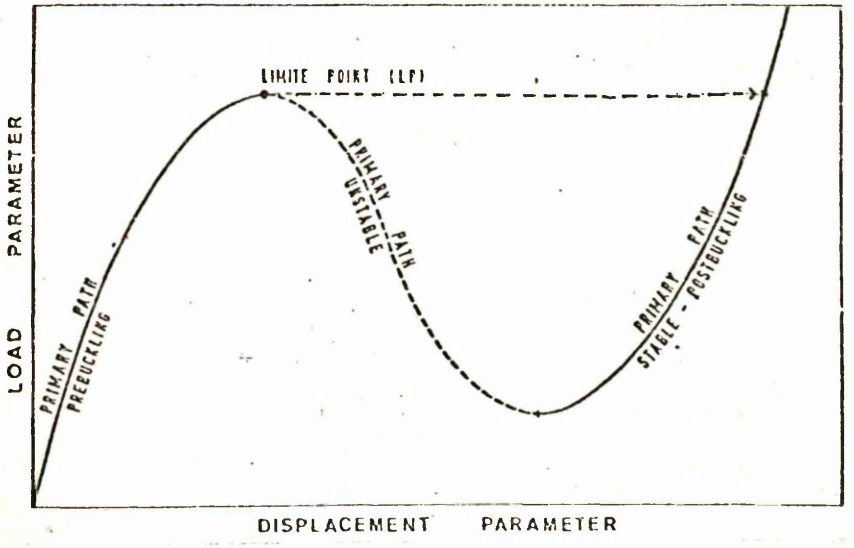

Fig. 3: Limit point for an equilibrium path with stable postbuckling behaviour

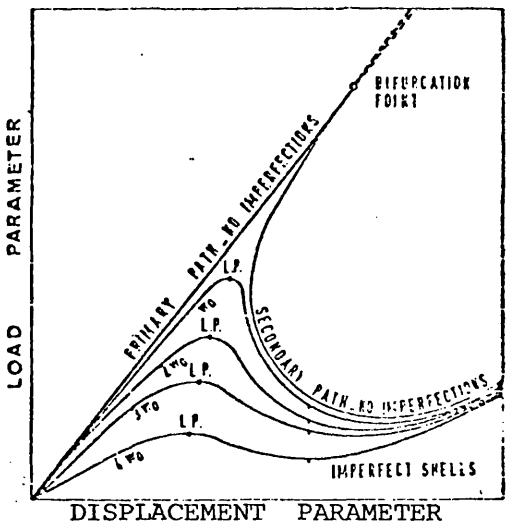

Fig. 4: Influence of initial shape imperfections on the equilibrium paths of cylinders and spheres under hydrostatic pressure

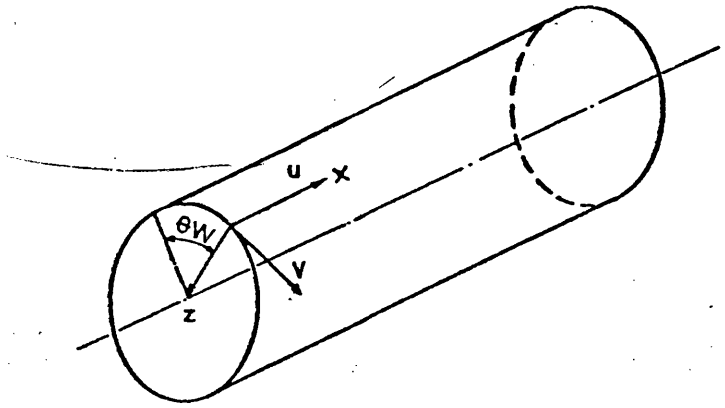

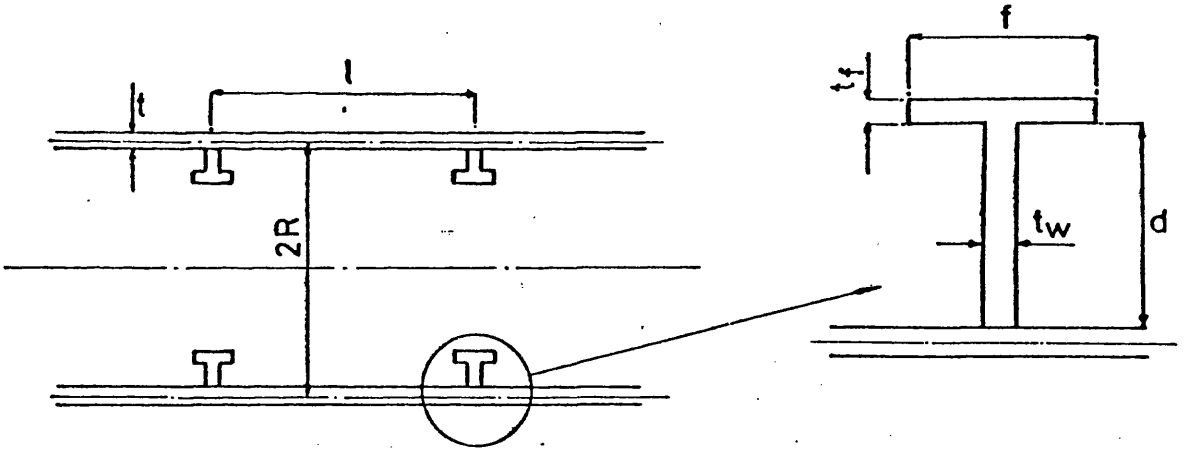

Coordinate System And Cross Section Of Stiffened Shell

Figure 5

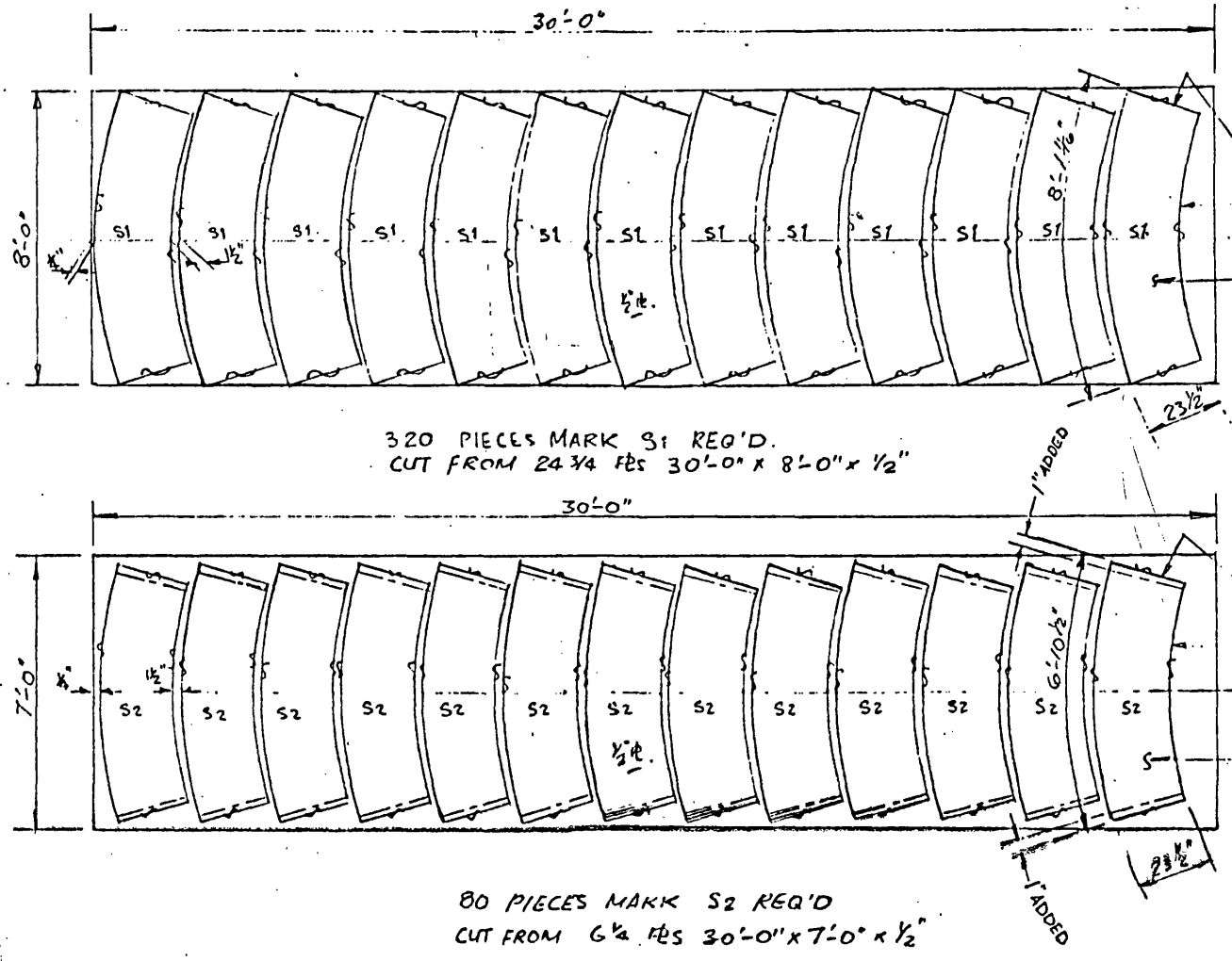

FIG. 6a

24 3/4	PCS 30'-0" x 8'-0" x 1/2"	C.S.		TITLE: PLATE LAYOUT.		
6 1/4	PCS 30'-0" x 7'-0" x 1/2"	C.S.				
					scale:	date: 31 – 7
					drawn:	checked:
				ref. draw'g	spec. section no.:	
q'd.	description	mat'l.	remarks	h no.	item	sketch no.: SK – – 16

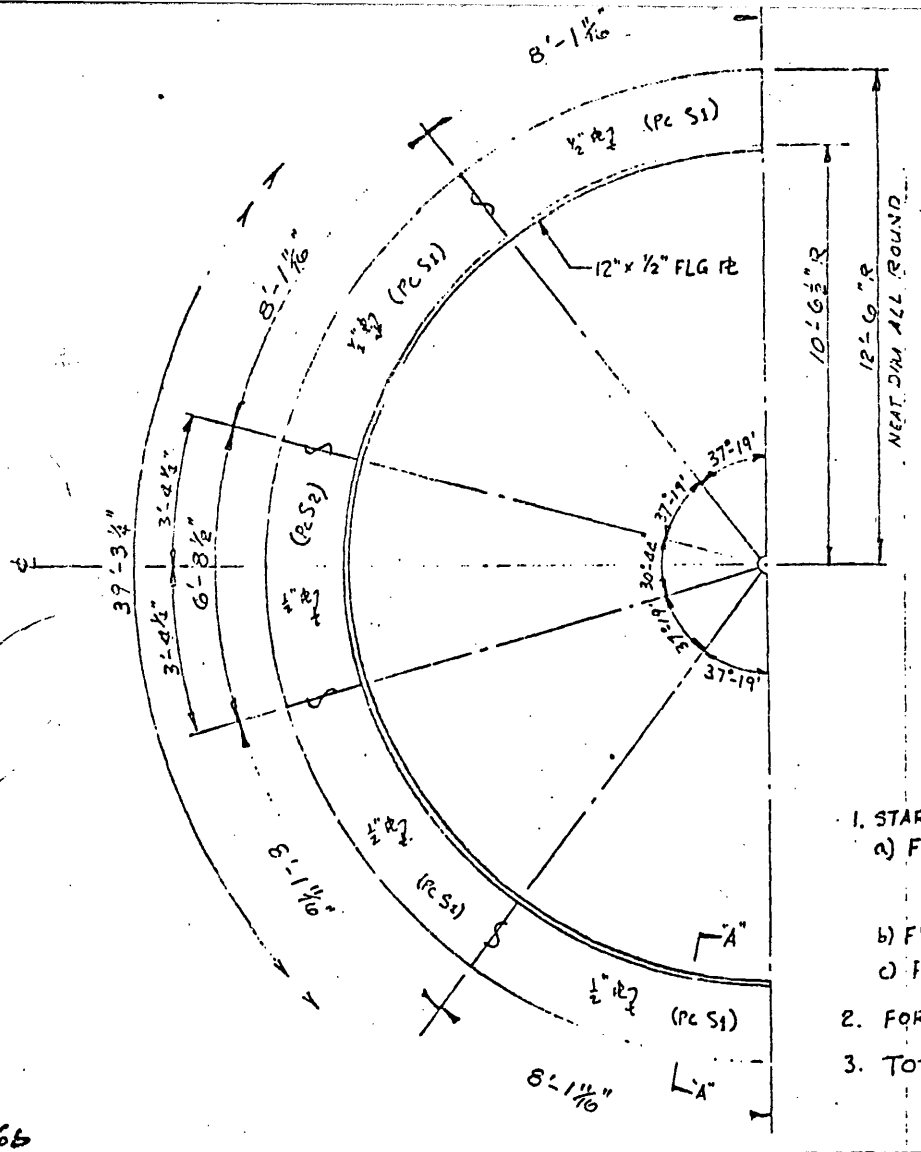

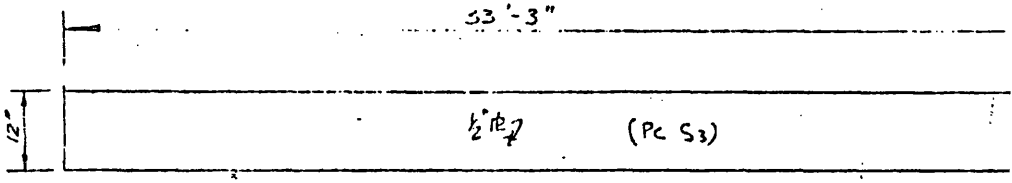

EXPANDED 12" x ½" FLG ℄

80 PIECES REQ'D.

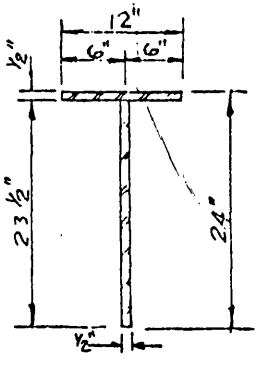

SECTION "H-A"

1. STARBOARD PONTOON REQ'D AT:-
   a) F'WD & AFT FRAMES — 2, 4 & 14 PORT SIDE ONLY.
      5, 6, 7, 9, 12 & 13 PORT & STARBOARD.
      10 & 11 STARBOARD SIDE ONLY.
   b) F'WD & AFT END OF PONTOON — 2 REQ'D.
   c) F'WD & AFT CORNERS OF PONTOON — 4 REQ'D.
2. FOR PORT PONTOON SIMILAR.
3. TOTAL REQ'D FOR TWO PONTOONS = 80 PIECES.

NOTE:
SEE SK- 76 & SK-7
FOR ℄ LAYOUT.

FIG. 66

qty'd	description	mat'l.	remarks

TITLE:
SEMI-CIRCUS TRANS FRAMES
SIDE CHORD.

ref. drawg
h no. 2. item

scale:
date: 29 - 7
drawn:
checked:
spec. section no.:
sketch no.: SK- - 7a

$E/\sigma_y = 841$, $R/t = 133.3$, $L/R = 0.675$

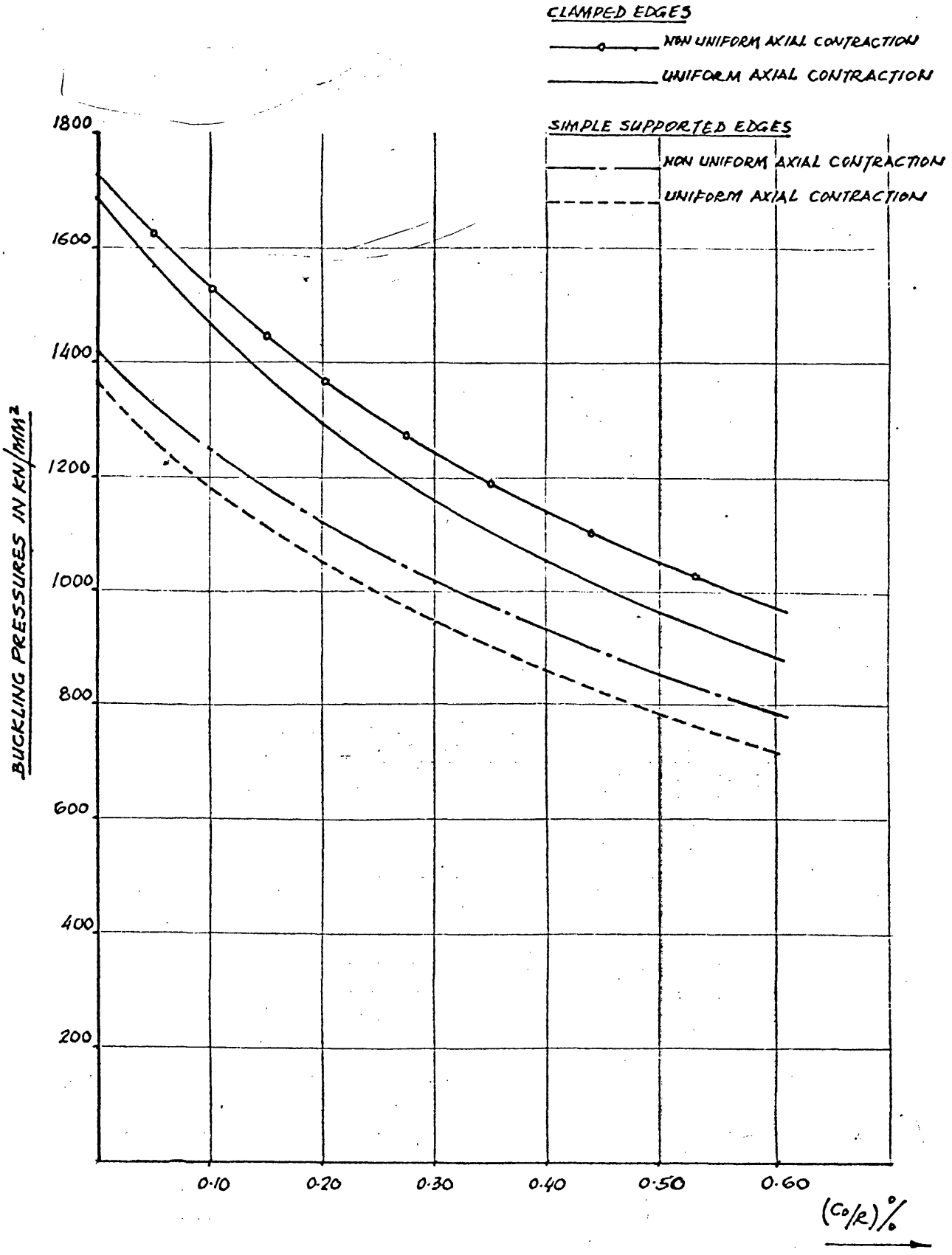

FIG.7 COMPARISON BETWEEN UNIFORM & NON-UNIFORM AXIAL CONTRACTION IN THE PREBUCKLING DISPLACEMENTS

DIMENSIONS: $R = 800\,mm$, $t = 6.0\,mm$, $l = 600\,mm$
$E = 207\ kN/mm^2$.

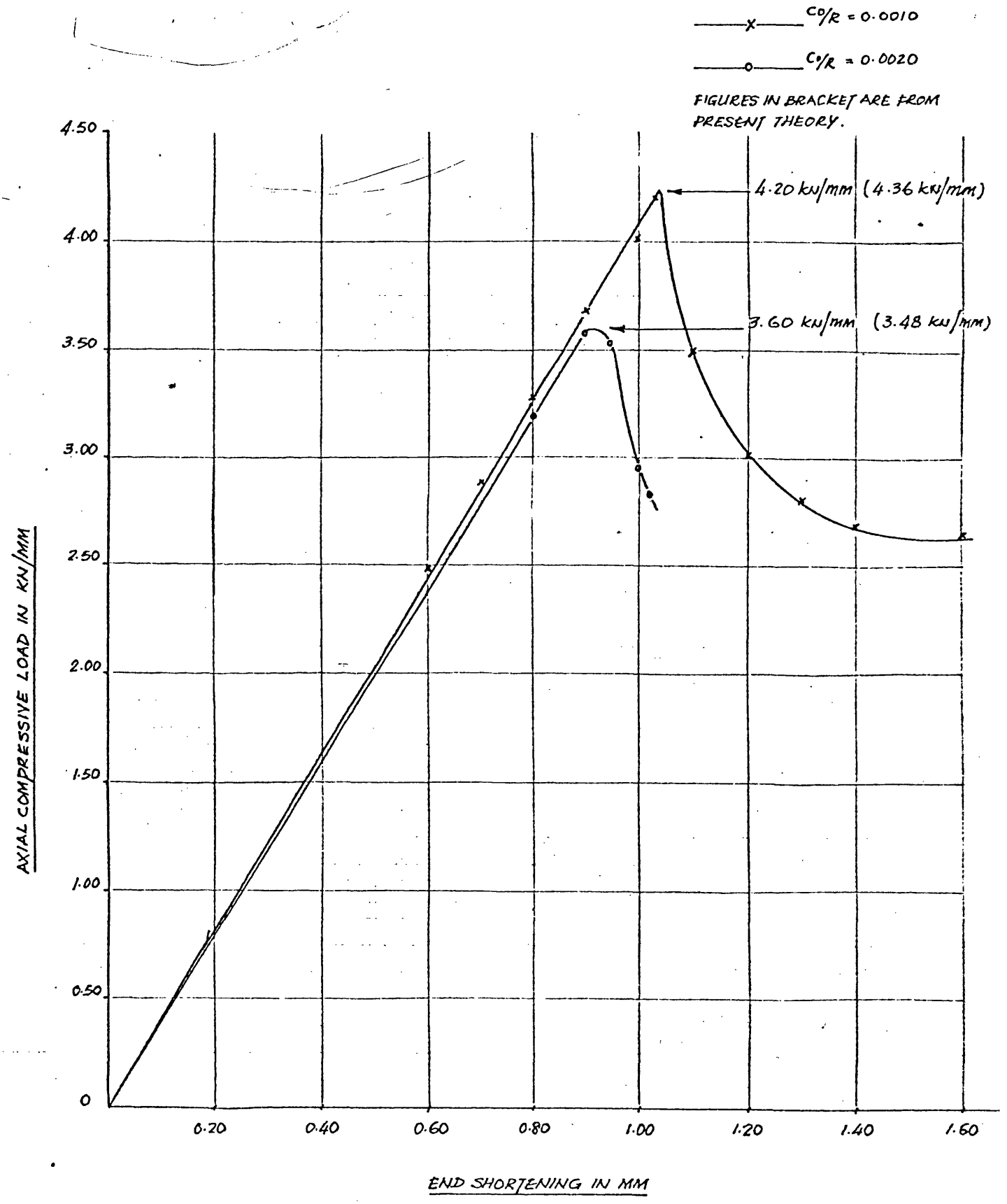

FIG. 8 COMPARISON OF PRESENT THEORY & DYNAMIC RELAXATION FINITE DIFFERENCE METHOD

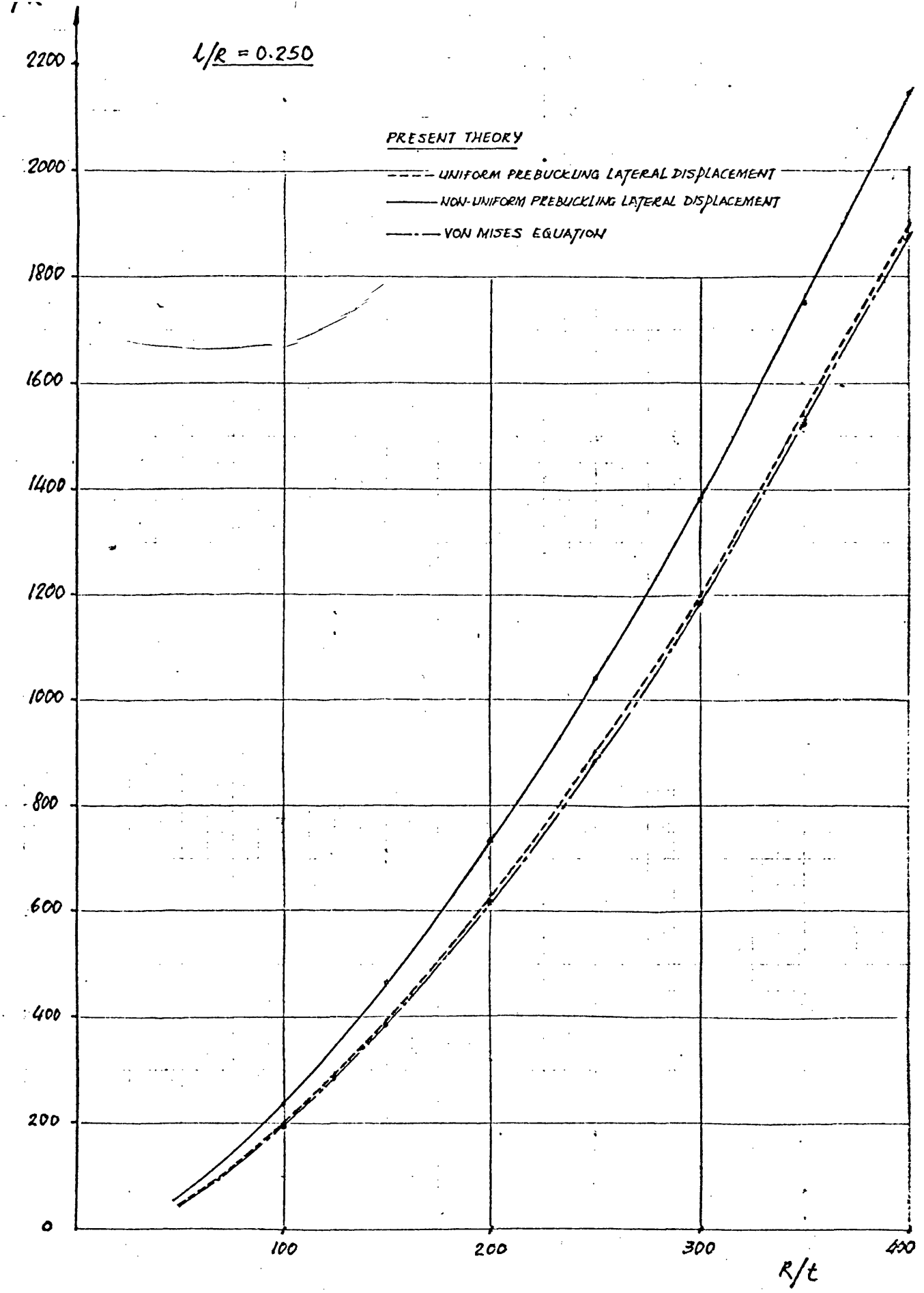

FIG. 9 COMPARISON BETWEEN PRESENT THEORY & VON MISES EQUATION

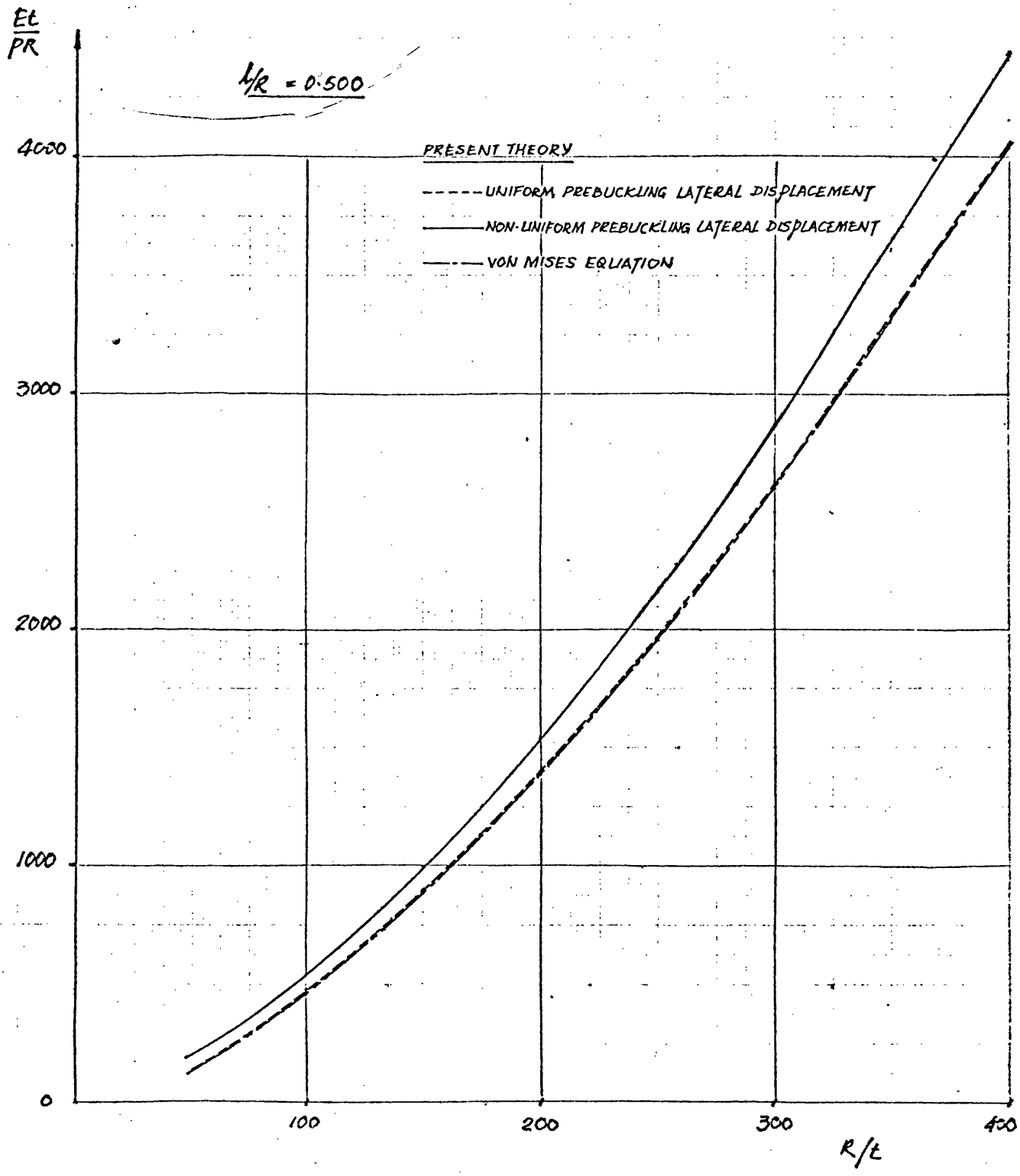

FIG.10 COMPARISON BETWEEN PRESENT THEORY & VON MISES EQUATION

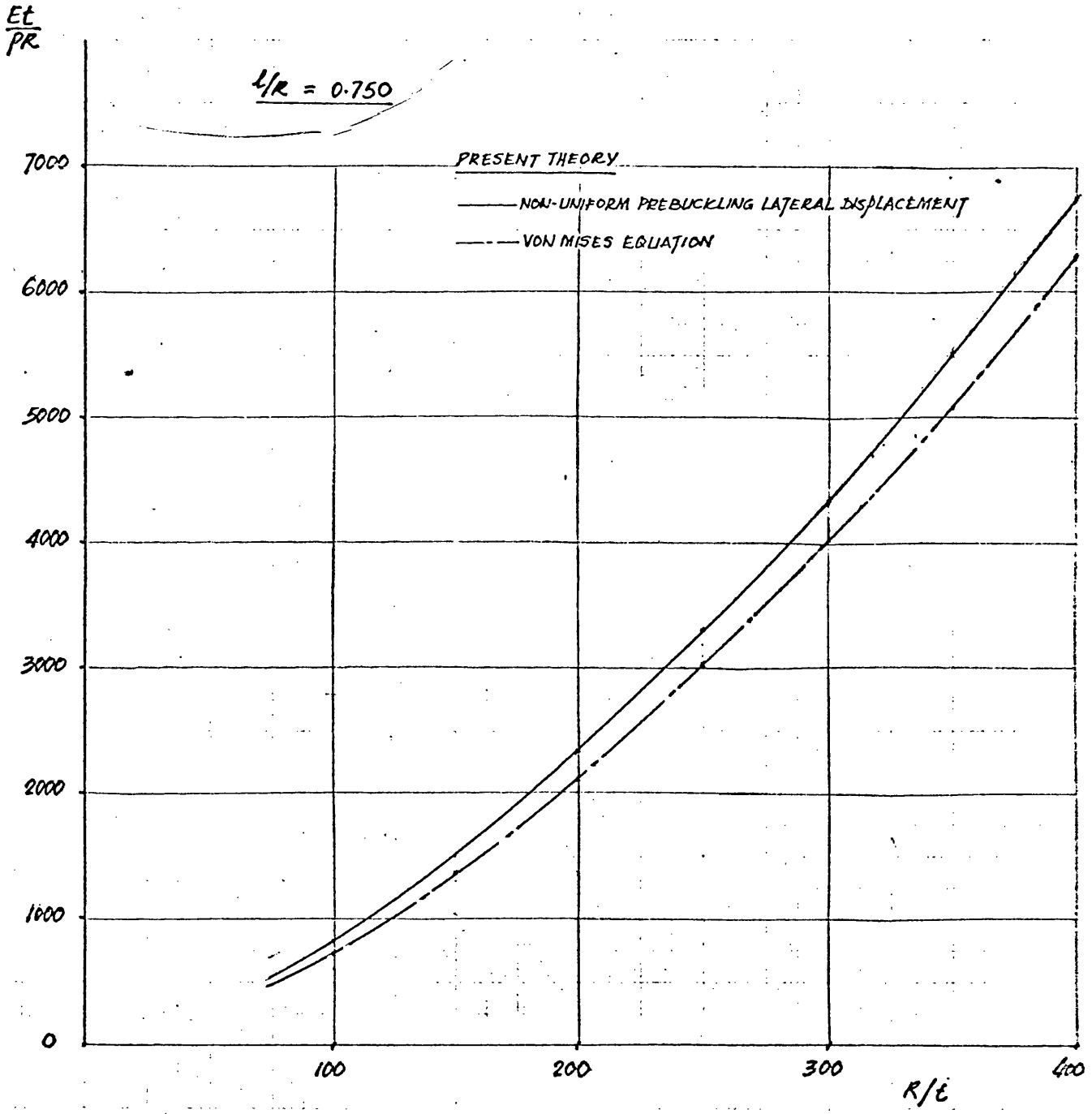

FIG. 11 COMPARISON BETWEEN PRESENT THEORY & VON MISES EQUATION

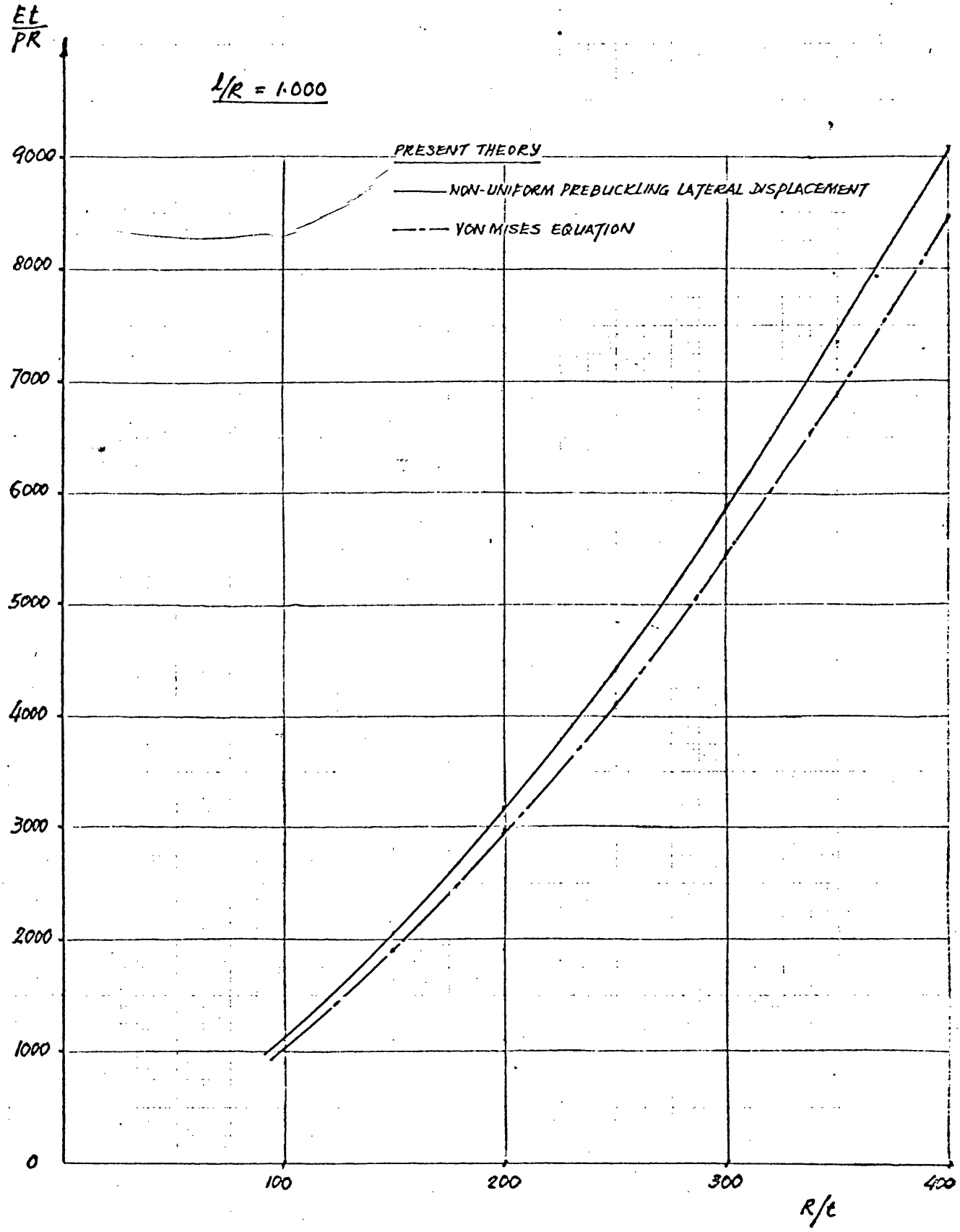

FIG. 12 COMPARISON BETWEEN PRESENT THEORY & VON MISES EQUATION

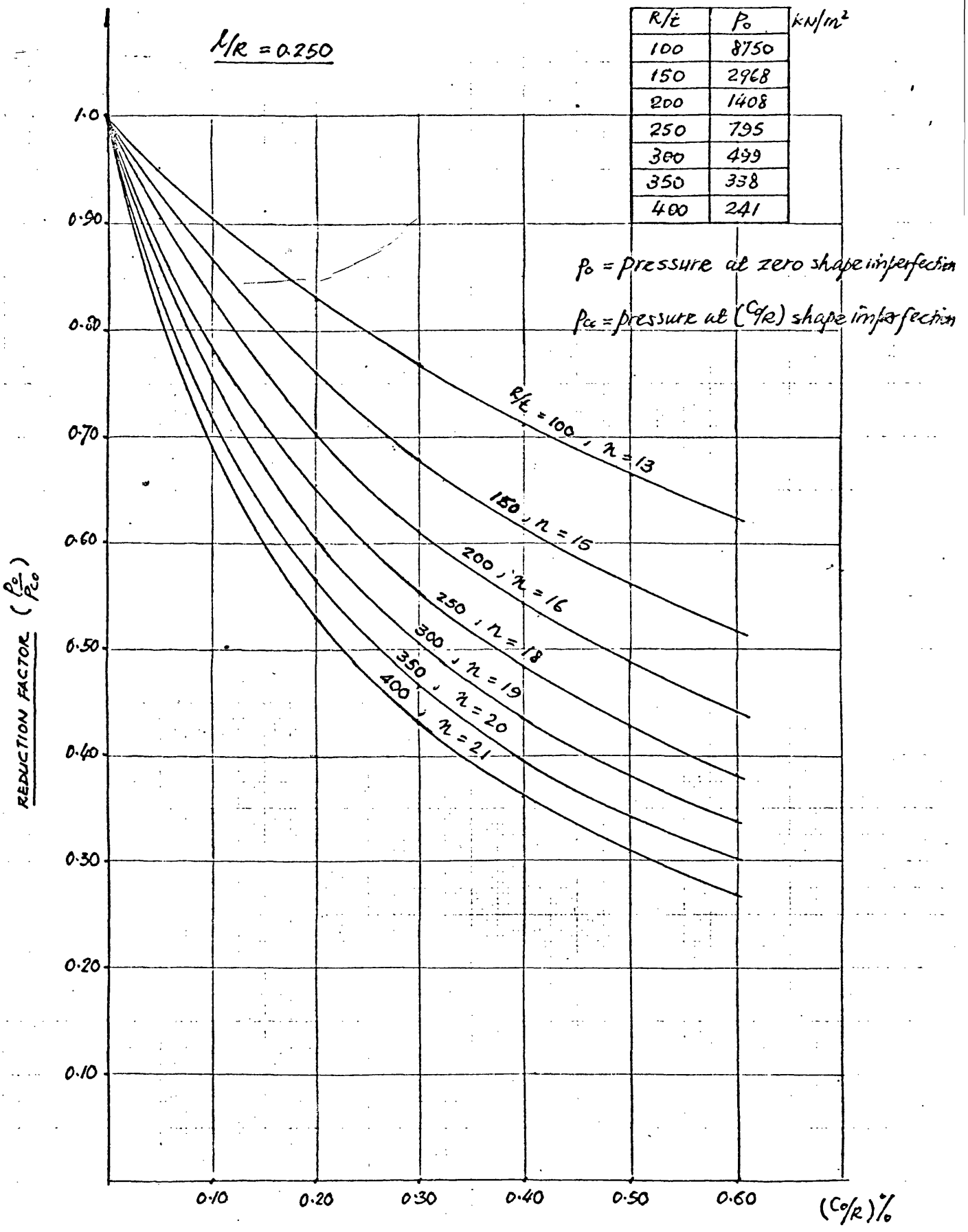

FIG.13 IMPERFECTION SENSITIVITY OF CYLINDERS UNDER UNIFORM EXTERNAL PRESSURE

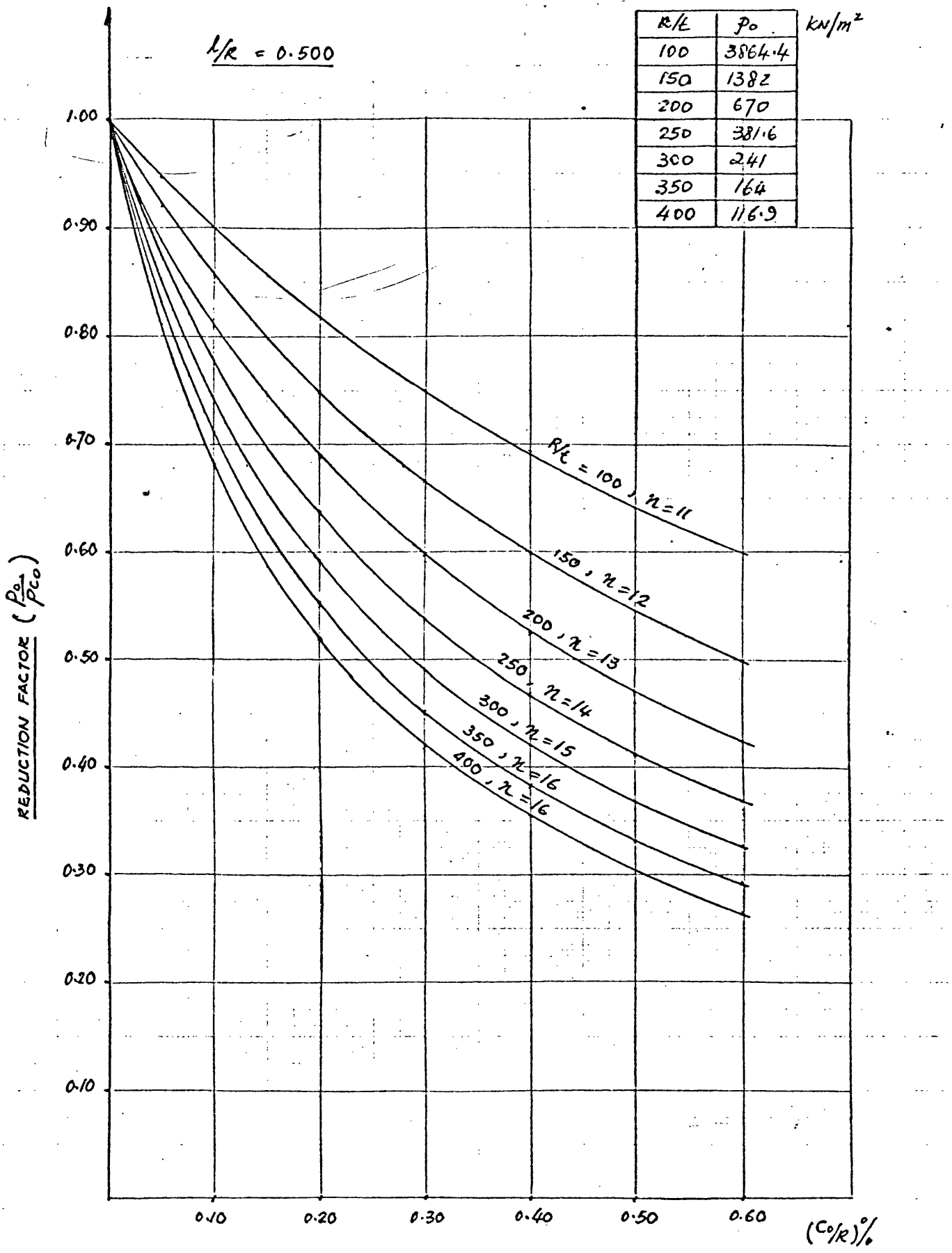

FIG.14 IMPERFECTION SENSITIVITY OF CYLINDERS UNDER UNIFORM EXTERNAL PRESSURE

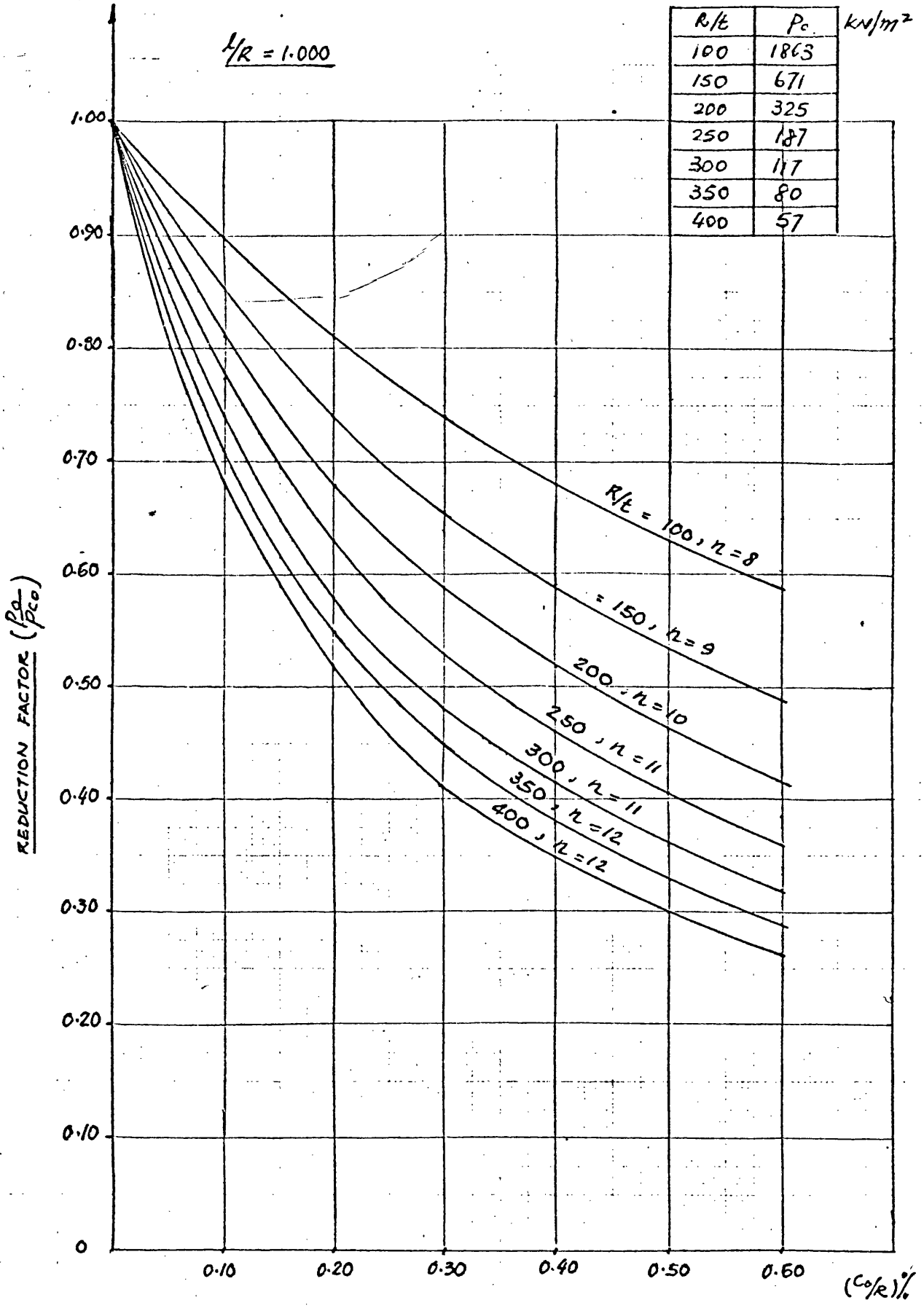

FIG.15 IMPERFECTION SENSITIVITY OF CYLINDERS UNDER UNIFORM EXTERNAL PRESSURE

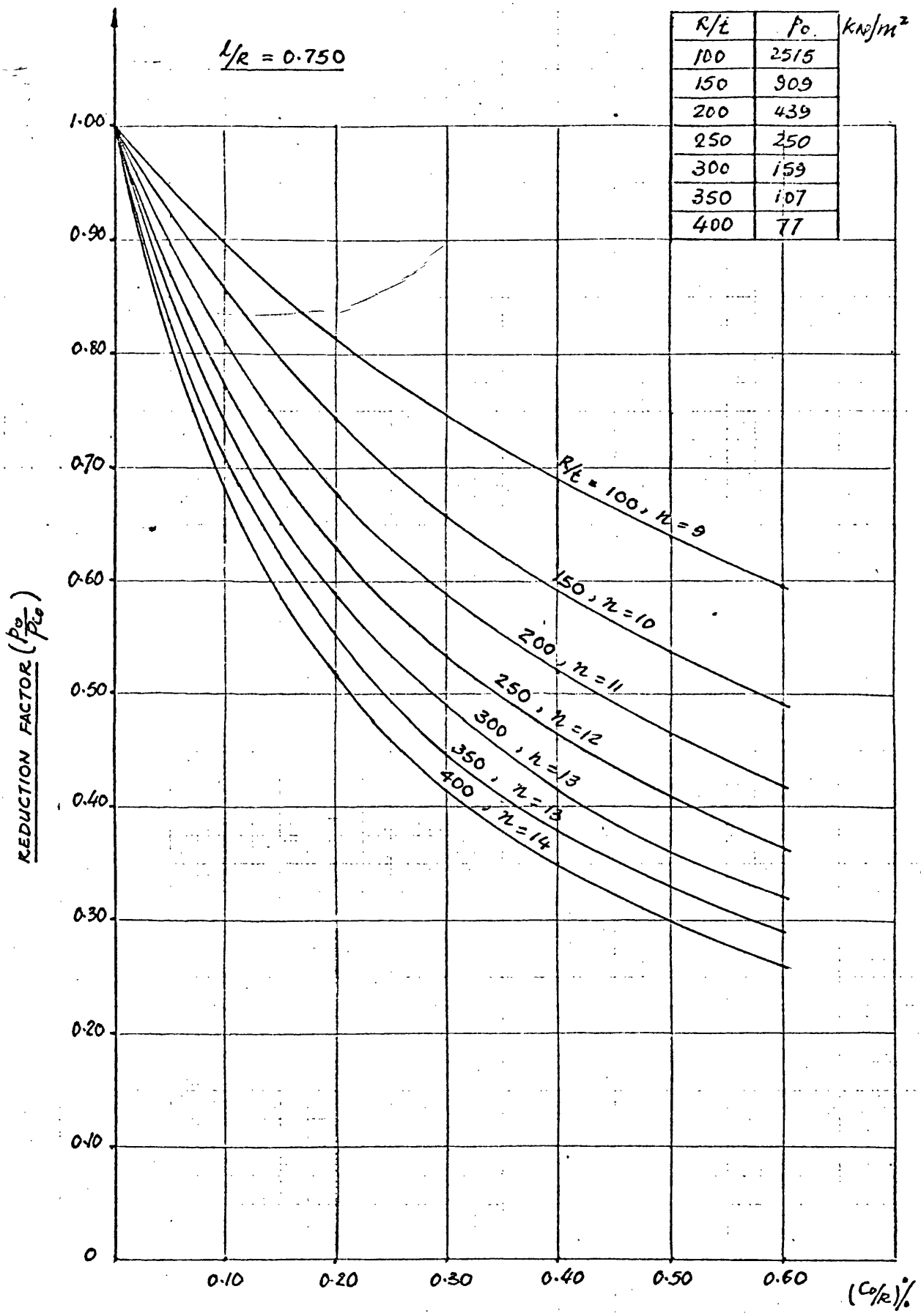

FIG.16 IMPERFECTION SENSITIVITY OF CYLINDERS UNDER UNIFORM EXTERNAL PRESSURE

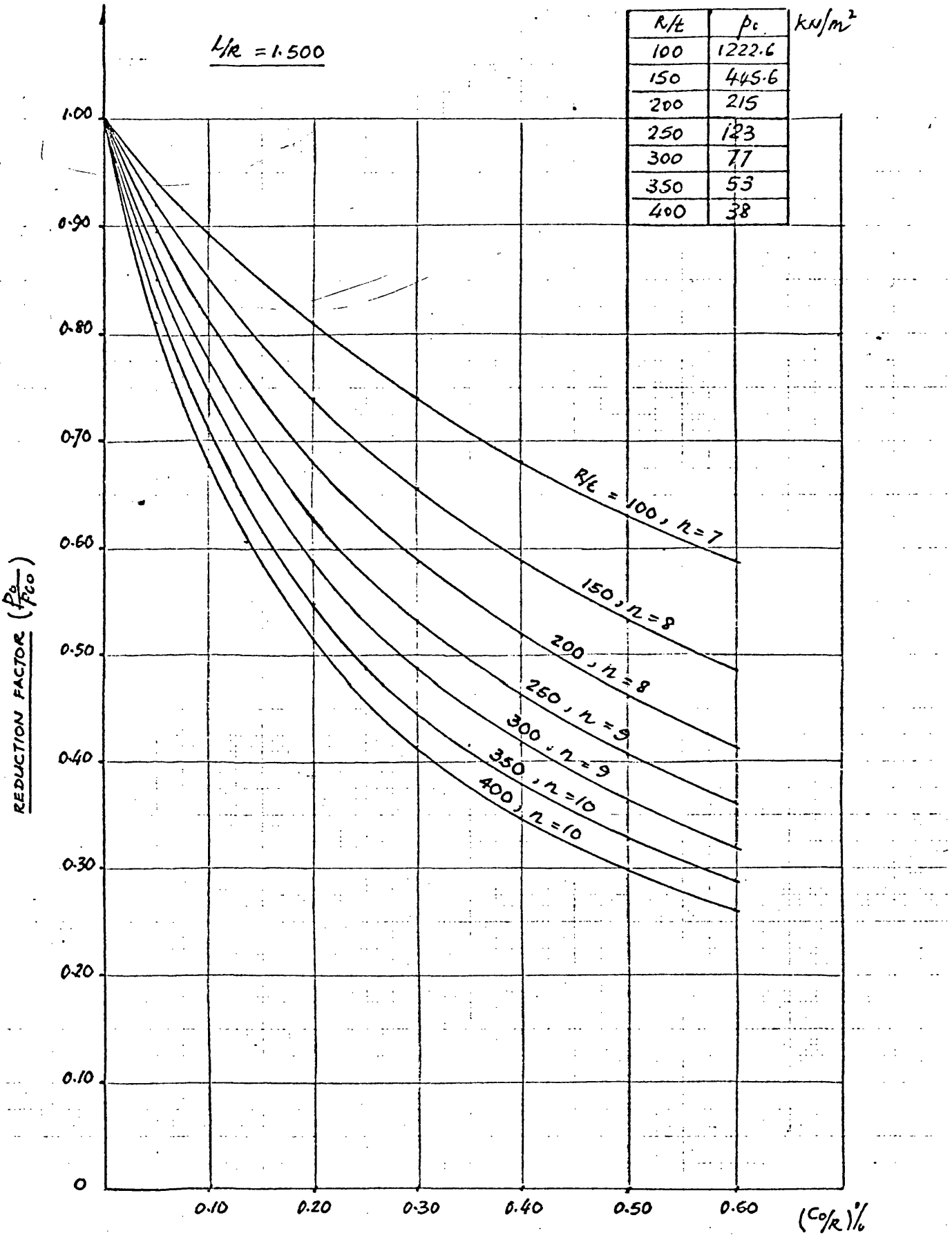

FIG.17 IMPERFECTION SENSITIVITY OF CYLINDERS UNDER UNIFORM EXTERNAL PRESSURE

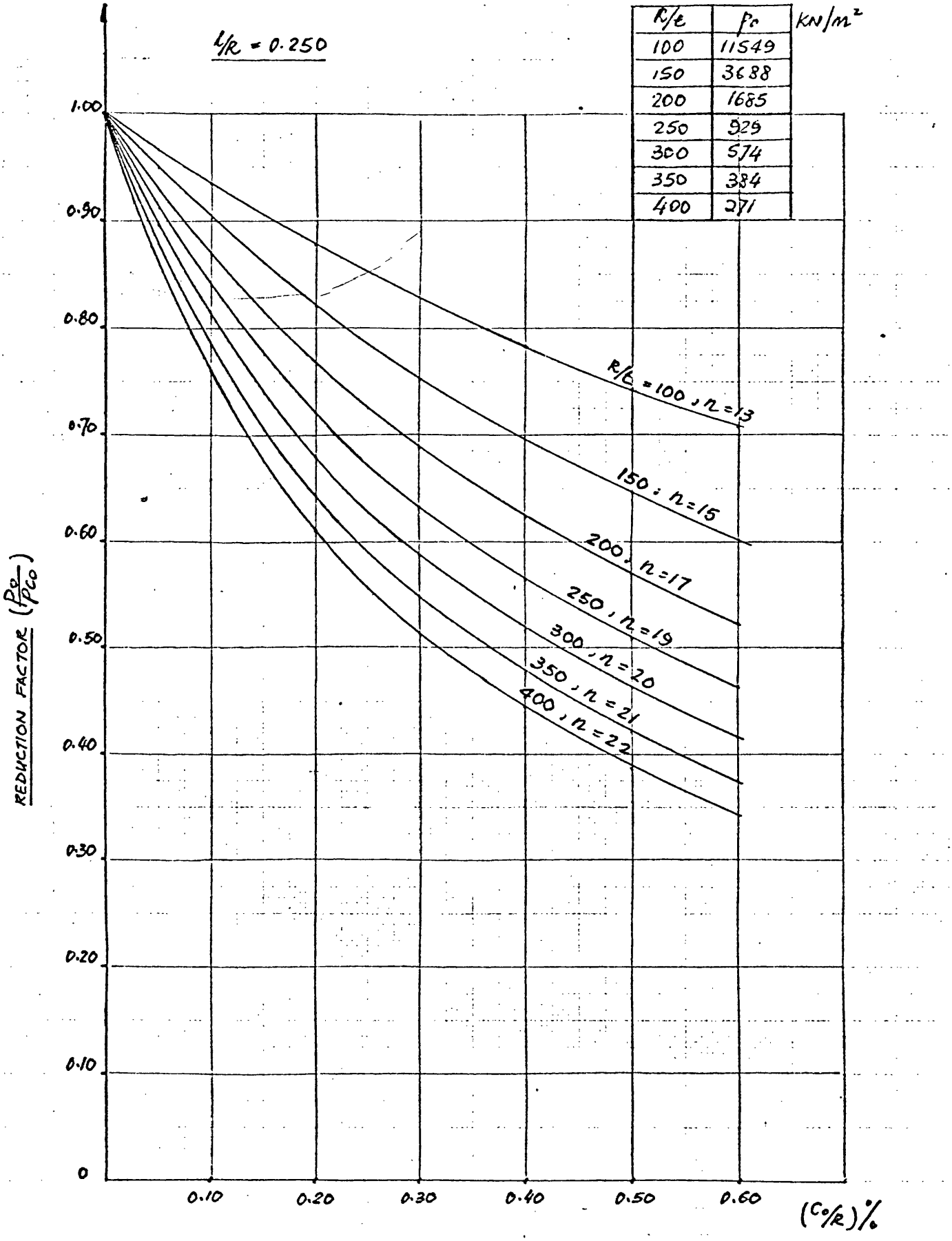

FIG.18 IMPERFECTION SENSITIVITY OF CYLINDERS UNDER RADIAL PRESSURE

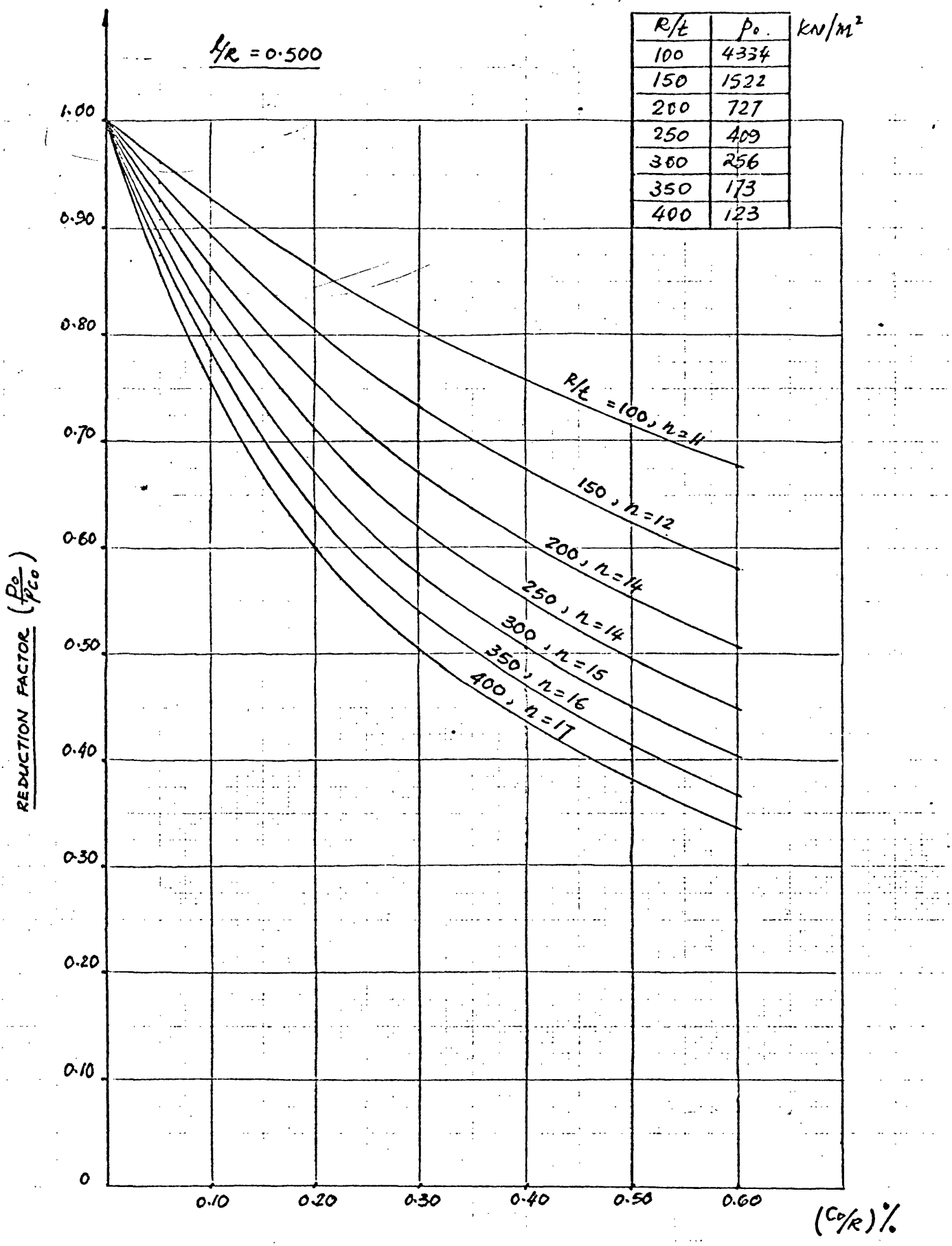

FIG.19 IMPERFECTION SENSITIVITY OF CYLINDERS UNDER RADIAL PRESSURE

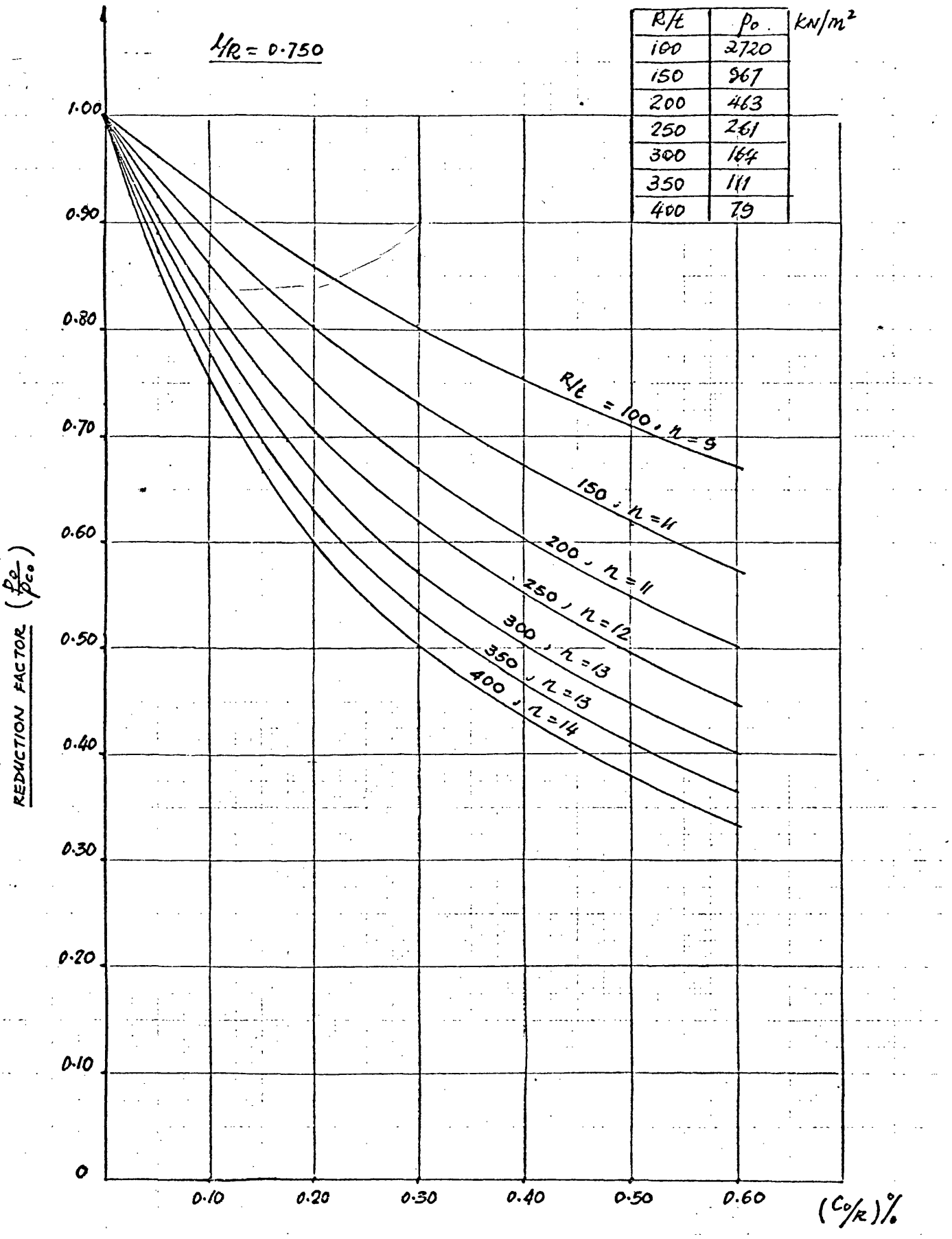

FIG. 20 IMPERFECTION SENSITIVITY OF CYLINDERS UNDER RADIAL PRESSURE

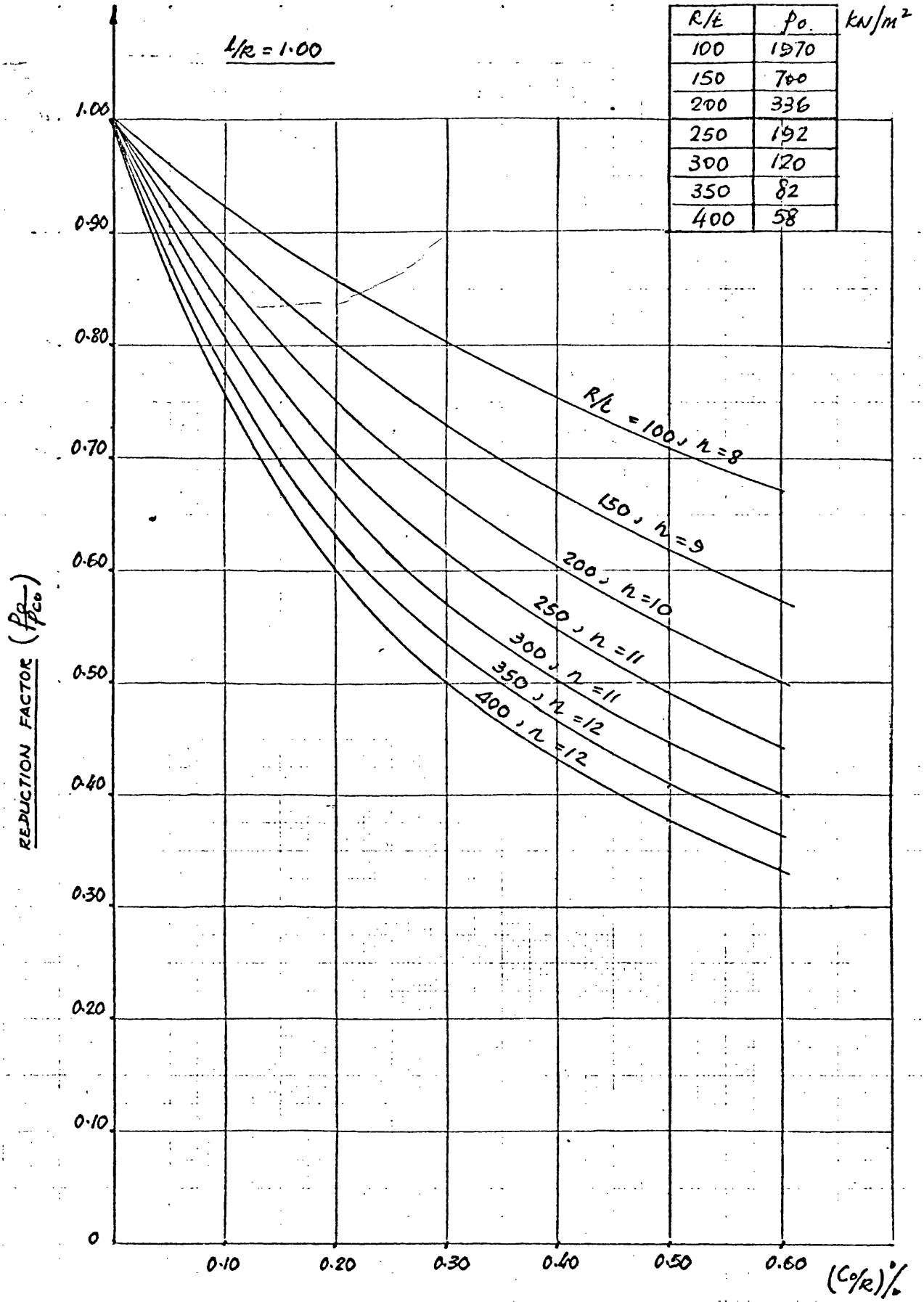

FIG.21 IMPERFECTION SENSITIVITY OF CYLINDERS UNDER RADIAL PRESSURE

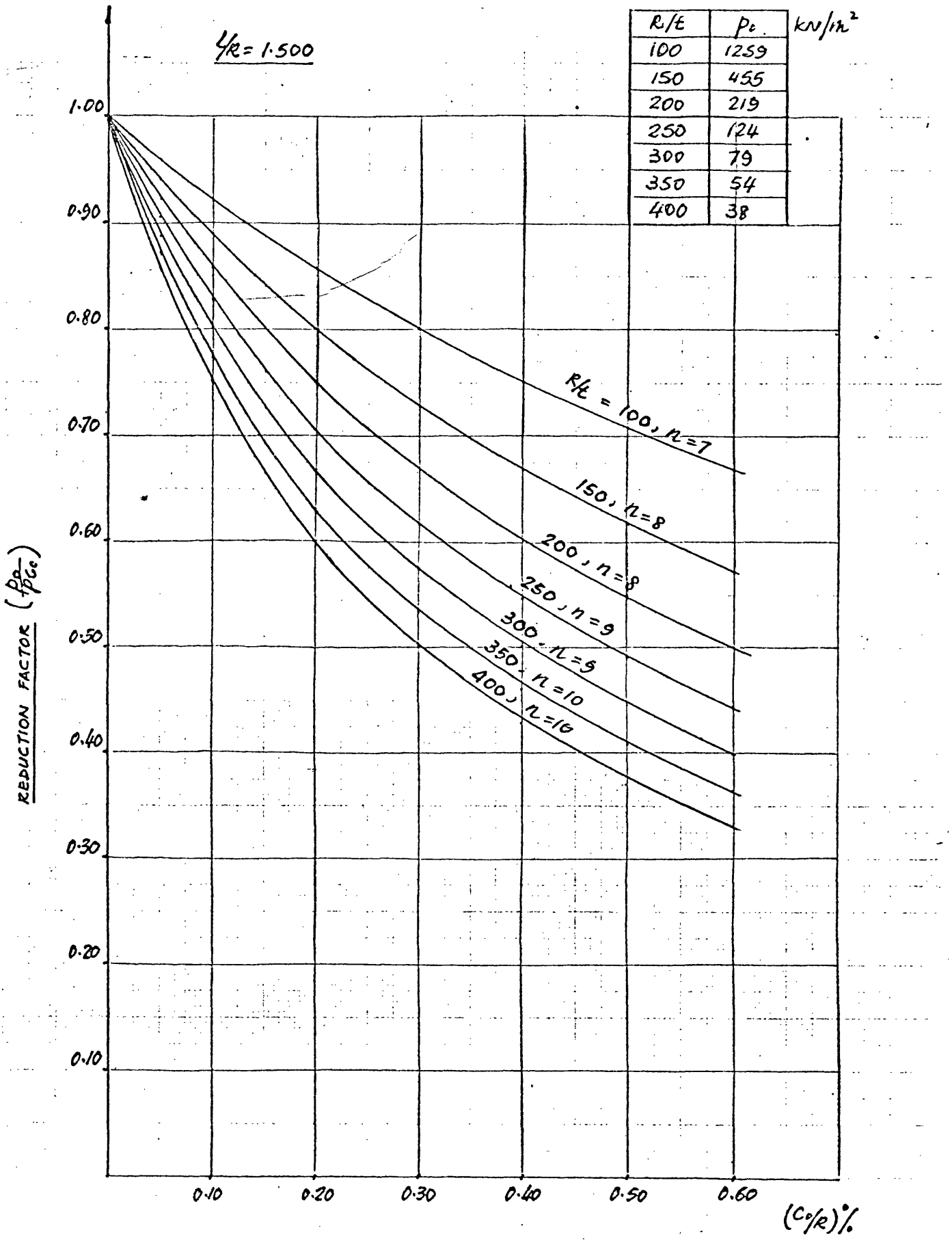

FIG. 22 IMPERFECTION SENSITIVITY OF CYLINDERS UNDER RADIAL PRESSURE

$L/R = 1.00$ $\quad \sigma_y = 246\ N/mm^2$

R/t	N_{x_0} (kN/mm)
100	9.25
150	4.02
200	2.22
250	1.39
300	0.945

N_{x_0} = axial load at zero shape imperfecti

$N_{x_{co}}$ = axial load at (c_0/t) shape imperfecti

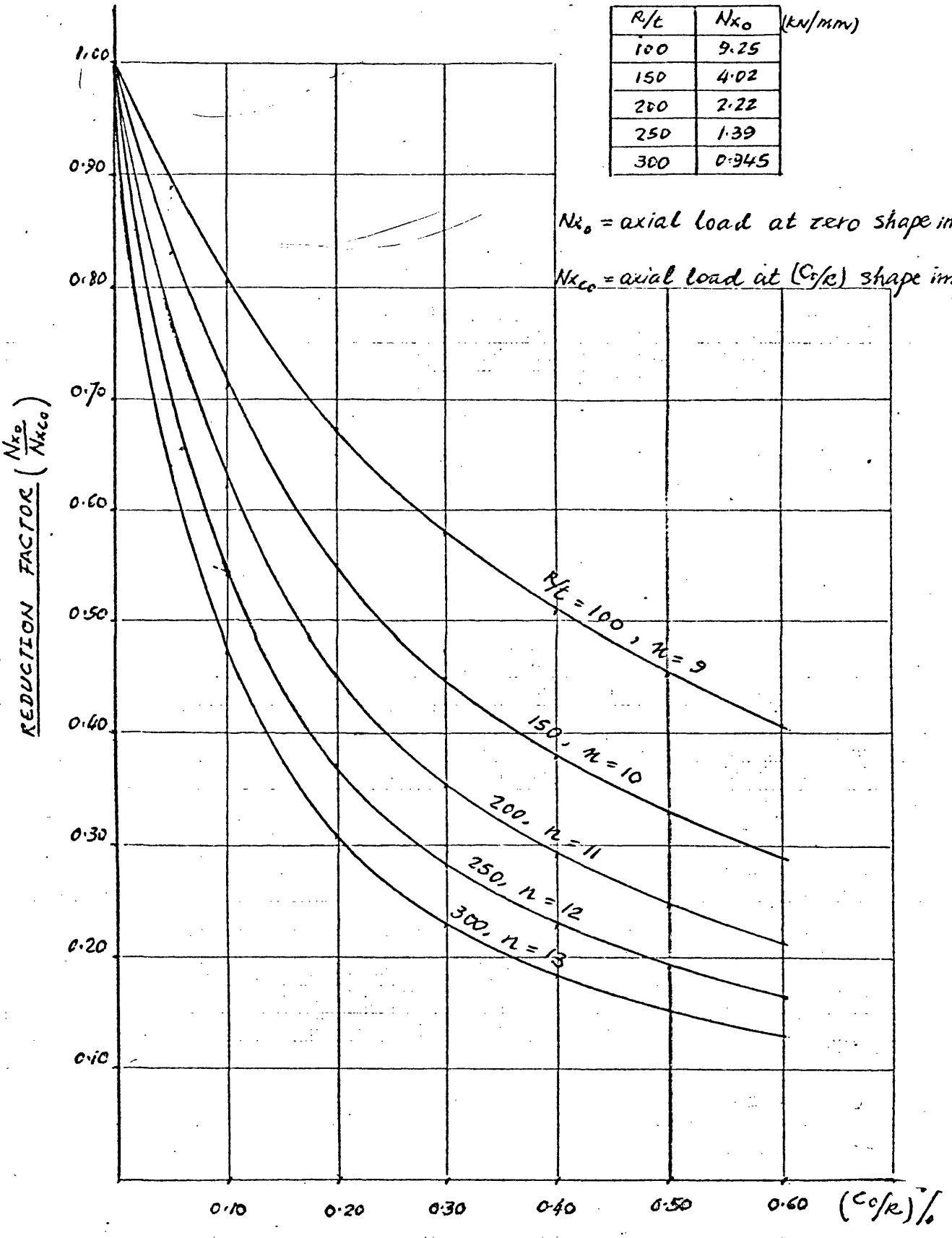

FIG. 23 IMPERFECTION SENSITIVITY OF CYLINDERS UNDER AXIAL COMPRESSION

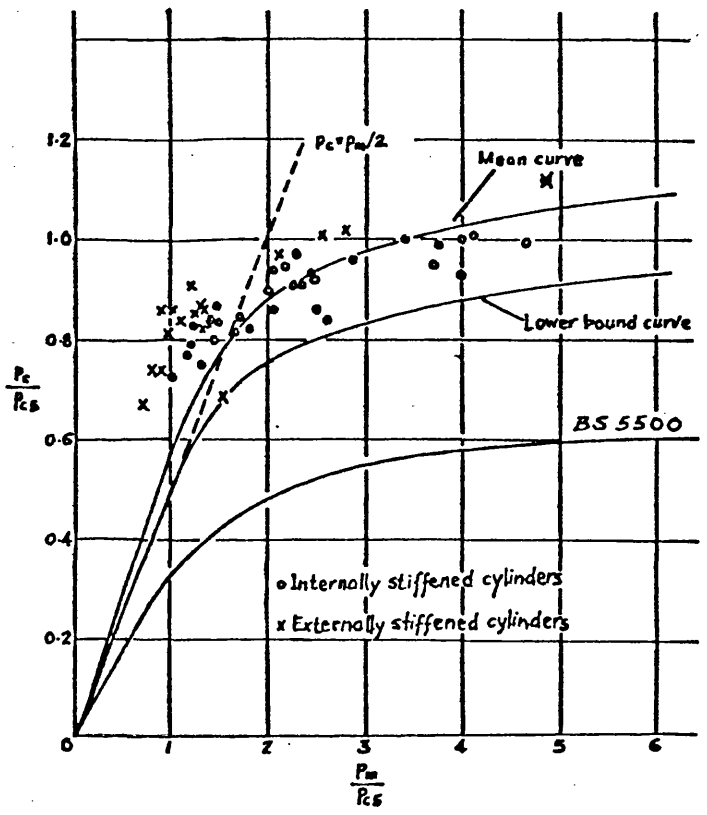

FIG. 24 PLOT OF INTERSTIFFENER COLLAPSE RESULTS

$L/R = 0.250$ $\frac{E}{\sigma_y} = 841$

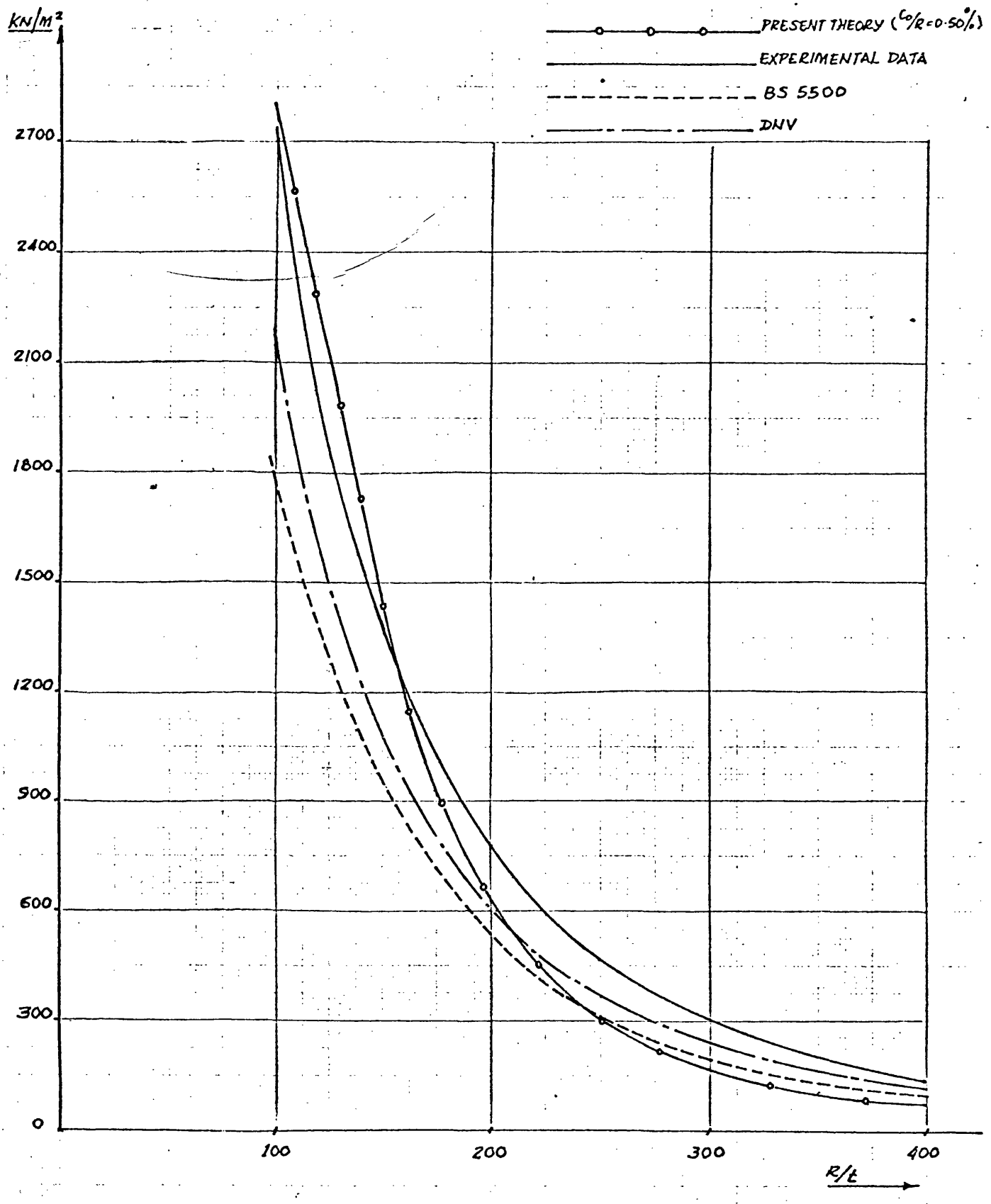

FIG.25 ANALYTICAL CURVES & DESIGN RULES - UNIFORM EXTERNAL PRESSURE

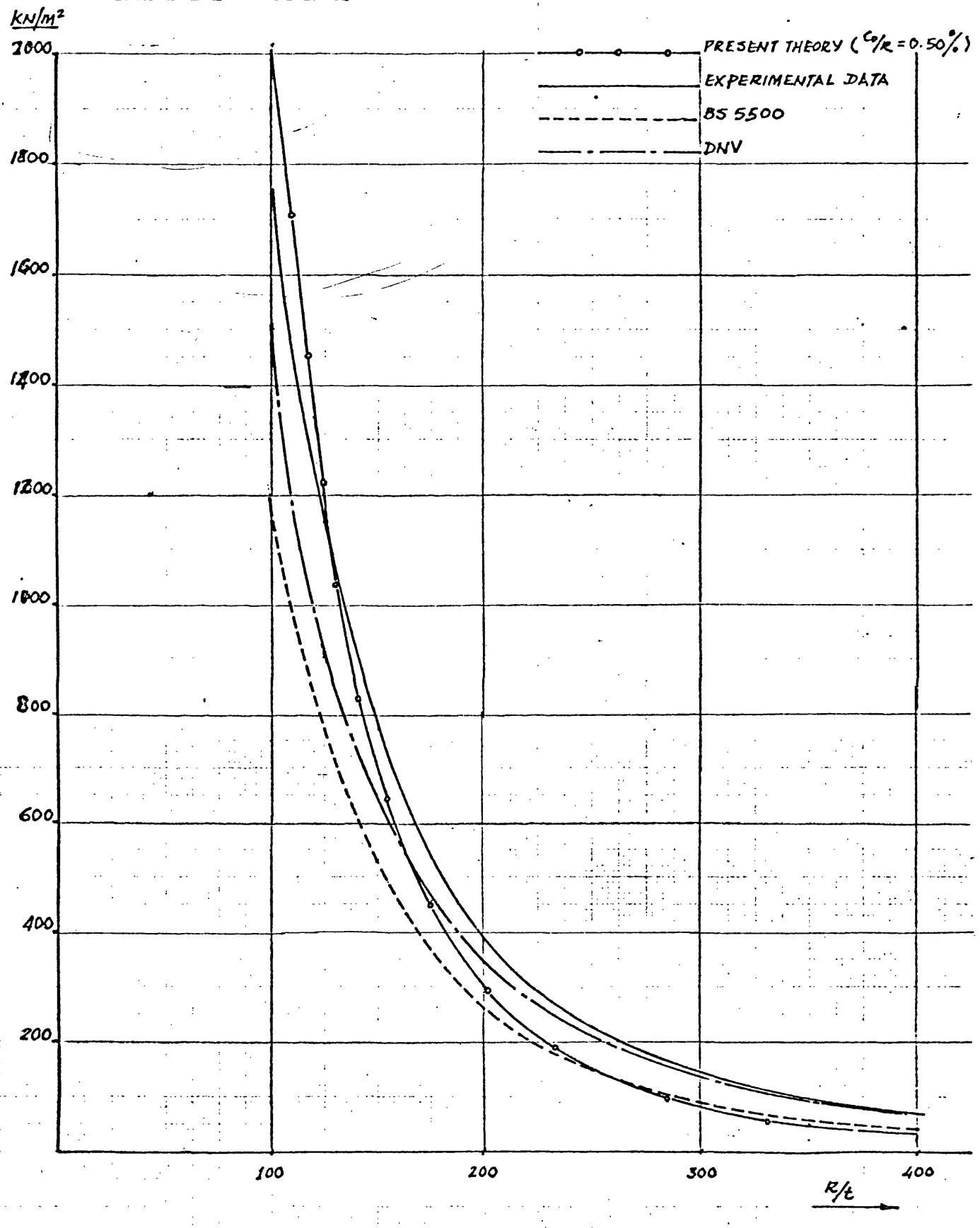

FIG.26 ANALYTICAL CURVES & DESIGN RULES - UNIFORM EXTERNAL PRESSURE

$L/R = 0.750$ $\frac{E}{\sigma_y} = 841$

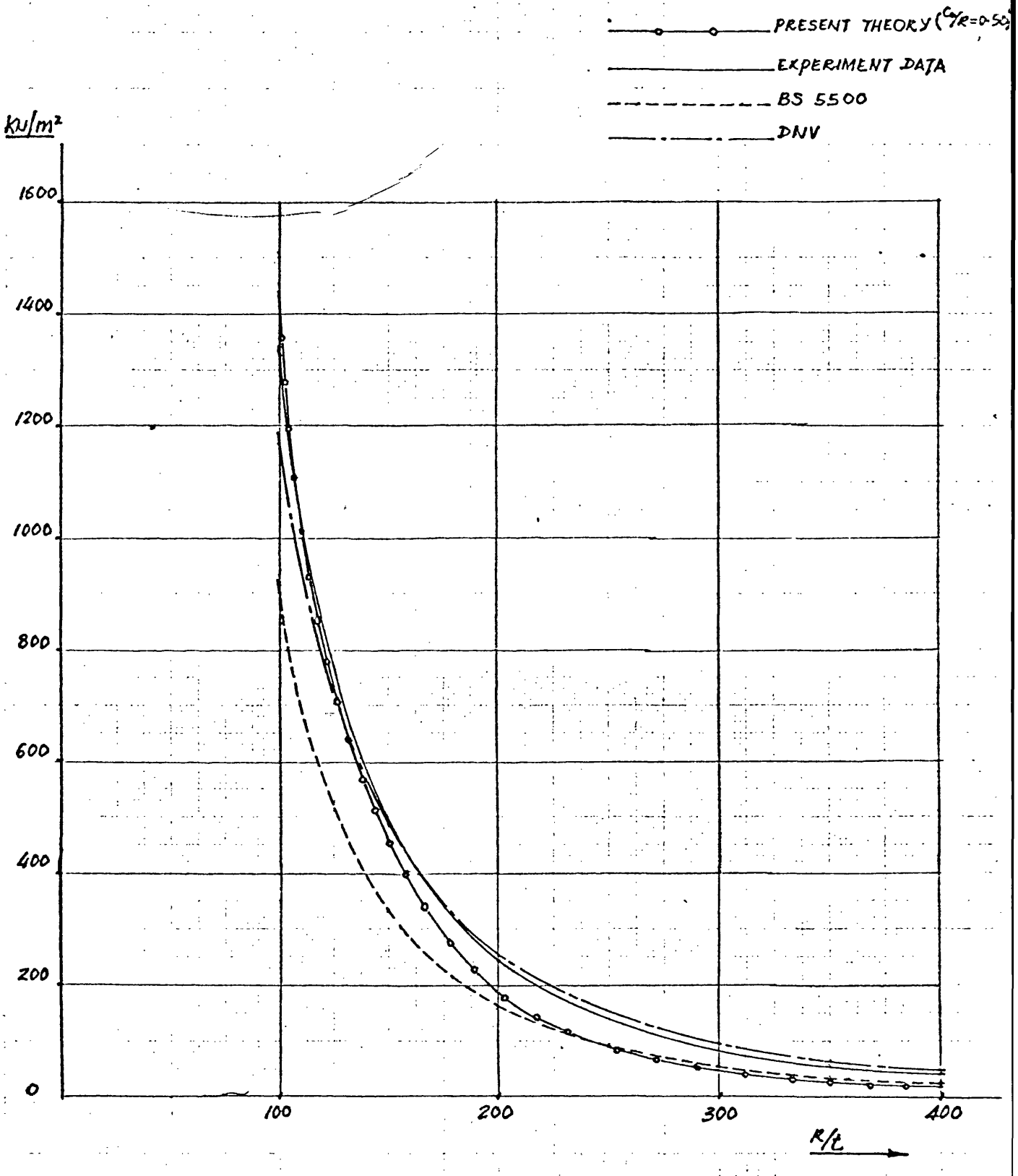

FIG. 27 ANALYTICAL CURVES & DESIGN RULES - UNIFORM EXTERNAL PRESSURE

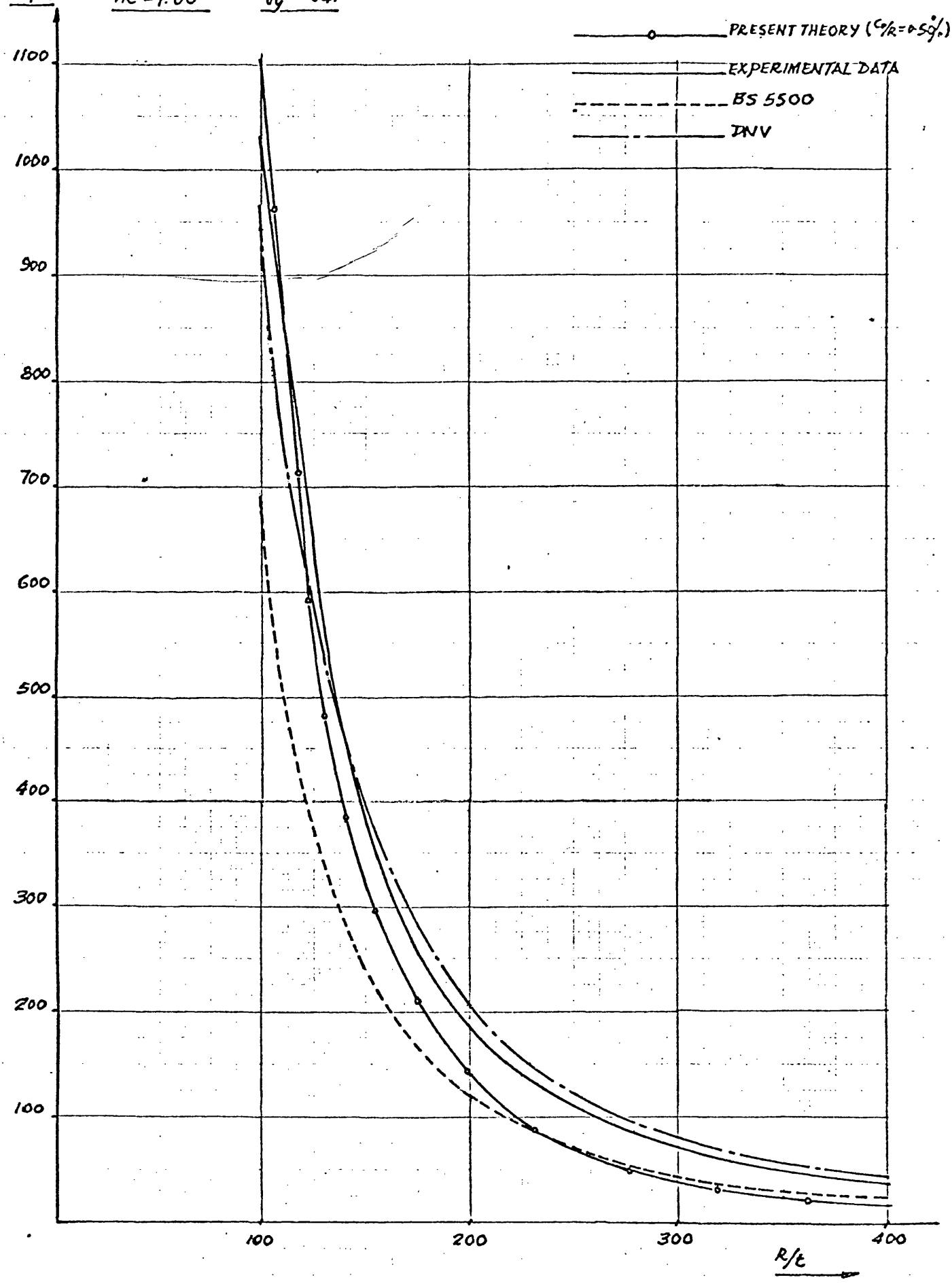

FIG. 28 ANALYTICAL CURVES & DESIGN RULES - UNIFORM EXTERNAL PRESSURE

$L/R = 1.500$ $\frac{E}{\sigma_y} = 841$

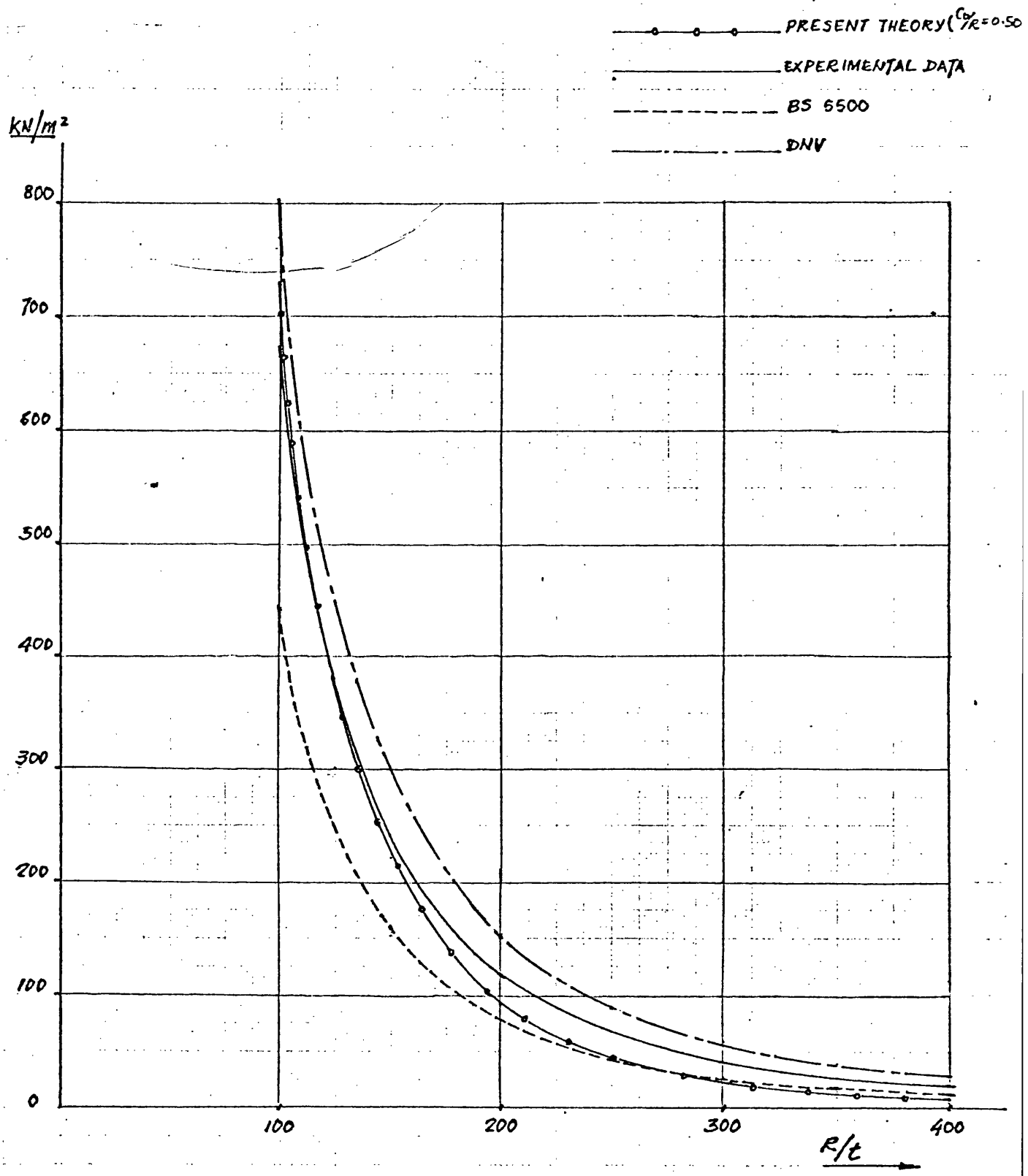

FIG. 29 ANALYTICAL CURVES & DESIGN RULES - UNIFORM EXTERNAL PRESSURE

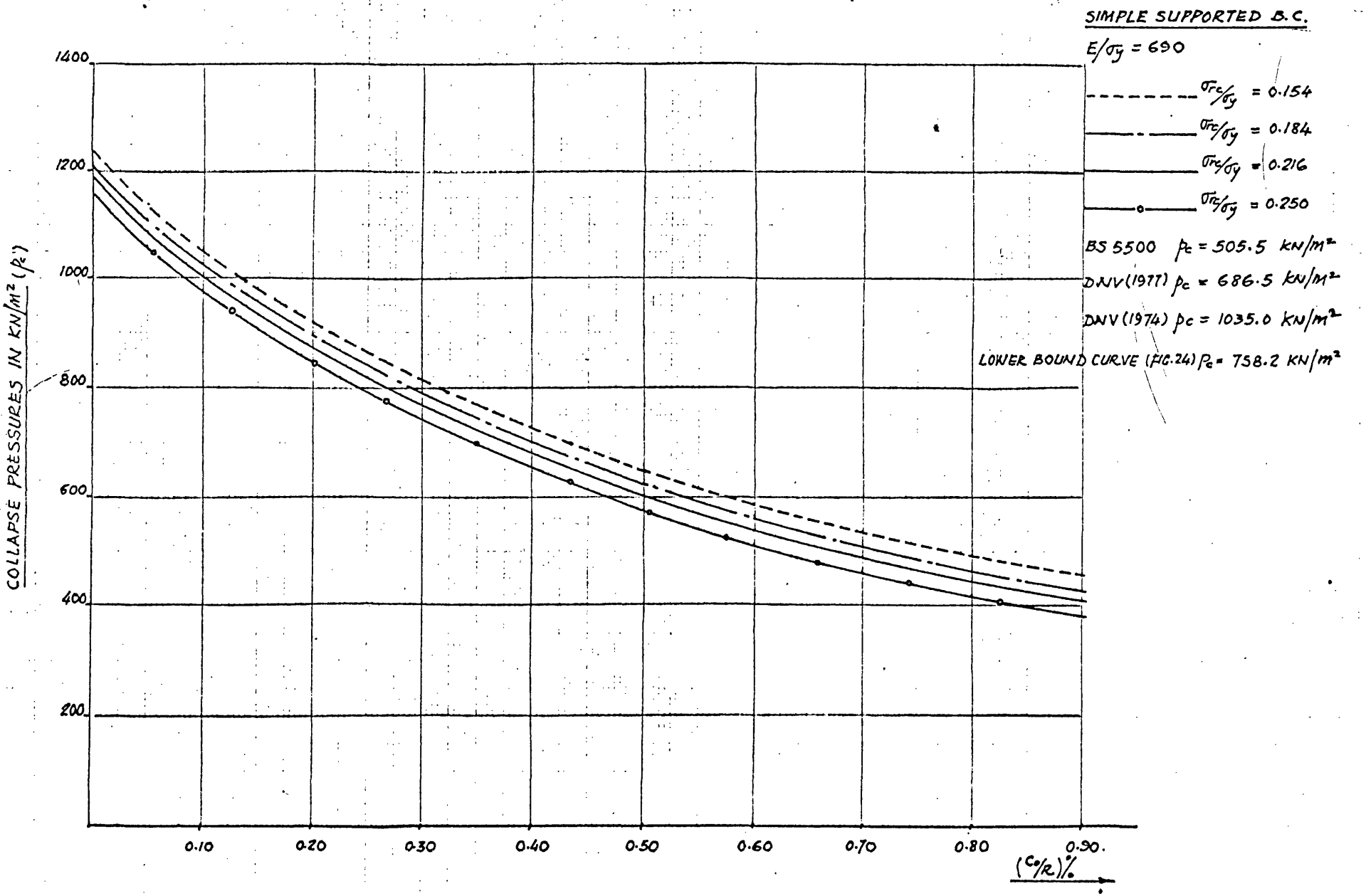

FIG.30 DPI FRIGG FIELD BUOYANCY TANK UNDER UNIFORM EXTERNAL PRESSURE

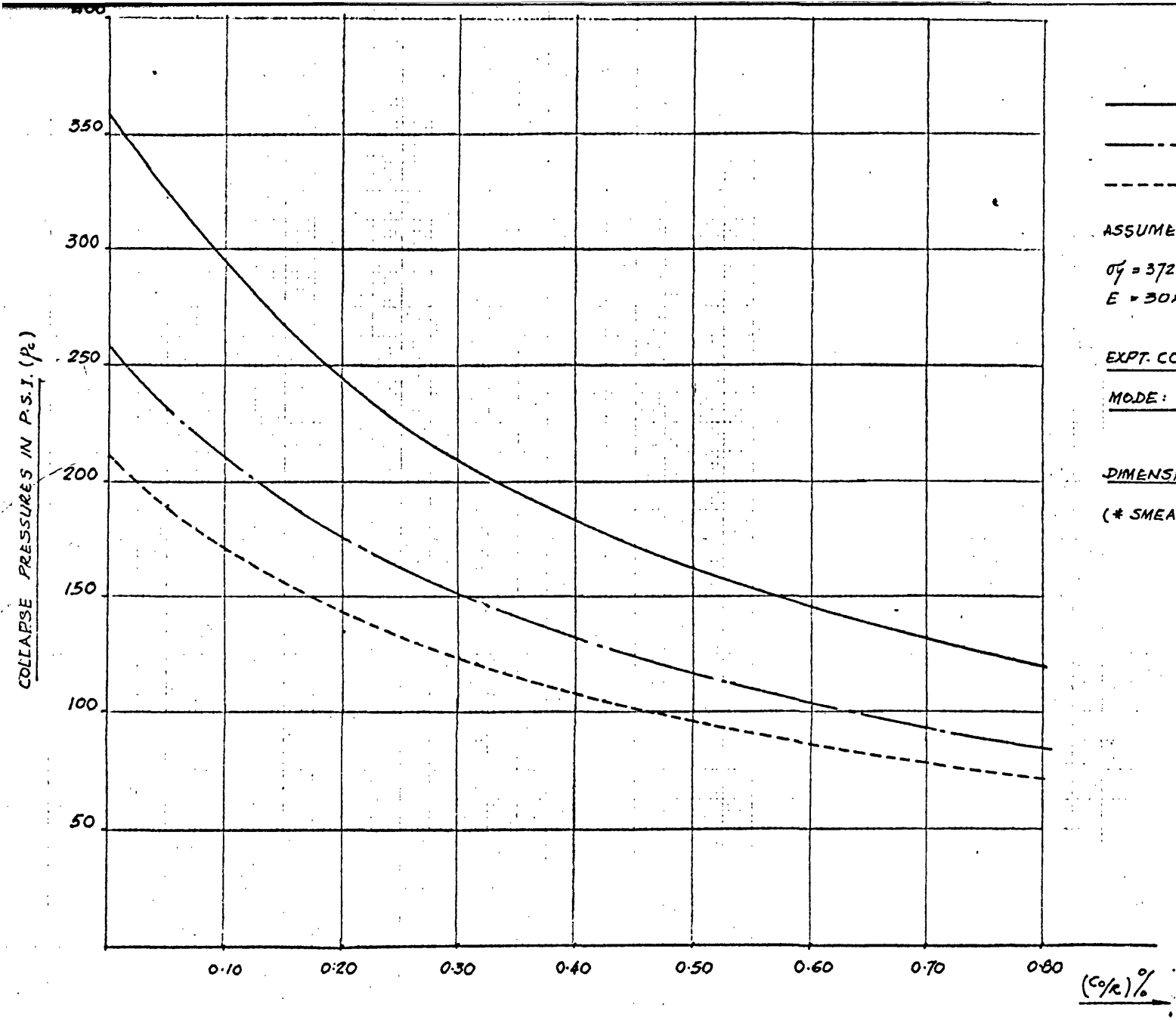

FIG. 31 COMPARISON OF THEORETICAL & EXPERIMENTAL COLLAPSE PRESSURES OF KNIRA'S 1/5 SCALE MODEL. REF. (96)

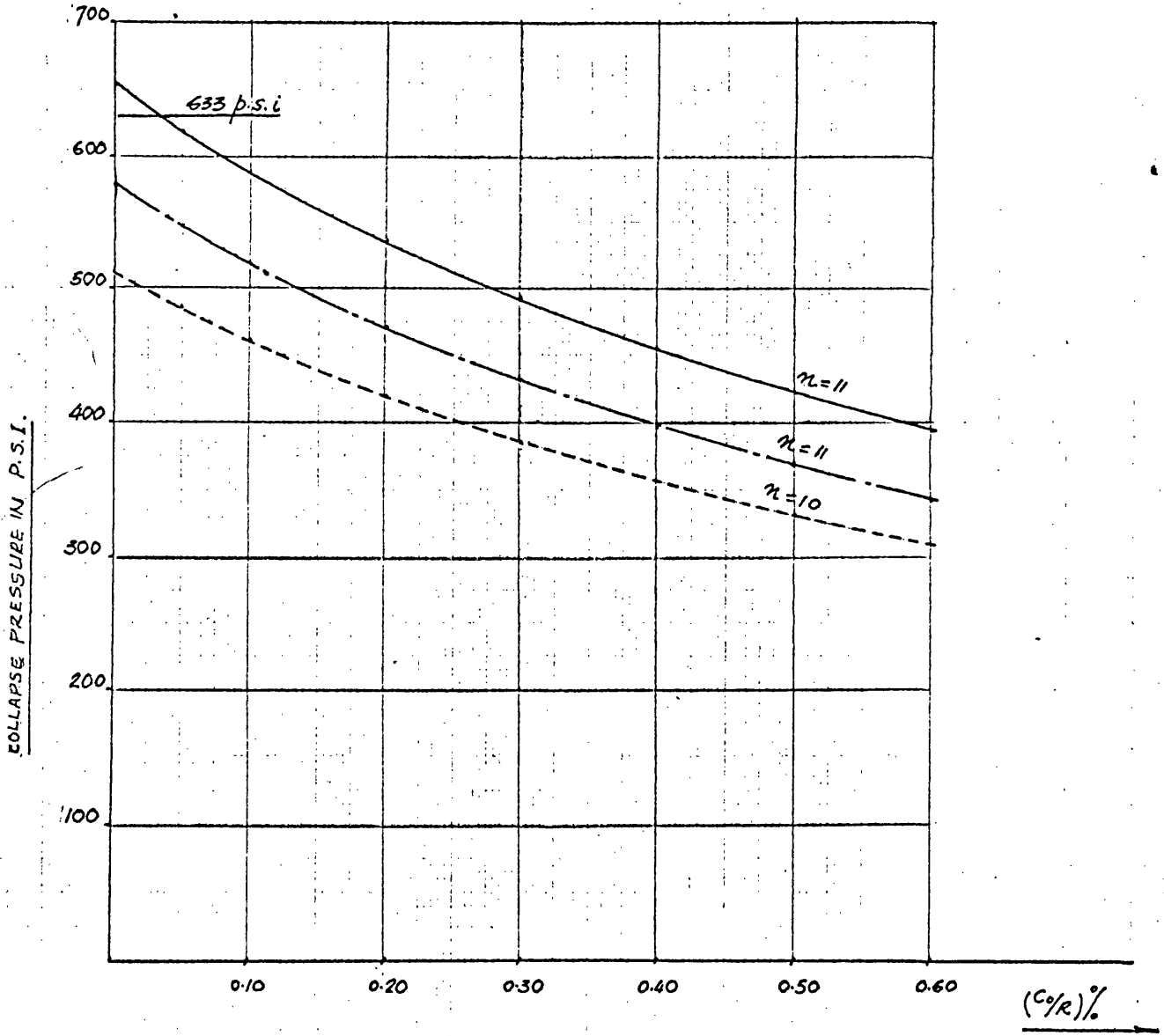

CLAMPED EDGE

PARTIALLY FIXED EDGE

SIMPLE SUPPORTED EDGE

$\sigma_y = 82500$ p.s.i.

$E = 28.7 \times 10^6$ p.s.i.

EXPERIMENTAL COLLAPSE PRESSURE = 633 p.s.i. AT $n = 11$

MODE: ELASTIC BUCKLING

DIMENSIONS: $t = 0.081''$, $R = 8.050''$, $l = 4.27''$

FIG. 32 COMPARISON OF THEORETICAL & EXPERIMENTAL COLLAPSE PRESSURES OF MACHINED MODEL BR-4B REF. (28)

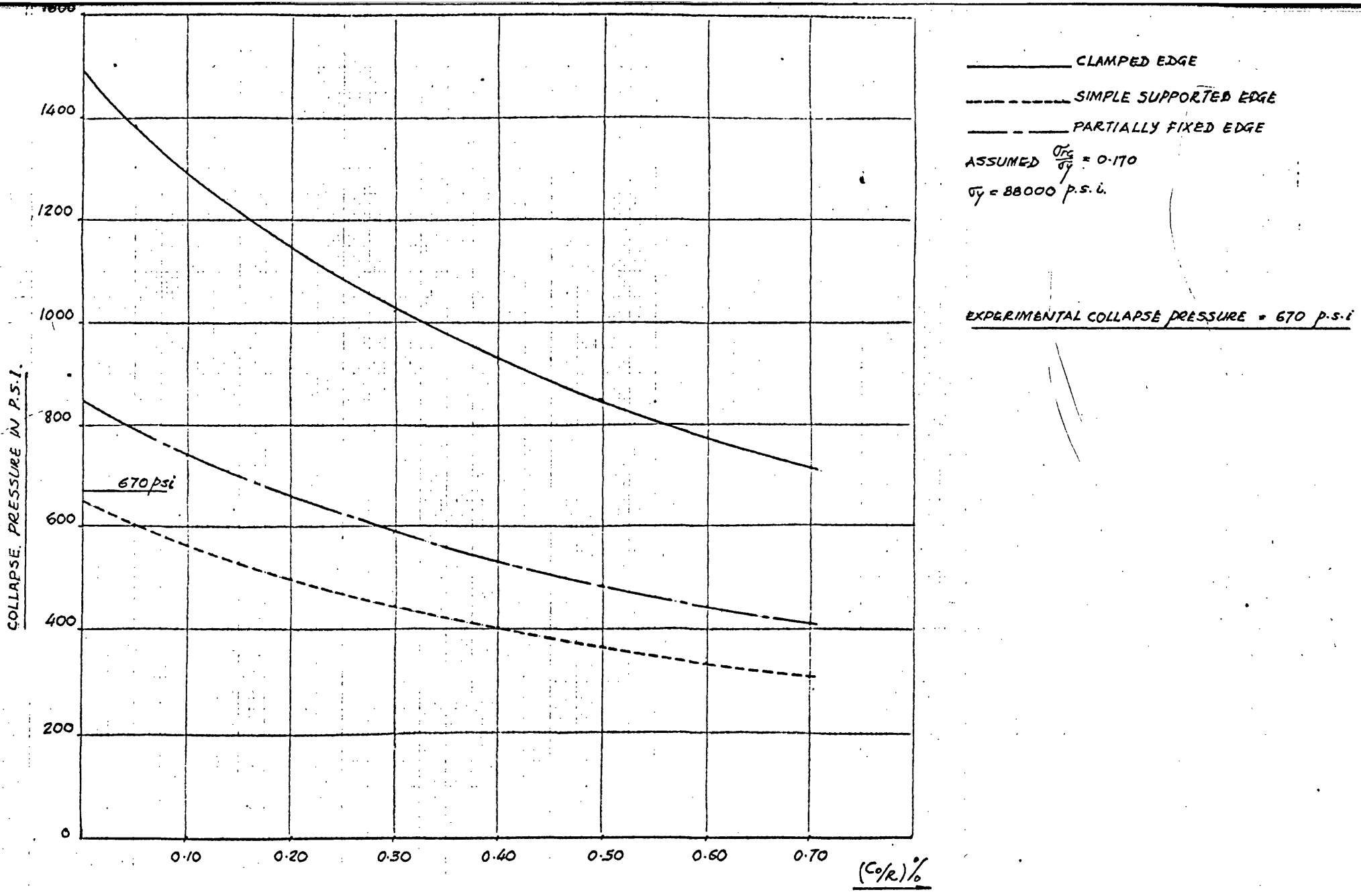

FIG. 33 COMPARISON OF THEORETICAL & EXPERIMENTAL COLLAPSE PRESSURES OF WELDED MODEL T-2 REF. (25)

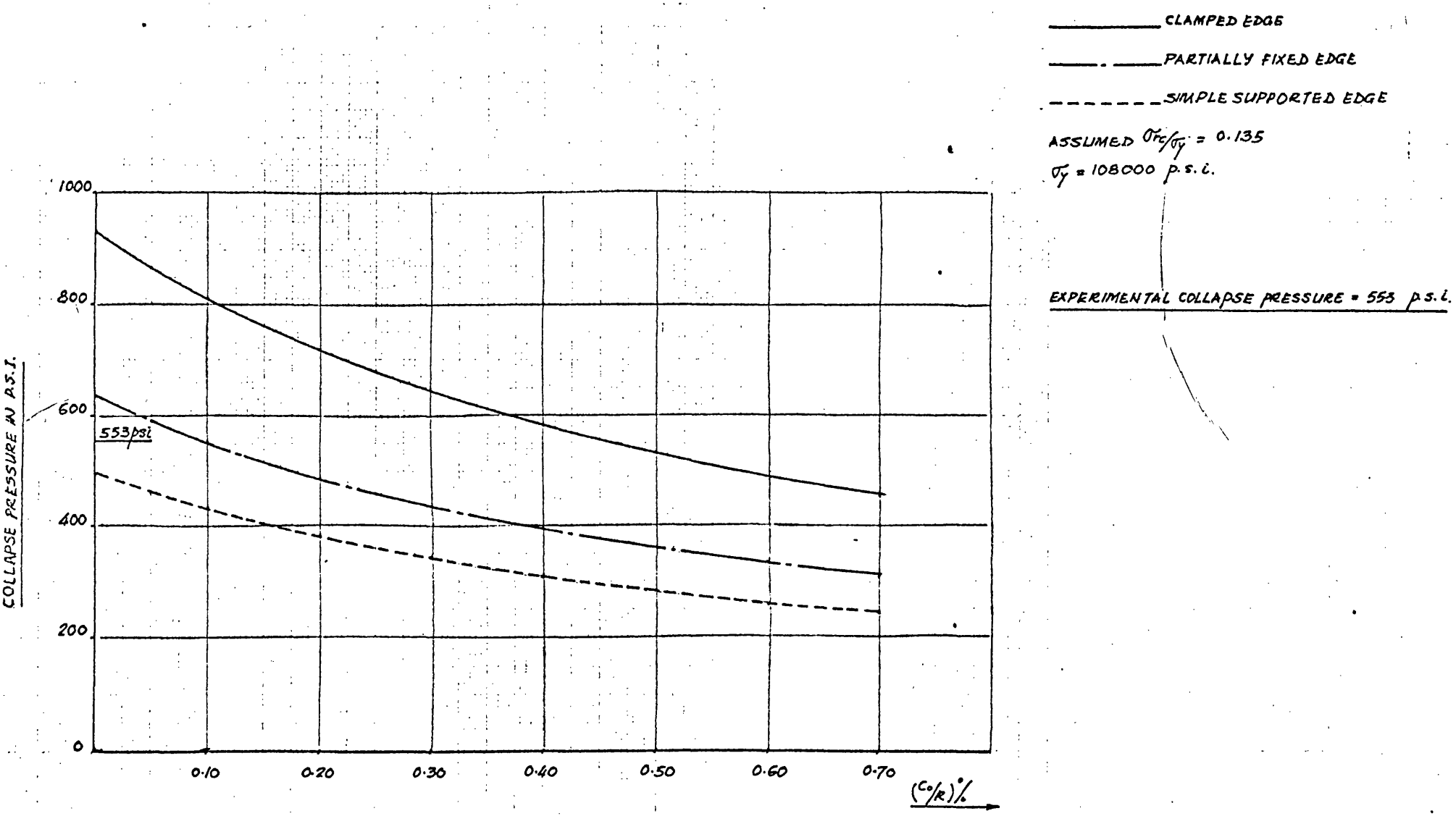

FIG.34 COMPARISON OF THEORETICAL & EXPERIMENTAL COLLAPSE PRESSURES OF WELDED MODEL T-3 REF:(25)

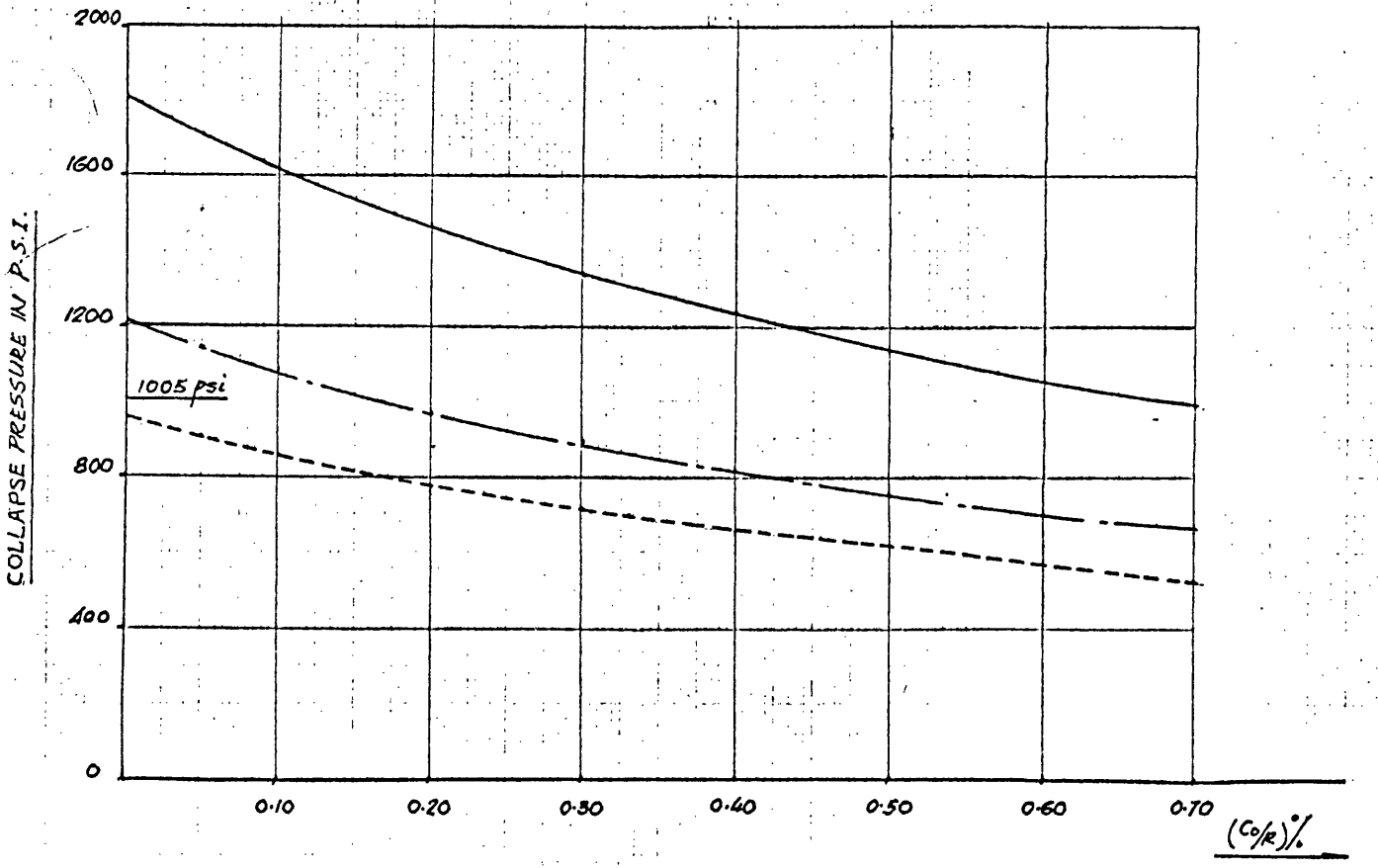

FIG. 35 COMPARISON OF THEORETICAL & EXPERIMENTAL COLLAPSE PRESSURES OF WELDED MODEL T-6 REF (25)

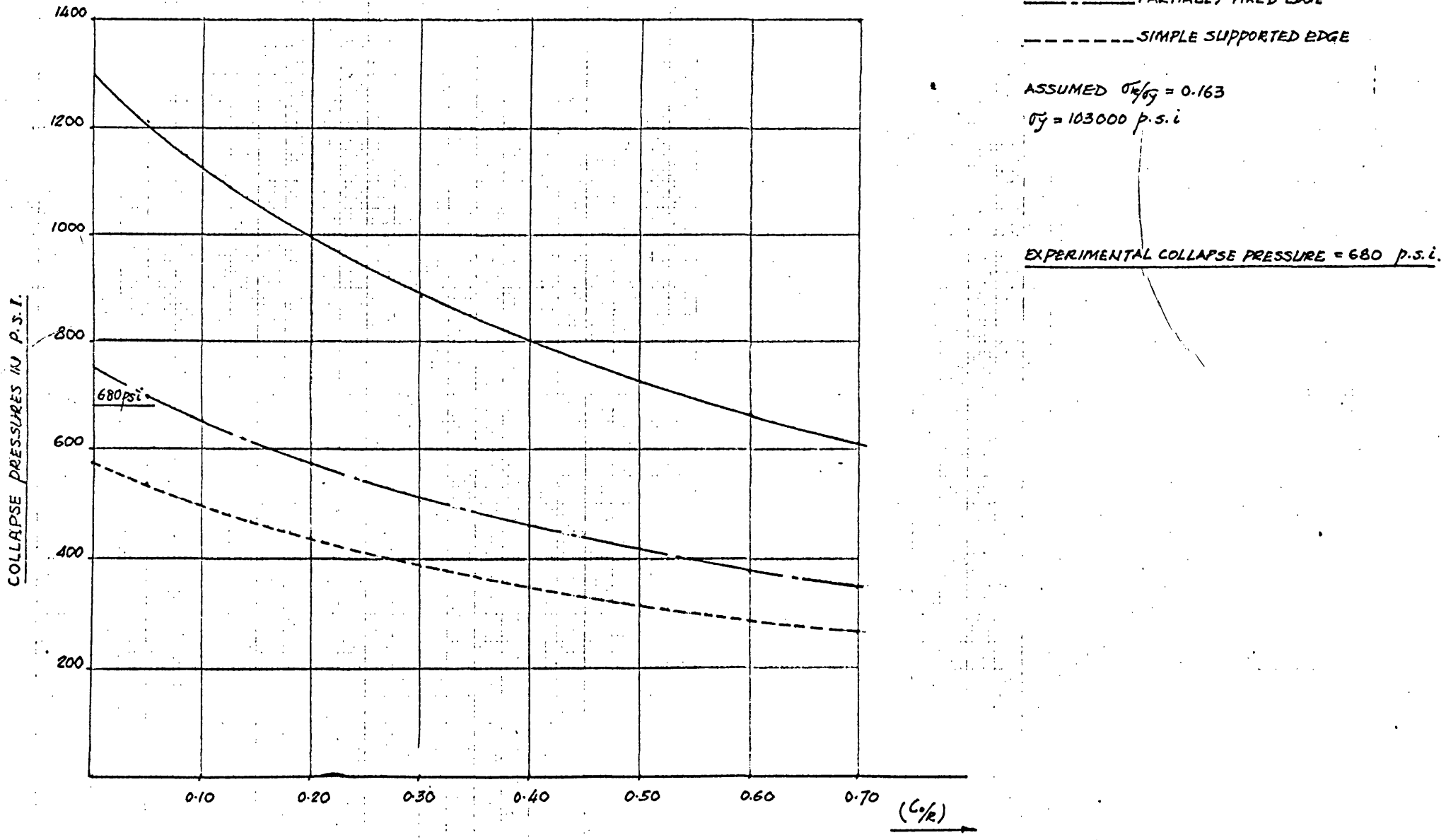

FIG. 36 COMPARISON OF THEORETICAL & EXPERIMENTAL COLLAPSE PRESSURES OF WELDED MODEL T-2A REF. (25)

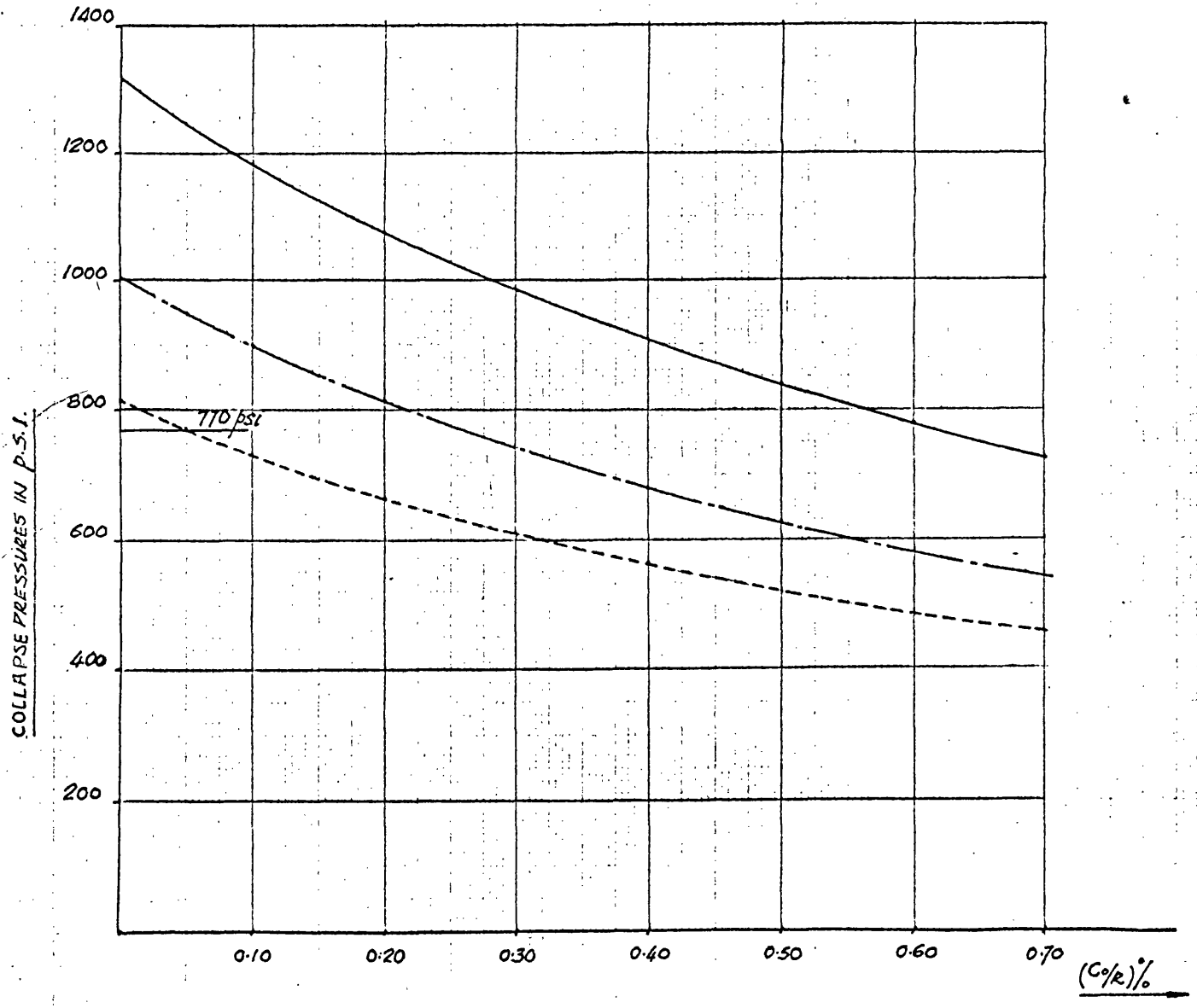

CLAMPED EDGE

PARTIALLY FIXED EDGE

SIMPLE SUPPORTED EDGE

ASSUMED $\sigma_{rc}/\sigma_y = 0.136$

$\sigma_y = 84000$ p.s.i.

EXPERIMENTAL COLLAPSE PRESSURE = 770 p.s.i.

FIG. 37 COMPARISON OF THEORETICAL & EXPERIMENTAL COLLAPSE PRESSURES OF WELDED MODEL T-7A REF: (25)

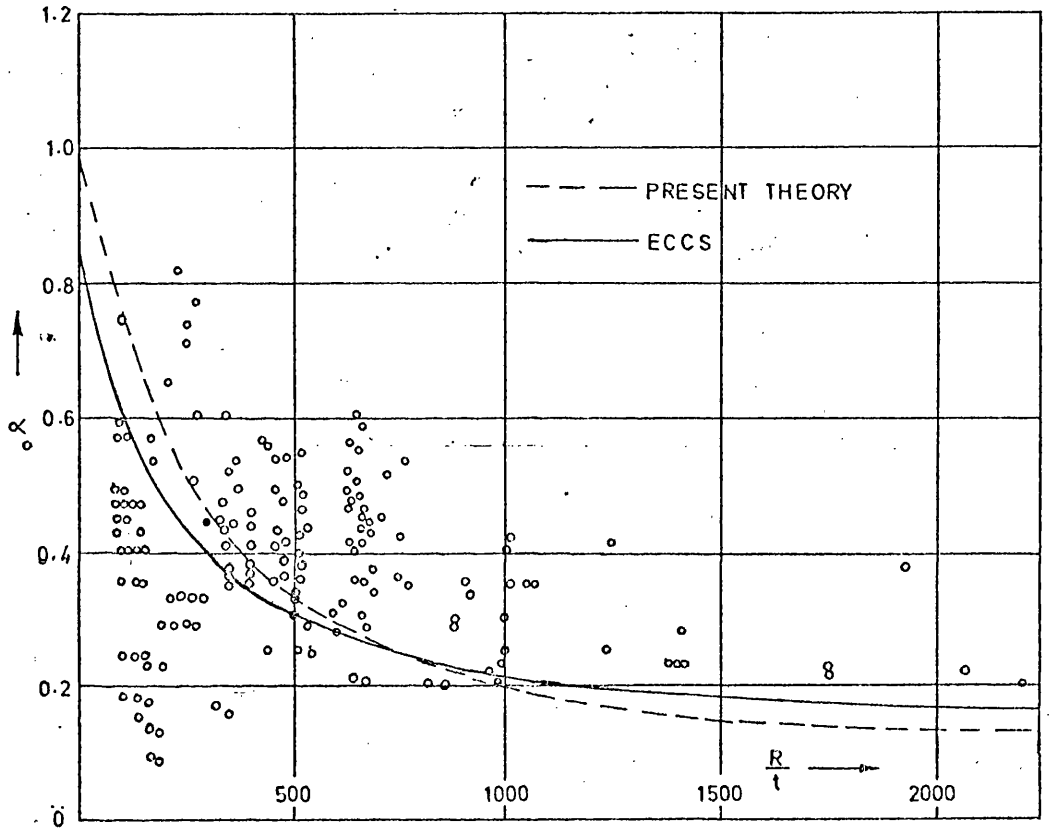

BUCKLING LOADS OF AXIALLY LOADED CYLINDERS

Fig. 38

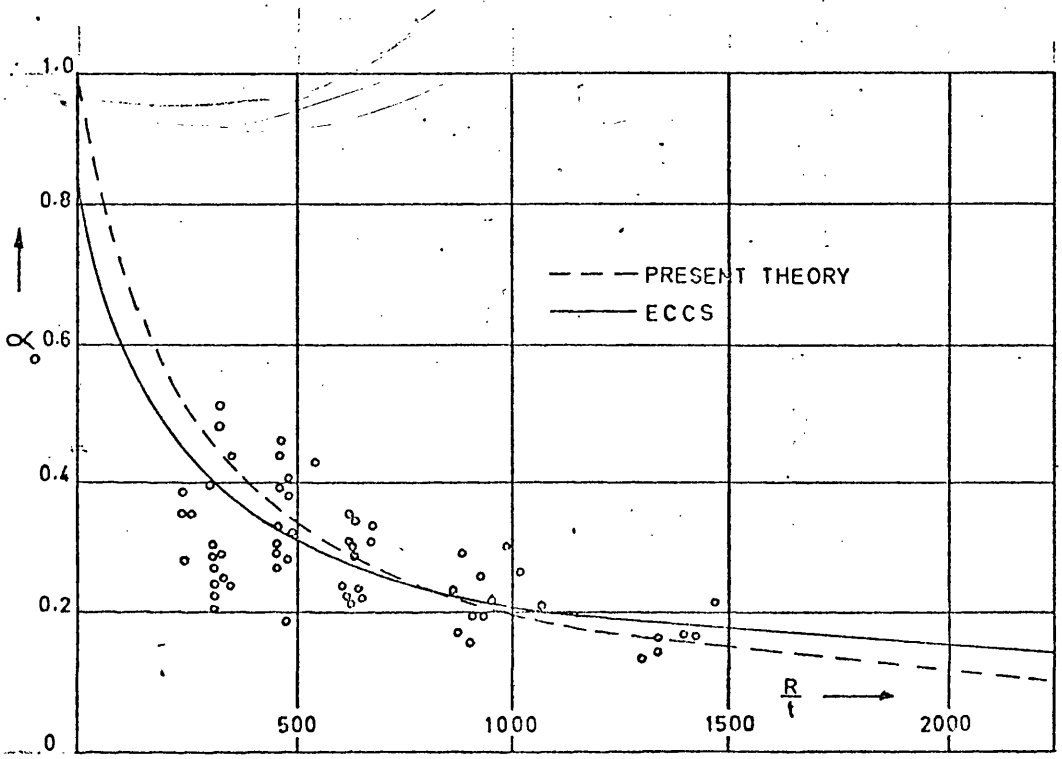

BUCKLING LOADS OF AXIALLY LOADED CYLINDERS

fig. 39

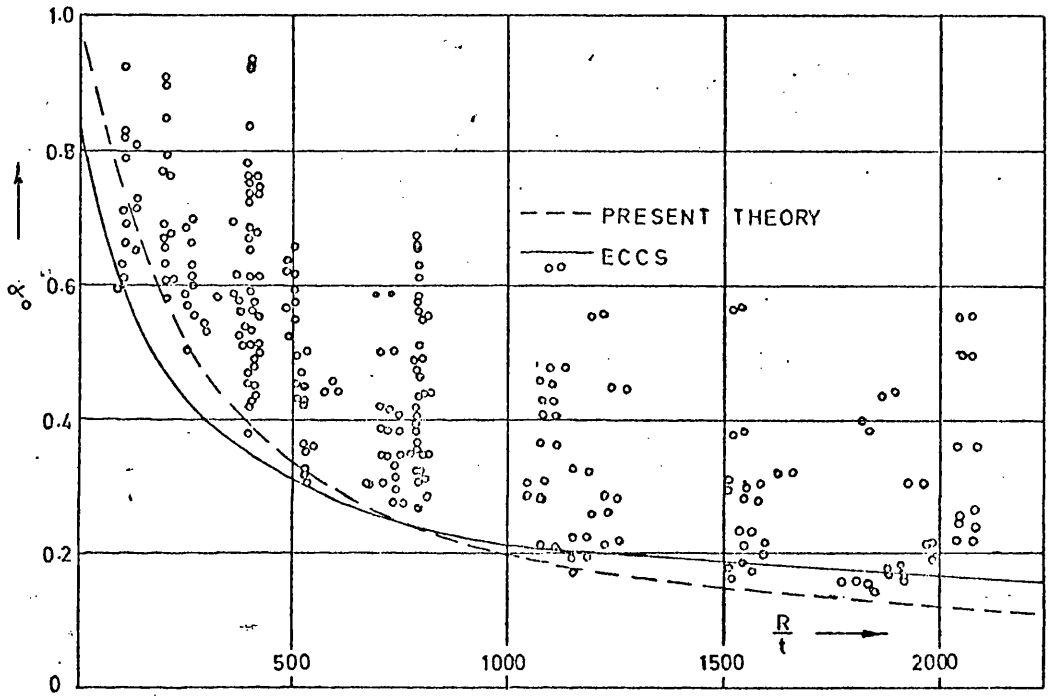

BUCKLING LOADS OF AXIALLY LOADED CYLINDERS

FIG.40

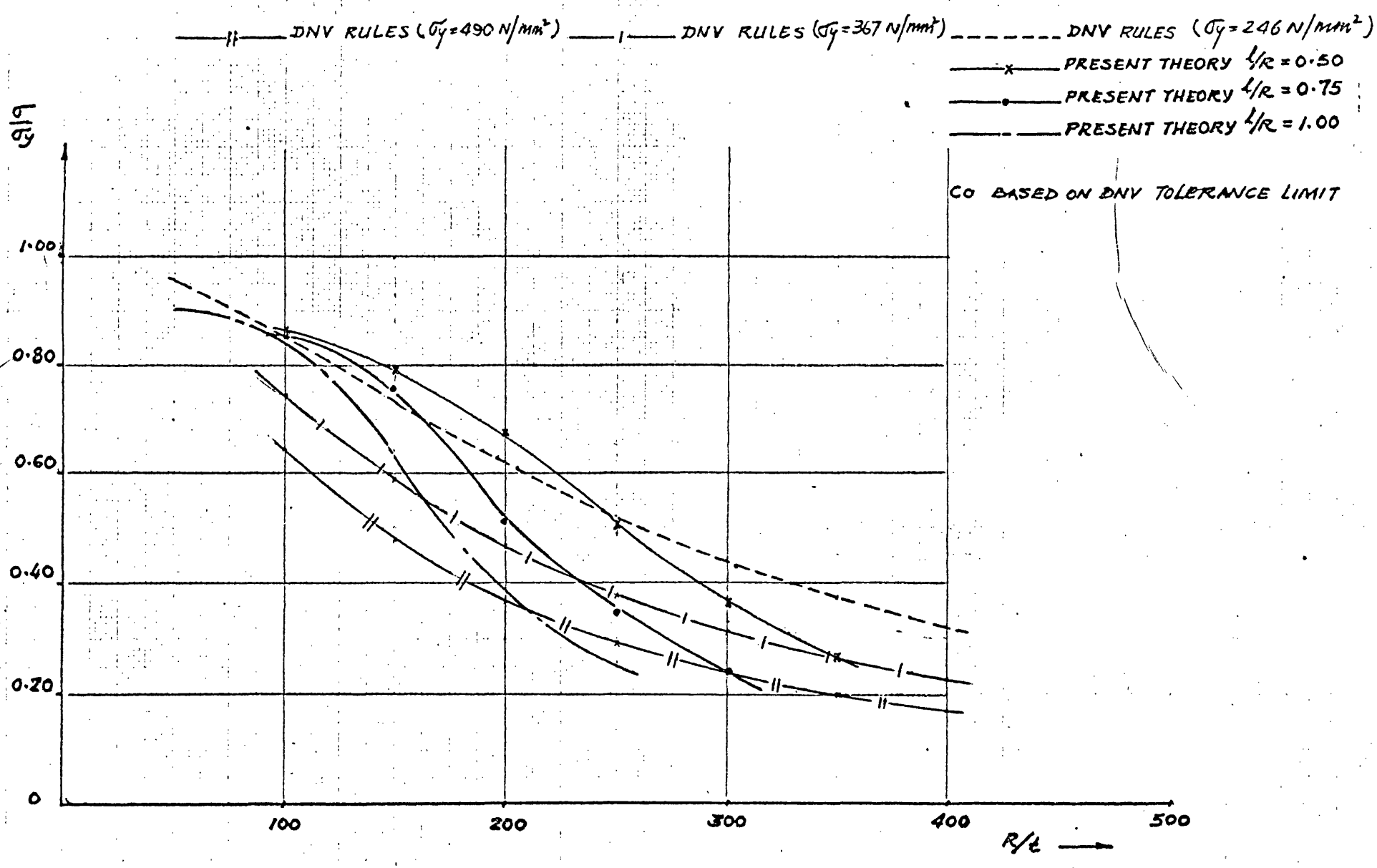

FIG. 41 COMPARISON BETWEEN PRESENT THEORY & DNV RULES — AXIAL COMPRESSION

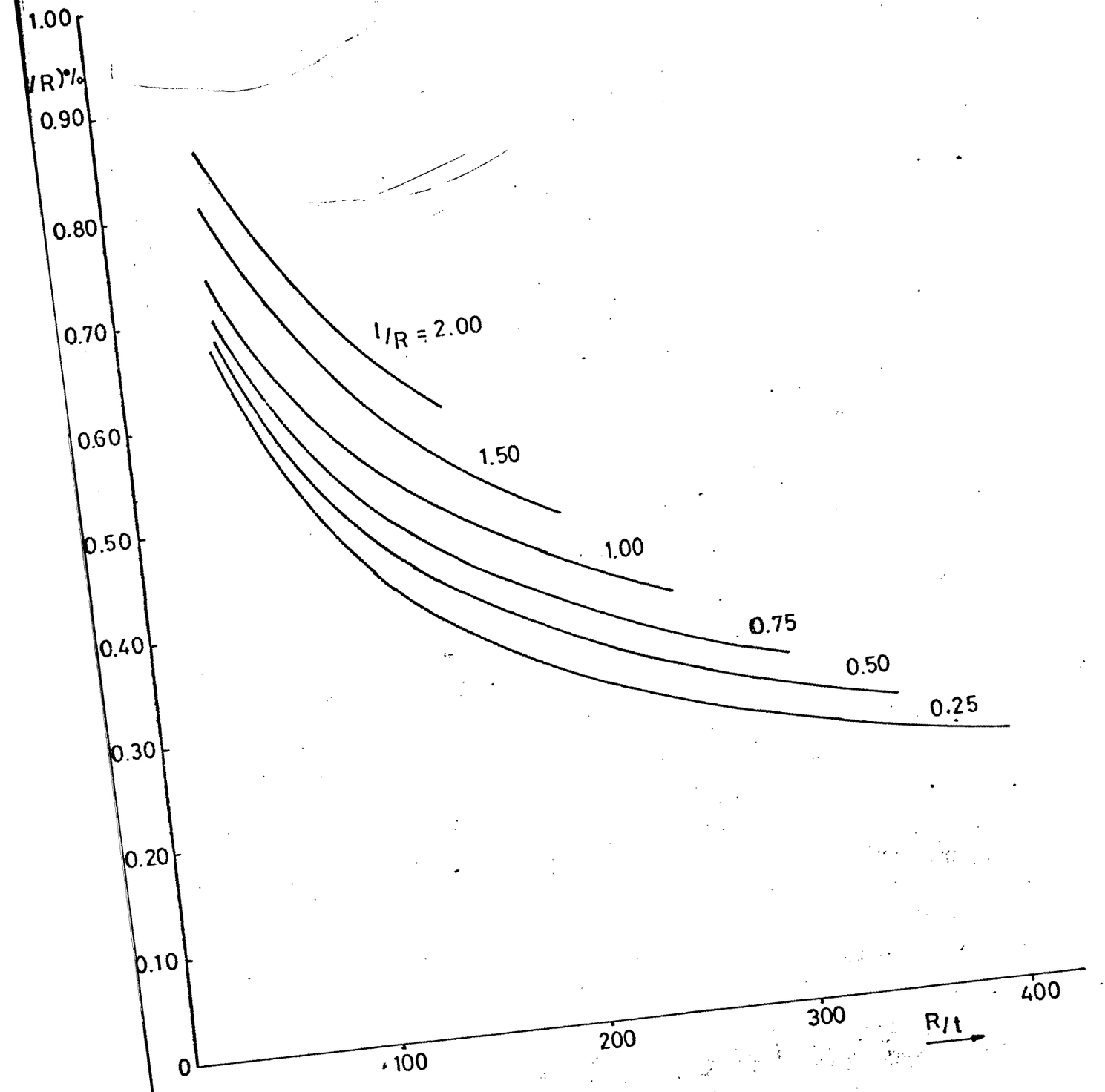

DNV Maximum Permissible Deviation From Circular Form

Fig. 42

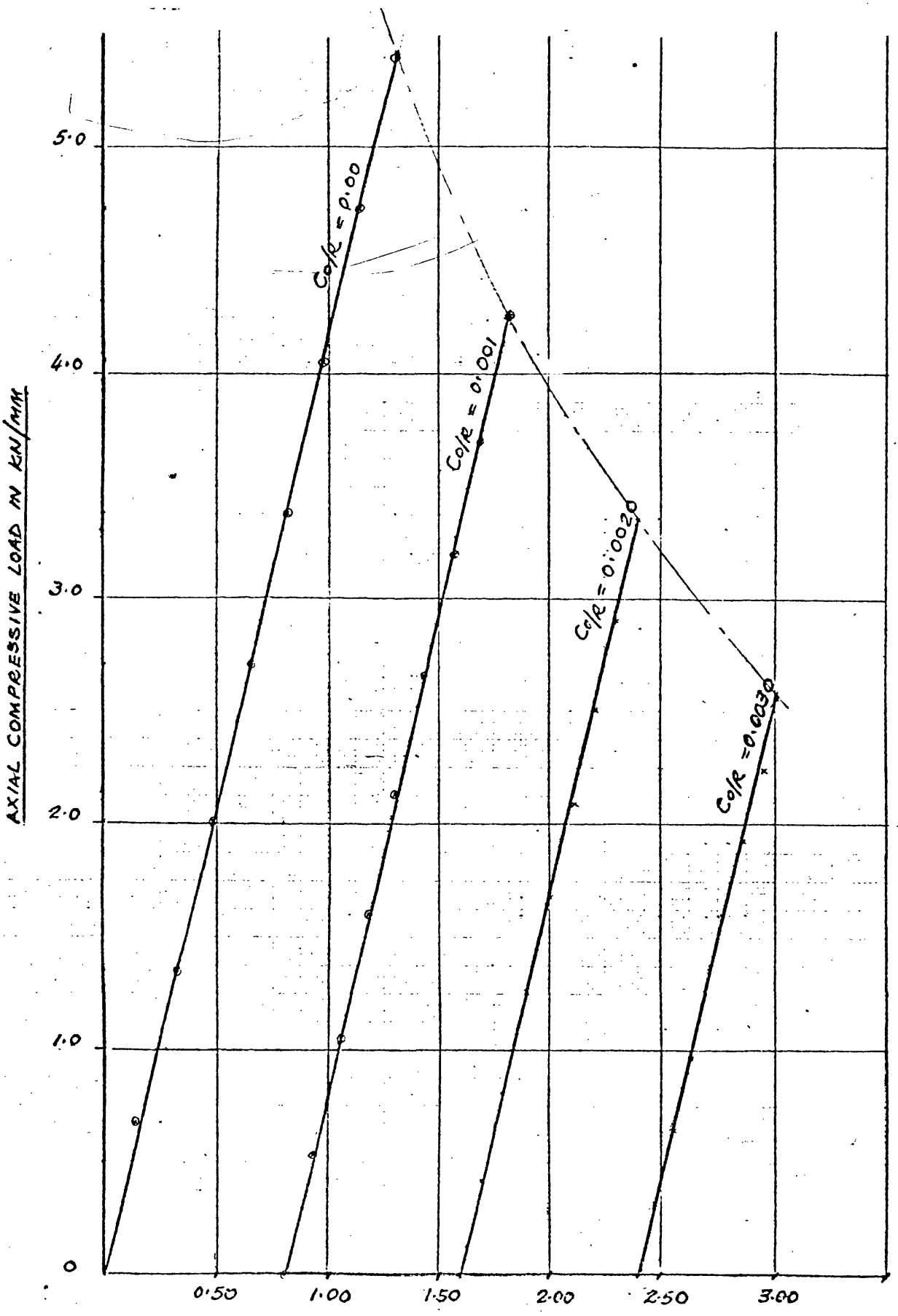

FIG. 43 DISPLACEMENT AMPLITUDE (MM)

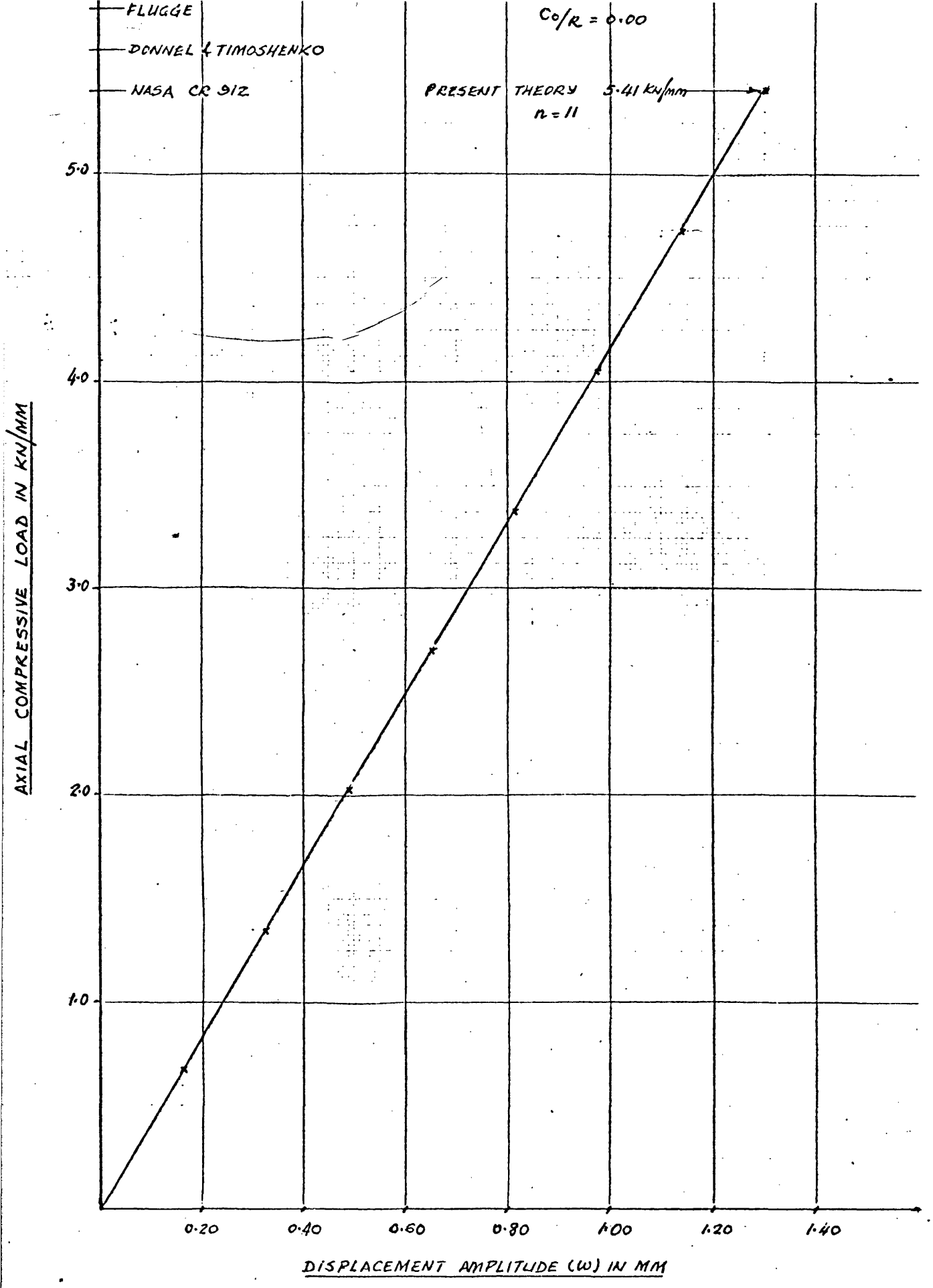

FIG. 44 COMPARISON BETWEEN PRESENT THEORY & CLASSICAL SOLUTIONS

REPRODUCED FROM FIG. 9 OF REF. (29)

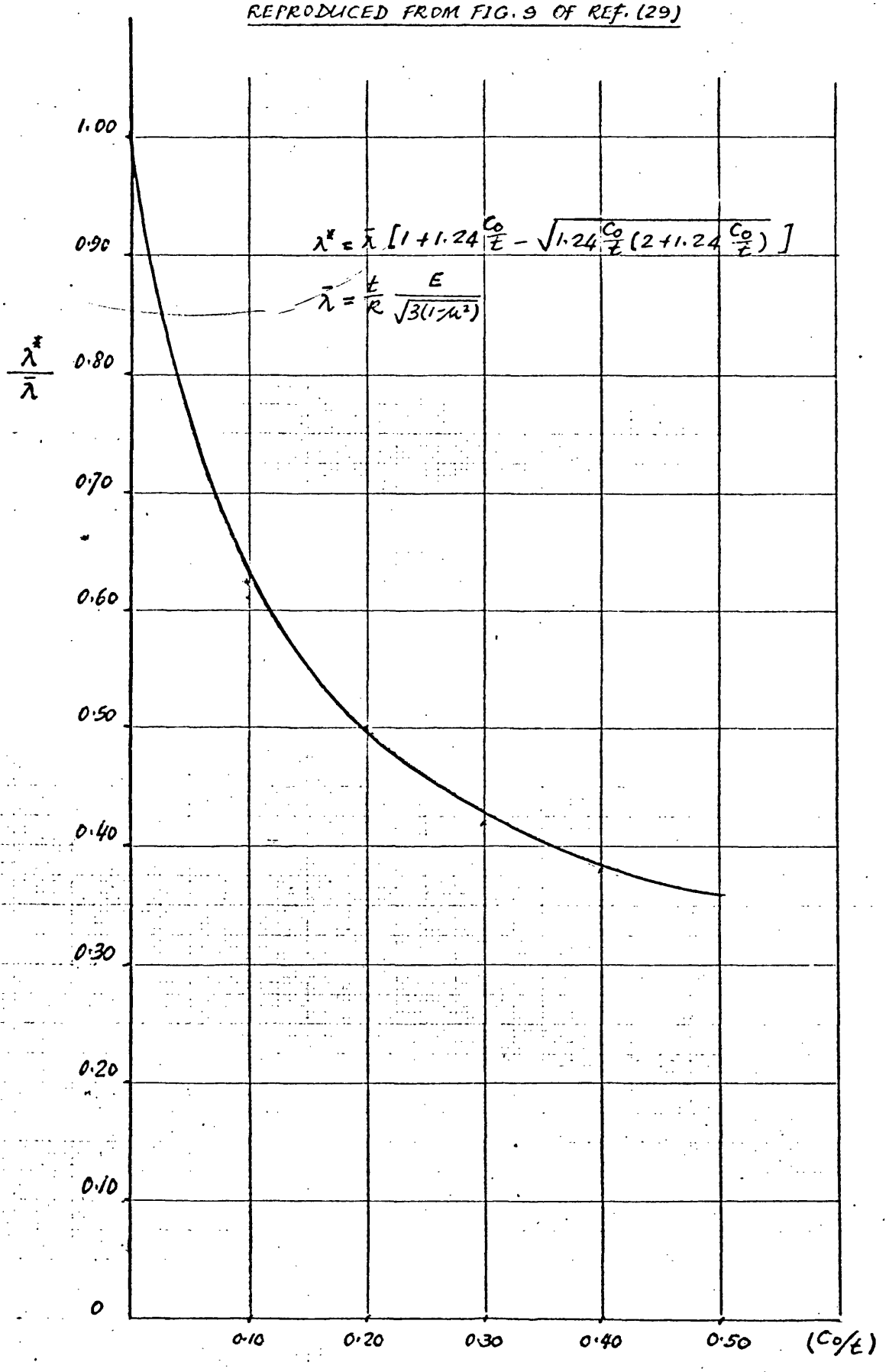

FIG. 45 KOITER'S SENSITIVITY OF THE AXIAL COMPRESSIVE LOAD

TABLE 1: INFLUENCE OF COLD-BENDING RESIDUAL STRESSES ON INTERFRAME COLLAPSE PRESSURE

$R/t = 133$, $\ell/R = 0.675$, $E/\sigma_y = 841$, $R = 800$ mm

$(C_o/R)\%$	SIMPLE SUPPORTED		CLAMPED	
	IR = 0	IR = 2	IR = 0	IR = 2
0.00	1369.4	1369.3	1687.9	1687.8
0.05	1273.0	1272.9	1569.2	1569.1
0.10	1189.3	1189.1	1466.1	1466.0
0.20	1051.0	1050.8	1295.8	1295.7
0.30	941.5	941.3	1160.9	1160.8
0.40	852.7	852.5	1051.5	1051.4
0.50	779.2	778.9	960.9	960.8
0.60	717.4	717.1	884.7	884.6

$R/t = 133$, $\ell/R = 0.338$, $E/\sigma_y = 841$

$(C_o/R)\%$	SIMPLE SUPPORTED		CLAMPED	
	IR = 0	IR = 2	IR = 0	IR = 2
0.00	2839.7	2839.6	4077.0	4077.0
0.05	2650.8	2650.7	3807.7	3807.5
0.10	2485.5	2485.4	3571.6	3571.4
0.20	2209.9	2209.8	3177.5	3177.4
0.30	1989.3	1989.3	2861.7	2861.6
0.40	1808.8	1808.7	2603.0	2602.9
0.50	1658.3	1658.2	2387.2	2387.1
0.60	1530.9	1530.8	2204.5	2204.4

Key: IR = 0 - without cold-bending residual stresses

IR = 2 - with cold-bending residual stresses

Pressures are in kN/m^2 .

TABLE 2: WELDING RESIDUAL STRESSES ON INTERFRAME COLLAPSE PRESSURE

Pressures in kN/m^2

$R/t = 133$, $\ell/R = 0.675$, $E/\sigma_y = 841$, $\sigma_{rc}/\sigma_y = 0.110$, $\eta = 4.5$

$(C_o/R)\%$	SIMPLE SUPPORTED			CLAMPED		
	IR = 0*	IR= 3*	% LOSS	IR = 0	IR = 3	% LOSS
0.00	1369.4	1287.6	6.0	1687.9	1561.5	7.5
0.05	1273.0	1191.8	6.4	1569.2	1443.8	8.0
0.10	1189.3	1108.6	6.8	1466.1	1341.5	8.5
0.20	1051.0	971.2	7.6	1295.8	1172.7	9.5
0.30	941.5	862.4	8.4	1160.9	1038.9	10.5
0.40	852.7	774.2	9.2	1051.5	930.4	11.5
0.50	779.2	701.1	10.0	960.9	840.6	12.5
0.60	717.4	639.7	10.8	884.7	765.1	13.5

* IR = 0 - without welding residual stresses

* IR = 3 - with welding residual stresses

$R/t = 133$, $\ell/R = 0.675$, $E/\sigma_y = 841$, $\sigma_{rc}/\sigma_y = 0.125$, $\eta = 5.0$

$(C_o/R)\%$	SIMPLE SUPPORTED			CLAMPED		
	IR = 0	IR = 3	% LOSS	IR = 0	IR = 3	% LOSS
0.00	1369.4	1277.7	6.7	1687.9	1546.6	8.4
0.05	1273.0	1182.0	7.1	1569.2	1429.0	8.9
0.10	1189.3	1098.8	7.6	1466.1	1326.8	9.5
0.20	1051.0	961.6	8.5	1295.8	1158.1	10.6
0.30	941.5	852.9	9.4	1160.9	1024.6	11.7
0.40	852.7	764.7	10.3	1051.5	916.2	12.8
0.50	779.2	691.7	11.2	960.9	826.4	14.0
0.60	717.4	630.4	12.1	884.7	750.9	15.1

R/t = 133/

TABLE 2: (Cont'd)

$R/t = 133$, $\ell/R = 0.675$, $E/\sigma_y = 841$, $\sigma_{rc}/\sigma_y = 0.154$, $\eta = 6.0$

$(C_o/R)\%$	SIMPLE SUPPORTED			CLAMPED		
	IR = 0	IR = 3	% LOSS	IR = 0	IR = 3	% LOSS
0.00	1369.4	1257.6	8.2	1687.9	1516.5	10.1
0.05	1273.0	1162.0	8.7	1569.2	1399.2	10.8
0.10	1189.0	1079.0	9.2	1466.1	1297.2	11.5
0.20	1051.0	941.9	10.3	1295.8	1128.9	12.9
0.30	941.5	833.4	11.5	1160.9	995.5	14.2
0.40	852.7	745.4	12.6	1051.5	887.4	15.6
0.50	779.2	672.6	13.7	960.9	797.8	16.9
0.60	717.4	611.3	14.8	884.7	722.5	18.3

TABLE 3: INFLUENCE OF WELDING RESIDUAL STRESSES IN INTERFRAME COLLAPSE PRESSURE

Pressure in kN/m^2 , R = 800 mm

$R/t = 200$, $\ell/R = 0.675$, $E/\sigma_y = 841$, $\sigma_{rc}/\sigma_y = 0.110$, $\eta = 6.7$

$(C_o/R)\%$	SIMPLE SUPPORTED			CLAMPED		
	IR = 0	IR = 3	% LOSS	IR = 0	IR = 3	% LOSS
0.00	490.4	433.8	11.5	612.1	524.3	14.3
0.05	439.7	383.8	12.7	548.7	462.1	15.7
0.10	398.5	343.3	13.8	497.2	411.5	17.2
0.20	335.6	281.3	16.2	418.7	334.4	20.1
0.30	289.8	236.2	18.5	361.5	278.3	23.0
0.40	255.1	201.9	20.8	318.1	235.7	25.9
0.50	227.7	174.9	23.2	284.0	202.3	28.7
0.60	205.7	153.3	25.5	256.5	175.3	31.6

$R/t = 200$, $\ell/R = 0.675$, $E/\sigma_y = 841$, $\sigma_{rc}/\sigma_y = 0.125$, $\eta = 7.5$

$(C_o/R)\%$	SIMPLE SUPPORTED			CLAMPED		
	IR = 0	IR = 3	% LOSS	IR = 0	IR = 3	% LOSS
0.00	490.4	426.4	13.0	612.1	512.9	16.2
0.05	439.7	376.5	14.4	548.7	450.9	17.8
0.10	398.5	335.9	15.7	497.2	400.5	19.4
0.20	335.6	335.9	18.3	418.7	323.6	22.7
0.30	289.8	229.1	20.9	361.5	267.6	25.9
0.40	255.1	194.9	23.6	318.1	225.1	29.2
0.50	227.7	168.0	26.2	284.0	191.7	32.5
0.60	205.7	146.4	28.8	256.5	164.8	35.7

R/t = 200/

TABLE 3: (Cont'd)

$R/t = 200$, $\ell/R = 0.675$, $E/\sigma_y = 841$, $\sigma_{rc}/\sigma_y = 0.154$, $\eta = 9.2$

$(C_o/R)\%$	SIMPLE SUPPORTED			CLAMPED		
	IR = 0	IR = 3	% LOSS	IR = 0	IR = 3	% LOSS
0.00	490.4	412.3	15.9	612.1	491.8	19.6
0.05	439.7	362.6	17.5	548.7	430.0	21.6
0.10	398.5	322.3	19.1	497.2	379.8	23.6
0.20	335.6	260.6	22.3	418.7	303.3	27.6
0.30	289.8	215.8	25.5	361.5	247.6	31.5
0.40	255.1	181.7	28.8	318.1	205.3	35.4
0.50	227.7	154.9	31.9	284.0	172.1	39.4
0.60	205.7	133.3	35.2	256.5	145.3	43.4

TABLE 4: INFLUENCE OF WELDING RESIDUAL STRESSES ON INTERFRAME COLLAPSE PRESSURE

Pressures in kN/m^2 , ℓ = 270 mm

$R/t = 133$, $\ell/R = 0.338$, $E/\sigma_y = 841$, $\sigma_{rc}/\sigma_y = 0.154$, $\eta = 3.0$

$(C_o/R)\%$	SIMPLE SUPPORTED			CLAMPED		
	IR = 0	IR = 3	% LOSS	IR = 0	IR = 0	% LOSS
0.00	2839.7	2745.6	3.3	4077.2	3930.7	3.6
0.05	2650.8	2557.2	3.5	3807.7	3661.7	3.8
0.10	2485.5	2392.2	3.7	3571.6	3426.0	4.1
0.20	2209.9	2117.2	4.2	3177.5	3032.5	4.6
0.30	1989.3	1897.0	4.6	2861.7	2717.3	5.0
0.40	1808.8	1716.0	5.2	2603.0	2459.0	5.5
0.50	1658.3	1566.6	5.5	2387.2	2243.6	6.0
0.60	1530.9	1439.5	6.0	2204.5	2061.1	6.5

$R/t = 133$, $\ell/R = 0.338$, $E/\sigma_y = 841$, $\sigma_{rc}/\sigma_y = 0.250$, $\eta = 4.5$

$(C_o R/)\%$	SIMPLE SUPPORTED			CLAMPED		
	IR = 0	IR = 3	% LOSS	IR = 0	IR = 3	% LOSS
0.00	2839.7	2692.5	5.2	4077.2	3852.9	5.5
0.05	2650.8	2504.3	5.5	3807.7	3584.0	5.8
0.10	2485.5	2339.5	5.9	3571.6	3348.5	6.2
0.20	2209.9	2064.7	6.6	3177.5	2955.5	7.0
0.30	1989.3	1844.8	7.3	2861.7	2640.5	7.7
0.40	1808.8	1664.8	8.0	2603.0	2382.5	8.5
0.50	1658.3	1514.8	8.5	2387.2	2167.2	9.2
0.60	1530.9	1387.8	9.3	2204.5	1984.9	10.0

TABLE 5: PROPERTIES OF CYLINDERS

Cylinder		Radius R in.	Thickness t in.	Unsupported Length of Shell ℓ in.	Frame Area A_f sq.in.	Frame Faying Width t_w in.	Yield Strength σ_y* psi
Welded with T-Frames	T-2	38.87	0.264	7.24	1.885	0.260	88000 (c)
	T-3	38.87	0.260	8.74	1.625	0.260	108000 (c)
	T-6	26.87	0.256	7.24	1.170	0.260	115000 (c)
	T-2A	38.87	0.254	7.24	0.796	0.260	103000
	T-7A	26.87	0.263	8.74	0.683	0.260	84000

* All yield strengths are defined at offset strain of 0.002.

(c) Specimens of shell material taken from collapsed cylinders

Specimens for all other cylinders were obtained prior to fabrication

TABLE 6: OVERALL BUCKLING PRESSURES

Comparison between Eq. (22a) and Eq. (22b)

Dimensions: $R = 100"$, $t = 1.00"$, $\ell = 30.0"$, $d = 7.36"$

$t_w = 0.32"$, $f = 4.0"$, $t_f = 0.64"$

Material Properties: $E = 30 \times 10^6$ psi , $\sigma_y = 50{,}000$ psi

Pressure in P.S.I.

n	L = 150"		L = 300"		L = 450"	
	Eq. (22a)	Eq. (22b)	Eq. (22a)	Eq. (22b)	Eq. (22a)	Eq. (22b)
2	768	724	846	801	871	827
3	2177	2087	2369	2279	2430	2341
4	3383	2712	3603	2899	3671	2962
5	3874	2635	4028	2788	4073	2834
6	3833	2499	3928	2614	3955	2644
7	3589	2356	3646	2439	3662	2459
8	3308	2225	3343	2285	3353	2299

n	L = 600"		L = 750"		L = 3000"	
	Eq. (22a)	Eq. (22b)	Eq. (22a)	Eq. (22b)	Eq. (22a)	Eq. (22b)
2	883	839	890	847	913	869
3	2460	2371	2478	2389	2532	2442
4	3704	2989	3723	3005	3780	3038
5	4095	2853	4108	2863	4146	2799
6	3968	2657	3975	2663	3997	2676
7	3669	2468	3674	2472	3687	2480
8	3358	2305	3361	2307	3369	2313

TABLE 7: COMPARISON BETWEEN PRESENT THEORY AND KENDRICK'S THEORY (80)

Overall Instability of Ring Stiffened Cylinder under External Pressure.

Dimensions[+]: R = 100" , ℓ = 30.00" , d - 7.36" , tw = 0.32"
f = 4.0" , t_f = 0.64" , t = 1.00"

Material Properties: E = 30 x 10^6 psi , σ_y = 50,000 psi

Buckling Pressures in P.S.I. L = 150"

n	Kendrick Ref. (80)	PRESENT THEORY				
		Eq. (19c)	Eq. (19b)	Eq. (20b)	Eq. (21b)	Eq. (22b)
2	4598	4656	4002	3979	3965	724*
3	4020	3939	3399	3344	3475	2087
4	3405	3425	2913	2839	2856	2712
5	3521	3634	2976	2943	2918	2635
6	3218	3318	2810	2801	2789	2499
7	2927	3018	2599	2598	2592	2356
8	2678	2763	2403	2404	2402	2225
14		2126*	1893*	1903*	1913*	

BS5500 p_{fy} = 622.4 psi , p_n = 3497 psi , n = 4
Present Theory p_{fy} = 531.9 psi
* critical value

Buckling Pressures in P.S.I. L = 300"

n	Kendrick Ref. (80)	PRESENT THEORY				
		Eq. (19c)	Eq. (19b)	Eq. (20b)	Eq. (21b)	Eq. (22b)
2	4138	4139	3534	3869	3869	801*
3	1946*	1959*	1931*	1957*	2197*	2279
4	2990	3044	2792	2743	2746	2899
5	3487	3592	3073	3052	3039	2788
6	3211	3310	2879	2877	2873	2814
7	2923	3022	2647	2647	2645	2439
8	2674	2774	2435	2436	2436	2285

BS5500 p_{Fy} = 583.8 psi , p_n = 1859 psi , n = 3
Present theory p_{Fy} = 563.9 psi

TABLE 7: (Cont'd)

Buckling Pressures in P.S.I. L = 450"

n	Kendrick Ref.(80)	PRESENT THEORY				
		Eq.(19c)	Eq.(19b)	Eq.:20b)	Eq.(21b)	Eq.(22b)
2	1677	1683*	1658*	1886	2728	827*
3	1666*	1688	1685	1694*	1822*	2341
4	2958	3023	2800	2756	2747	2962
5	3494	3593	3103	3085	3074	2834
6	3206	3313	2897	2895	2892	2644
7	2916	3027	2657	2658	2656	2459
8	2666	2779	2442	2443	2443	2299

BS5500 p_{Fy} = 554.0 psi , p_n = 1541 , n = 3

Present Tehory p_{Fy} = 582.3 psi.

Buckling Pressurs in P.S.I. L = 600"

n	Kendrick Ref.(80)	PRESENT THEORY				
		Eq.(19c)	Eq.(19b)	Eq.(20b)	Eq.(21b)	Eq.(22b)
2	1000*	1007*	1014*	1167*	1747	839*
3	1603	1631	1628	1628	1702*	2371
4	2953	3024	2808	2766	2752	2989
5	3491	3595	3114	3098	3088	2853
6	3200	3315	2903	2901	2899	2657
7	2908	3029	2661	2662	2660	2468
8	2656	2781	2444	2446	2445	2305

BS5500 p_{Fy} = 529.2 psi , p_n = 938.7 , n = 2

Present Theory p_{Fy} = 574.5 psi

TABLE 7: (Cont'd)

Buckling Pressures in P.S.I. L = 750"

n	Kendrick Ref. (80)	PRESENT THEORY				
		Eq. (19c)	Eq. (19b)	Eq. (20b)	Eq. (21b)	Eq. (22b)
2	775*	784*	795*	898*	1294*	847*
3	1583	1613	1609	1603	1651	2389
4	2951	3027	2813	2771	2754	3005
5	3487	3596	3120	3105	3094	2863
6	3193	3316	2906	2905	2903	2663
7	2900	3030	2663	2663	2662	2472
8	2647	2783	2446	2447	2446	2307

BS5500 p_{Fy} = 459.0 psi , p_n = 717 psi , n = 2

Present Theory p_{Fy} = 498.0 psi

Buckling Pressures in P.S.I. L = 3000"

n	Kendrick Ref. (80)	PRESENT THEORY				
		Eq. (19c)	Eq. (19b)	Eq. :20b)	Eq. (21b)	Eq. (22b)
2	579*	592*	600*	605*	633*	869*
3	1563	1599	1589	1574	1575	2442
4	2945	3039	2822	2780	2760	3038
5	3404	3600	3129	3115	3106	2799
6	3068	3320	2911	2910	2908	2676
7	2740	3035	2666	2666	2666	2480
8	2462	2787	2449	2449	2448	2313

BS5500 p_{Fy} = 381.0 psi , p_n = 546 , n = 2

Present Theory p_{Fy} = 403.0 psi

* Critical Value

\+ A cylinder designed to collapse under external pressure in the range 400-700 psi according to the steel uses (80)

TABLE 8: COMPARISON BETWEEN PRESENT THEORY AND BS5500 RULES

Overall instability of ring stiffened cylinder under external pressure.

Dimensions: $R = 100"$, $\ell = 50.00"$, $d = 7.36"$, $t_w = 0.32"$, $f = 4.0"$, $t_f = 0.64"$

Material Properties: $E = 30 \times 10^6$ psi , $\sigma_y = 50{,}000$ psi

Pressures in P.S.I.

L (inch)	Eq. (22b) p_n	Eq. (19b) p_n	Eq. (19c) p_n	p_{Fy}+	BS5500	
					p_n	p_{Fy}
150	343.9*(2)	844.2 (12)	1008.9 (12)	241.5	2400.0 (4)	586.3
300	418.2 (2)	1373.5 (3)	1391.5 (3)	293.7	1268.0 (3)	522.8
450	442.7 (2)	1107.1 (3)	1101.6 (3)	310.9	950.2 (3)	456.9
600	454.8 (2)	783.2 (2)	778.6 (2)	319.4	715.5 (2)	461.7
750	462.1 (2)	565.8 (2)	556.6 (2)	324.6	493.8 (2)	354.7
3000	483.4 (2)	381.7 (2)	372.1 (2)	254.5	323.0 (2)	247.6

* Circumferential buckling wave number, n

+ p_{Fy} calculated from the lowest p_n of either eq. (22b) or eq. (19b) and $C_{ol}/R = 0.0050$.

TABLE 9: COMPARISON BETWEEN PRESENT THEORY AND EXPERIMENTAL RESULTS OF REF. (100)

Overall Instability of Ring-Stiffened Machined Aluminium Cylinder Under External Pressure.

Dimensions: $R = 1.015"$, $t = 0.030"$ (0.762 mm) , $\ell = 2.50"$
$L = 12.50"$, $d = 0.150"$, $t_w = 0.040"$ (external stiffeners)

Properties of Material: $E = 10.7^6$ psi ± 3% , $\sigma_y = 39.1$ tons/in².

Experimental collapse pressure = 450 psi , n = 2

$(\bar{C}_{o2}/R)$ %	C_{o2} (inch)	C_{o2} (mm)	Buckling Pressure Eq. (22b)	Buckling Pressure Eq. (19b)
0.00	0.0000	0.0000	612.3 (2)*	611.9 (2)
0.10	0.0010	0.0254	588.6 (2)	584.9 (2)
0.20	0.0020	0.0515	566.6 (2)	560.3 (2)
0.30	0.0030	0.0762	546.2 (2)	537.1 (2)
0.40	0.0040	0.1030	527.3 (2)	516.9 (2)
0.50	0.0050	0.1288	509.6 (2)	497.6 (2)
0.60	0.0061	0.1547	493.1 (2)	479.8 (2)
0.70	0.0071	0.1800	477.7 (2)	463.2 (2)
0.80	0.0081	0.2060	463.2 (2)	447.8 (2)
0.90	0.0090	0.2280	440.0 (2)	430.0 (2)

*Circumferential buckling wave number, n

buckling pressures in p.s.i.

BS5500 $p_n = 510.6$, n = 2

TABLE 10: COMPARISON BETWEEN PRESENT THEORY AND EXPERIMENTAL RESULTS OF REF. (96)

Overall Instability of Orthogonally Stiffened Welded Steel Cylinder under External Pressure.

Dimensions: $R = 35.85"$, $t^* = 0.297"$, $\ell = 9.00"$, $d = 0.150"$

$t_w = 0.040"$, $L = 189.0"$

(*smeared shell thickness - all 24 stringers of 0.186" x 2.033" are smeared)

Measured out-of-circularity = 0.234" (or 0.0065R)

Properties of Material: $E = 29.0 \times 10^6$ psi , $\sigma_y = 39000$ psi

Experimental collapse pressure = 270 psi

Assumed $(C_{o1}/R)\%$	Assumed $(C_{o2}/R)\%$	n	Collpase Pressure Eq. (22b) psi	σ_F/σ_{YF}
0.650	0.00	2	272.3	0.955
0.650	0.05	2	265.8	0.942
0.625	0.00	2	276.0	0.948
0.625	0.05	2	269.4	0.934

Assumed $(C_{o1}/R)\%$	Assumed $(C_{o2}/R)\%$	n	Collapse Pressure Eq. (19b) psi	σ_F/σ_{YF}
0.650	0.00	3	275.9	1.00
0.650	0.05	3	269.7	1.00
0.625	0.00	3	282.5	1.00
0.625	0.05	3	276.3	1.00

Assumed $(C_{o1}/R)\%$	Assumed $(C_{o2}/R)\%$	n	Collapse Pressure BS5500 psi	σ_F/σ_{YF}
0.650	0.00	3	275.0	1.00
0.625	0.00	3	280.0	1.00

TABLE 11A: COMPARISON BETWEEN PRESENT THEORY AND FINITE ELEMENT METHOD OF REF. (52)

Influence of out-of-circularity on collapse strength of typical long externally pressurised ring-stiffened cylinder.

Dimensions: $R = 120t$, $\ell = 20t$, $d = 8t$, $t_w = 0.75t$, $f = 5t$, $t_f = 1.5t$, $L = 440t$

Buckling Mode (n)	C_{ol}/R	% Less of strength due to out-of-circularity		
		SMITH(52)	Eq. (19b)	Eq. (22b)
2	0.0002	3	2	2
2	0.001	11	10	6
2	0.005	31	35	23

TABLE 11B: OVERALL INSTABILITY OF RING STIFFENED CYLINDER UNDER UNIFORM EXTERNAL PRESSURE

Dimensions: $L = 720"$, $t = 1.00"$, $\ell = 30.0"$, $d = 7.36"$, $t_w = 0.32"$, $f = 4.0"$, $t_f = 0.64"$

Pressure in P.S.I.

Radius, R (inches)	Eq. (19b)	Eq. (22b)
101.0	811.4 (2)	823.1 (2)
105.0	767.8 (2)	739.9 (2)

TABLE 12: COMPARISON BETWEEN PRESENT THEORY AND FINITE ELEMENT METHOD OF REF. (91)

Overall Instability of Ring Stiffened Steel Cylinder under External Pressure.

Dimensions: $t = 0.010R$, $\ell = 0.15R$, $L = 2R$, $d = 0.033R$

$t_w = 0.0052R$, $f = 0.032R$, $t_f = 0.007R$

Properties of Material: $E = 30 \times 10^6$ psi , $\mu = 0.300$

Solution from finite element method = 1525 psi , n = 4

PRESENT THEORY

BUCKLING PRESSURE IN PSI		n
Eq. (19c)	Eq. (19b)	
11213.0	8985.4	2
2188.4	1985.2	3
1550.7	1466.1	4

Eq. (19c) consists of the same buckling displacements as Eq. (19b), but a different pre-buckling displacement, i.e. $\frac{\partial u}{\partial x}$ = constant and w = constant, uniform lateral and axial contraction prior to buckling.

Eq. (19c) represents a dead load situation and Eq. (19b) represents a live load model, where the loading changes direction as the structure deforms.

TABLE 13: DNV RULES - AXIAL COMPRESSIVE BUCKLING STRESSES (N/mm^2)

σ_y = 245 N/mm^2

ℓ/R \ R/t	100	150	200	250	300	350	400	450	500
0.50	210.3	179.9	151.4	127.3	107.3	92.10	79.32	68.87	60.20
1.00	210.3	179.9	151.4	127.3	107.3	92.10	79.32	68.87	60.20
1.50	210.3	179.9	151.4	127.3	107.3	92.10	79.32	68.87	60.20
2.00	210.3	179.9	151.4	127.3	107.3	92.10	79.32	68.87	60.20

σ_y = 367.5 N/mm^2

0.50	273.6	214.9	170.5	138.1	114.1	95.92	81.74	70.43	61.23
1.00	273.6	214.9	170.5	138.1	114.1	95.92	81.74	70.43	61.23
1.50	273.6	214.9	170.5	138.1	114.1	95.92	81.74	70.43	61.23
2.00	273.6	214.9	170.5	138.1	114.1	95.92	81.74	70.43	61.23

σ_y = 490.0 N/mm^2

0.50	314.4	233.1	179.2	142.6	116.6	97.38	82.63	71.0	61.61
1.00	314.4	233.1	179.2	142.6	116.6	97.38	82.63	71.0	61.61
1.50	314.4	233.1	179.2	142.6	116.6	97.38	82.63	71.0	61.61
2.00	314.4	233.1	179.2	142.6	116.6	97.38	82.63	71.0	61.61